

B Meson Decays in the Covariant Confined Quark Model

Stanislav Dubnička ^{1,†} , Anna Z. Dubničková ^{2,†} , Mikhail A. Ivanov ^{3,†}  and Andrej Liptaj ^{1,*,†} ¹ Institute of Physics, Slovak Academy of Sciences, 845 11 Bratislava, Slovakia² Faculty of Mathematics, Physics and Informatics, Comenius University, 842 48 Bratislava, Slovakia³ Bogoliubov Laboratory of Theoretical Physics, Joint Institute for Nuclear Research, 141980 Dubna, Russia

* Correspondence: andrej.liptaj@savba.sk

† These authors contributed equally to this work.

Abstract: The aim of this text is to present the covariant confined quark model (CCQM) and review its applications in the decays of B mesons. We do so in the context of existing experimental measurements and theoretical results of other authors, which we also review. The physics principles are, in detail, exposed for the CCQM; the other results (theoretical and experimental) are surveyed in an enumerative way with comments. We proceed by considering, successively, three categories of decay processes: leptonic, semileptonic and non-leptonic.

Keywords: quark model; symmetry; B meson decay

1. Introduction

The confinement property of quantum chromodynamics (QCD) implies that it is not possible to study the strong force using the scattering of free quarks. Since the confinement itself is a manifestation of the strong force, one cannot help but analyze more complex systems such as hadrons, i.e., bound states of quarks. All hadrons are colorless (white) objects, including mesons consisting of two quarks only. Even though no stable mesons exist, meson physics is often seen as the most simple testing ground for QCD.

Various measurements have provided us so far with a large amount of experimental data (masses, decay rates), which challenge our ability to provide theoretical predictions. For the above-mentioned reasons, the perturbative calculations performed at the partonic level need to be complemented by the so-called hadronic effects, which are non-perturbative in nature and originate in the long-range interaction between quarks and gluons. As of now, we do not have a well-established general method for reliable computation of hadronic effects for arbitrary processes from first principles.

Our ability to describe mesons and other QCD states without model dependence is limited, but has improved in time. Light meson physics is often treated within the chiral perturbation theory (ChPT), based on an (approximate) flavor chiral symmetry of the QCD which is spontaneously broken. Assuming this symmetry, together with constraints from the analyticity and unitarity, phenomenological Lagrangians were proposed in [1]. This allowed the authors to reproduce the results from complicated methods using the current algebra. In [1], the Lagrangians were given in the leading order only; the extension of this approach, which included meson loops, was formulated in two original papers [2,3]. Since then, the ChPT proved to be a successful effective field theory approach with remarkable results [4,5]; however, the large masses of other quarks—other than u , d and s —exclude the heavy-quark physics from ChPT's applicability range.

A different approach is represented by non-perturbative methods, such as the Dyson–Schwinger equations. The latter were formulated decades ago [6–8] in terms of an infinite number of coupled differential equations imposed on the Green functions of the theory. With necessary simplifications, results were derived first for abelian theories. Then, the approach was extended also to the more complicated case of non-abelian theories [9], thus



Citation: Dubnička, S.; Dubničková, A.Z.; Ivanov, M.A.; Liptaj, A. B Meson Decays in the Covariant Confined Quark Model. *Symmetry* **2023**, *15*, 1542. <https://doi.org/10.3390/sym15081542>

Academic Editors: Michal Hnatič and Juha Honkonen

Received: 28 June 2023

Revised: 24 July 2023

Accepted: 1 August 2023

Published: 4 August 2023



Copyright: © 2023 by the authors. Licensee MDPI, Basel, Switzerland. This article is an open access article distributed under the terms and conditions of the Creative Commons Attribution (CC BY) license (<https://creativecommons.org/licenses/by/4.0/>).

including QCD and hadronic physics. The application to heavy quarks was, for the first time, presented in [10].

A distinctive non-perturbative theoretical technique to investigate the strong-interaction physics are the QCD sum rules [11,12]. The central objects of interest are the correlation functions of interpolating quark currents, treated using the operator product expansion (OPE) and expressed in term of a perturbative continuum contribution and a low-energy parameterization. These are then matched by assuming the quark–hadron duality. The results are derived in the form of sum rules, while the uncertainties have to take into account various necessary approximations. Among others, the results for leptonic decay constants and hadron transition form factors have been derived [13,14].

In the domain of heavy meson physics (which we are interested in), a specific tool is available: the approximate realization of the heavy quark symmetry gives rise to the heavy quark effective theory (HQET) [15–17]. The symmetry appears when the mass of the heavy quark goes to infinity; it is the combination of a heavy quark flavor symmetry and the independence of hadronic properties on the heavy quark spin state. It allows for important simplifications and leads to results expanded in the inverse of the heavy quark mass.

An important model-independent approach with possibly very broad applicability is represented by numerical QCD calculations on the lattice. Here, important progress was made over last decades [18]; nowadays, predictions of form factors in weak decays of heavy particles become available [19–22]. The potential of this method is immense, since, as is evident from [23], the bulk of experimental data in high-energy physics are related to hadrons and explaining them at a few-percent level accuracy would be a triumph.

However we are not at this point now and the possibility for lattice calculations to become the mainstream of theoretical predictions will depend on the future developments. Thus, despite the important achievements of the lattice QCD, model-dependent methods remain the most popular and versatile tools in making QCD predictions with hadronic effects included. This is mainly due to the fact that the lattice QCD remains limited to a narrow set of specific processes, while the model framework can be usually easily adopted to various settings, thus making predictions more easy to produce. This is especially true in relation to the B factories, i.e., very high-luminosity accelerator facilities which are nowadays in operation, where a large number of various heavy hadron decays are registered and measured. Many of these approaches can be described as “quark” models, since they describe the hadron by considering its valence quarks using some specific assumptions or ansätze (see, e.g., [24,25]).

The Nambu–Jona-Lasinio (NJL) model, based on the ideas of Y. Nambu and G. Jona-Lasinio (Refs. [26,27] are the original papers), is widely used in the low-energy phenomenology of light quarks (u, d, s). The hadron masses are generated by the spontaneous breaking of chiral symmetry, where the pion plays the role of the Goldstone boson. This approach has found many applications in light meson physics due to the simplicity of calculations; for review, see, e.g., Ref. [28]. Some efforts have been made to extend the NJL model to applications in heavy mesons by taking into the account the heavy quark symmetry [29,30]. In our earlier paper [31], which was a predecessor to the CCQM, a clear relation of the so-called compositeness condition (addressed later) with the requirement for the correct normalization of the kinetic term in the NJL Lagrangian after the spontaneous breaking of chiral symmetry was shown.

As far as quark models are concerned, for weak decays, they are usually combined with a perturbative computation at the quark level. Here, it is customary to use an effective four-fermion theory derived using the OPE and governed by the low-energy Hamiltonian:

$$\mathcal{H}_{\text{eff.}}^{b \rightarrow q} = \frac{G_F}{\sqrt{2}} V_{tb} V_{tq}^* \sum_i C_i(\mu) Q_i(\mu) \quad (1)$$

here written for the $b \rightarrow q \in \{s, d\}$ transition. $Q_i(\mu)$ are local operators expressed in terms of quark fields, $C_i(\mu)$ are the Wilson coefficients which can be evaluated perturbatively, V_{ij} are Cabibbo–Kobayashi–Maskawa (CKM) matrix elements and μ is the QCD renormal-

ization scale. Its value is set to a typical momentum transfer which is, for weak decays, significantly smaller than the W mass. Thus, W is effectively removed from (1) and it enters in computations of $C_i(\mu)$. An excellent overview of weak decays is given in [32].

The heavy decay processes are of special interest for the particle physics community for several reasons [33]. One of them is the determination of the CKM matrix elements and the study of related questions such as the CP violation, unitarity triangle, baryogenesis and weak physics in general. Further, B factories are used to search for new exotic states, including tetraquarks, pentaquarks, glueballs and so on. The collected data also allowed researchers to study fragmentation processes, test the lepton universality, investigate possible lepton flavor violation and address the questions related to a new set beyond Standard Model (SM) physics [34,35].

Indeed, various new physics (NP) scenarios [36–42] predict deviations from the SM in B meson decay processes. Because of the very high luminosity possessed by colliders nowadays, there is a hope that even rare (small in number) deviations from SM physics can be detected.

We present here how the covariant confined quark model (CCQM) [43] has been used to investigate the B-physics processes. A dedicated effort was made in previous years and decades to cover most of the measured B meson data, and, since the number of articles is large, we believe it is appropriate to review them. We provide in this text an overview of the results from the perspective of the CCQM, but we also point out contributions and achievements from other approaches and authors. With some exceptions, the majority of the outcomes were formulated in terms of the SM predictions, which were then compared to data. In this way, possible tensions or deviations were identified or hypotheses about the nature of an exotic state were expressed. This then points to possible NP phenomena or better understanding of exotic particles, especially when there is agreement with other theoretical works.

The large quantity of various B-related results which have been published in the past does not allow us to review each decay in full details. We therefore define three categories and for each we present a demonstrative calculation with one or two example processes. The categories are leptonic, semileptonic and non-leptonic (radiative) decays.

The text is structured as follows. In Section 2 the general features of the CCQM are presented. The following three sections are dedicated to specific process categories, as mentioned above. Each has three subsections, one with a general overview, the second presenting in more detail the computations for a chosen example process and the third where results obtained within the CCQM framework are summarized. The text ends with conclusions and an outlook.

2. Covariant Confined Quark Model

The key points for the model construction are the following:

- Lorentz symmetry and invariant Lagrangian;
- Compositeness and double counting;
- Confinement of quarks;
- Gauge symmetry and inclusion of electromagnetic (EM) fields.

The above are addressed in the order shown. In an additional subsection, we also briefly describe the computational techniques.

2.1. Lagrangian

To construct a theory with Lorentz symmetry, one naturally uses a Lagrangian formulation. This was carried out for the CCQM, which is an effective field approach where both quark and hadronic fields occur. The quark–meson interaction term is written as

$$\mathcal{L}_{int} = g_M M(x) J_M(x) + \text{H.c.}, \quad J_M(x) = \int dx_1 \int dx_2 F_M(x; x_1, x_2) \bar{q}_2(x_2) \Gamma_M q_1(x_1), \quad (2)$$

where M represents the mesonic field, q the quark field, g_M is their coupling and H.c. stands for the Hermitian conjugate. The interpolating quark current J_M is non-local and the integral over the positions x_1, x_2 of constituent quarks is weighted by a vertex function F_M . The symbol Γ_M represents a combination of gamma matrices that depend on the spin of M . For a scalar M , one has $\Gamma_M = 1$, while, for pseudoscalar, $\Gamma_M = \gamma^5$ and, for a vector particle, the expression is $\Gamma_M = \gamma^\mu$. In the latter case, the mesonic field has a Lorentz index too (M_μ) and the indices are contracted.

It is interesting to see what happens in the case of local interaction when $F_M(x; x_1, x_2) = \delta(x - x_1 - x_2)$. Then, one clearly observes that the interaction Lagrangian given by Equation (2), together with free meson and quark Lagrangians, corresponds to the NJL model after bosonization.

The explicit form of F_M is driven by two requirements. First, the positions of quarks are constrained so as to make the hadron be situated in their barycenter. For this, a delta function is introduced, where the weights in its argument depend on the constituent quark masses $w_i = m_i / (m_1 + m_2)$. Second, to manifestly respect the Lorentz symmetry, the remaining dependence is written as a function of the spacetime interval:

$$F_M(x; x_1, x_2) = \delta(x - w_1 x_1 - w_2 x_2) \Phi_M[(x_1 - x_2)^2]. \quad (3)$$

Further steps in the construction of F_M are performed with respect to the computational convenience. Φ_M is assumed to have a Gaussian form in the momentum representation:

$$\Phi_M[(x_1 - x_2)^2] = \int \frac{d^4 k}{(2\pi)^4} e^{-ik(x_1 - x_2)} \tilde{\Phi}_M(-k^2), \quad \tilde{\Phi}_M(-k^2) = e^{k^2/\Lambda_M^2}, \quad (4)$$

where Λ_M is a free parameter of the model related to the meson M . The square of the momentum in the argument of the exponential becomes negative in the Euclidean region $k^2 = -k_E^2$, which implies an appropriate fall-off behavior and removes ultraviolet divergences in Feynman diagrams. The question of other possible function forms of Φ_M was addressed in [31], where four different ansätze were tested, each having a meaningful physical interpretation. The dependence of the results on the function form was found to be small.

The S-matrix is constructed from the interaction Lagrangian as $S = T \exp\{i \int d^4 x \mathcal{L}_{\text{int}}(x)\}$. The calculation of the matrix elements in S proceeds in a standard manner: first, by making convolution of the quark fields with the help of T-product and, second, by using the Fourier transforms of quark propagators and vertex functions to transfer to the momentum space. Note that we use the ordinary local forms of the quark propagators $S(k) = 1/(m_q - \not{k})$ in our approach.

In addition to the hadron-related Λ_M , the CCQM comprises four “global” parameters: three constituent quark masses and one universal cutoff which plays a role in the quark confinement (as explained later). The values expressed (in GeV) are

$$m_q = m_{u,d} = 0.241, \quad m_s = 0.428, \quad m_c = 1.67, \quad m_b = 5.05, \quad \lambda = 0.181, \quad (5)$$

where one does not distinguish between the two light quarks, using the same mass for both. The values changed slightly in the past because they were updated a few times [44,45] as significant new data became available. They were extracted by over-constrained global fits of the model on available experimental points.

The CCQM does not include gluons. The gluonic effects are effectively taken into account by the vertex function, which is adjusted to describe data by tuning the contained free parameter.

Finally, we have to mention that the CCQM is suitable for description of various multi-quark states, including baryons [46,47] and tetraquarks [48]. In this text, we focus on mesons; the approach is, in other cases, very similar: the interpolating quark current

is constructed for a given number of quarks (more alternatives can be considered) and multiplied by the hadronic field to provide the interaction Lagrangian.

2.2. Compositeness Condition

The interaction of a meson is given by the Lagrangian (2): the meson fluctuates into its constituent quarks; these interact and, afterwards, combine back into a mesonic final state. However, (2) implies that both, quarks and mesons, are elementary and this raises concerns about double counting.

These questions were addressed by implementing the so-called compositeness condition [43,44,49], which originated in the works [50–52] (see [53] for a review). The interaction of a meson through the creation of virtual quark states implies the mesonic field is dressed, i.e., its vertex and wave function need to be renormalized. This is reflected in the renormalization constant Z_M , which can be interpreted as the overlap between the physical state and the corresponding bare state. By requiring $Z_M = 0$, one makes this overlap vanish, i.e., the physical state does not contain a bare state and can be regarded as a bound state. As a consequence, the quarks exist only virtually and quark degrees of freedom do not appear on the level of the physical state.

Z_M is expressed in terms of the derivative of the meson mass operator Π'_M (its scalar part for vector mesons):

$$Z_M = 1 - g_M^2 \Pi'_M(m_M^2) = 0 \tag{6}$$

and, at the one-loop level (Figure 1) is given by

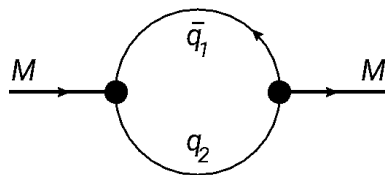


Figure 1. Meson mass function diagram.

$$\Pi'_{PS}(p^2) = \frac{-i}{2p^2} p^\alpha \frac{d}{dp^\alpha} \int d^4k \tilde{\Phi}_{PS}^2(-k^2) \text{tr} \left[\gamma^5 S_1(k + w_1 p) \gamma^5 S_2(k - w_2 p) \right], \tag{7}$$

$$\Pi'_V(p^2) = \frac{-i}{3} \left(g_{\mu\nu} - \frac{p_\mu p_\nu}{p^2} \right) \frac{1}{2p^2} p^\alpha \frac{d}{dp^\alpha} \int d^4k \tilde{\Phi}_V^2(-k^2) \text{tr} \left[\gamma^\mu S_1(k + w_1 p) \gamma^\nu S_2(k - w_2 p) \right], \tag{8}$$

for pseudoscalar and vector mesons, respectively. The symbol S_i denotes the quark propagator $S_i = 1/(m_{q_i} - \gamma^\mu k_\mu)$ and the differentiation is carried out by using the identity $d\Pi/dp^2 = (p^\mu d\Pi/dp^\mu)/(2p^2)$.

To reach equality (6), one benefits from the as-of-yet undetermined coupling constant g_M , tuning its value so that (6) is satisfied. As a consequence, the coupling g_M becomes a function of Λ_M . In this way, the number of parameters in the model is reduced and one increases its predictive power and stability. If the values Λ_M and g_M are unknown from previous studies, their determination is the first step in the application of the CCQM.

As is discussed in the next sections, the adjustable parameters of the model (quark masses, size parameters and infrared cutoff) are determined by fitting the experimental data of physical observables. For instance, in the case of the B meson, the size parameter is found to be equal to $\Lambda_B = 1.96$ GeV. By using the compositeness condition it gives the numerical value of the coupling constant $g_B = 4.80$.

2.3. Infrared Confinement

The CCQM is a successor to the so-called relativistic constituent quark model (see [54]) and, in [43], it was proposed to refine the latter by effectively implementing quark confinement into it. This was motivated by data on heavy particles which required an extension to situations where the hadron is heavier than the sum of its constituent quarks. To prevent

the decay into free quarks in such a scenario, a technique inspired by confined propagators is used. Here, the propagators are written in the Schwinger representation and a cutoff is introduced in the upper integration limit. The propagator then becomes an entire function:

$$\frac{S_i(k)}{(m_{q_i} + \gamma^\mu k_\mu)} = \int_0^\infty d\alpha e^{-\alpha(m_{q_i}^2 - k^2)} \rightarrow \int_0^{1/\lambda^2} d\alpha e^{-\alpha(m_{q_i}^2 - k^2)} = \frac{1 - e^{-(m_{q_i}^2 - p^2)/\lambda^2}}{m_{q_i}^2 - p^2}, \quad (9)$$

where the absence of singularities indicates the absence of a single quark asymptotic state. A modified version of this strategy was adopted and the cutoff was applied to the whole structure F of the Feynman diagram. It can be formally written as

$$\Pi = \int_0^\infty d^n \alpha F(\alpha_1, \dots, \alpha_n) = \int_0^{\infty \rightarrow 1/\lambda^2} dt t^{n-1} \int_0^1 d^n \alpha \delta(1 - \sum_{i=1}^n \alpha_i) F(t\alpha_1, \dots, t\alpha_n) \quad (10)$$

which can be obtained by inserting the unity $1 = \int_0^\infty dt \delta(t - \sum_{i=1}^n \alpha_i)$ into the expression on the left hand side. The single cutoff (indicated by the arrow) in the t variable is performed in the last step; the remaining integration variables are confined to an n dimensional simplex. After the cutoff is applied, the integral becomes convergent for arbitrary values of the kinematic variables, meaning that the quark thresholds are removed, with quarks never being on the mass shell. Then, the cutoff value (5) is the same for all processes.

2.4. Electromagnetic Interactions and Gauge Symmetry

Radiative decays represent another important class of processes measured in heavy meson factories. For their description, one has to include the interactions with photons into the CCQM [43,55]. Because of the non-local interaction Lagrangian, this is not straightforward and requires a dedicated approach. Taking into the account quarks and scalar mesons, the free parts of the Lagrangian are treated in the usual way, i.e., the minimal substitution is used:

$$\partial^\mu \psi \rightarrow (\partial^\mu - ie_\psi A^\mu) \psi, \quad \partial^\mu \bar{\psi} \rightarrow (\partial^\mu + ie_\psi A^\mu) \bar{\psi}, \quad (11)$$

where $\psi \in \{q, M\}$ and e_ψ is its electric charge in the units of the proton charge. One then obtains

$$\mathcal{L}^{EM_1} = eA_\mu(x)J_M^\mu(x) + e^2 A^2(x)M^-(x)M^+(x) + \sum_q e_q A_\mu(x)J_q^\mu(x), \quad (12)$$

$$J_M^\mu(x) = i[M^-(x)\partial^\mu M^+(x) - M^+(x)\partial^\mu M^-(x)], \quad J_q^\mu(x) = \bar{q}(x)\gamma^\mu q(x). \quad (13)$$

The compositeness condition formulated above, however, prevents a direct interaction of the dressed particle, i.e., the meson, with photons: the contributions from the photon-meson tree-level diagram, and analogous diagrams with self-energy insertions into the external mesonic line, determine the renormalization constant Z and $Z = 0$ implies they cancel. The interaction thus proceeds only through intermediate virtual states.

The gauging of the non-local interaction (2) is carried out in a manner similar to [56]. First, one multiplies the quark fields in (2) by a gauge field exponential:

$$q_i(x) \rightarrow e^{-ie_{q_i} I(x_i, x, P)} q_i(x), \quad I(x_i, x, P) = \int_x^{x_i} dz_\mu A^\mu(z), \quad (14)$$

where P is the path connecting x_i and x , the latter being the position of the meson. One can verify that the Lagrangian is invariant under the following gauge transformations:

$$q_i(x) \rightarrow e^{ie_{q_i} f(x)} q_i(x), \quad \bar{q}_i(x) \rightarrow \bar{q}_i(x) e^{-ie_{q_i} f(x)}, \quad (15)$$

$$M(x) \rightarrow e^{ie_M f(x)} M(x), \quad A^\mu(x) \rightarrow A^\mu(x) + \partial^\mu f(x). \quad (16)$$

Here, $f(x)$ is some scalar function. The apparent path-dependence of the definition (14) is not an actual one: in the perturbative expansion, only derivatives of the path integral appear and these are path-independent:

$$\frac{\partial}{\partial x^\mu} I(x, y, P) = A_\mu(x). \tag{17}$$

The individual terms of the Lagrangian are generated by expanding the gauge field exponential by orders in A^μ . At first order, one has

$$\mathcal{L}^{EM_2}(x) = g_M M(x) \iiint dx_1 dx_2 dy E_M^\mu(x; x_1, x_2, y) A_\mu(y) \bar{q}_2(x_2) \Gamma_M q_1(x_1), \tag{18}$$

where E_M is defined through its Fourier transform $\tilde{E}_M: (x_1 - x, x_2 - x, y - x) \xrightarrow{FT} (p_1, p_2, q)$,

$$\tilde{E}_M^\mu(p_1, p_2, q) = \sum_{i=1,2} \vartheta_i e_{q_i} w_i (w_i q^\mu + \vartheta_{i+1} 2l^\mu) \int_0^1 dt \tilde{\Phi}'_M \left[-t(w_i q + \vartheta_{i+1} l)^2 - (1-t)l^2 \right], \tag{19}$$

$$l = w_1 p_1 + w_2 p_2, \quad \vartheta_i = (-1)^i. \tag{20}$$

The symbol $\tilde{\Phi}'_M$ denotes the derivative with respect to the argument. In corresponding Feynman diagrams, the photon is attached to the non-local vertex.

2.5. Computations

From the Lagrangian, one derives the Feynman diagrams. Gaussian expressions in the vertex function (4) and in the Fock–Schwinger propagator (9) can be joined into a single exponent, which takes a quadratic form in the loop momenta k . It can be formally written as $\exp(ak^2 + 2rk + z)$, $a = a(\{\alpha\})$, $r = r(\{\alpha\}, \{p\})$, where $\{\alpha\}$ denotes the set of Schwinger parameters and $\{p\}$ denotes external momenta. The exponential is preceded by a polynomial P in loop momenta which originates from the trace of Dirac matrices (numerators of propagators). Since the powers of k can be generated by differentiation with respect to r , the loop momenta integration is formally written as

$$\int d^4k P(k) \exp(ak^2 + 2rk + z) = \exp(z) P\left(\frac{1}{2} \frac{\partial}{\partial r}\right) \int d^4k \exp(ak^2 + 2rk). \tag{21}$$

Using the substitution $u = k + r/a$, the argument of the exponential is transformed:

$$\int d^4k \exp(ak^2 + 2rk) = \int d^4u \exp(au^2 - r^2/a) = \exp(-r^2/a) \int d^4u \exp(au^2) \tag{22}$$

and the integration is performed in the Euclidean region as a simple Gaussian integral. Further, the differential operator and the r -dependent exponential can be interchanged, i.e.,

$$P\left(\frac{1}{2} \frac{\partial}{\partial r}\right) \exp\left(-\frac{r^2}{a}\right) = \exp\left(-\frac{r^2}{a}\right) P\left(-\frac{r}{a} + \frac{1}{2} \frac{\partial}{\partial r}\right) \tag{23}$$

which simplifies the action of the differential operator. One arrives at

$$\int_0^\infty d\alpha_1 \cdots \int_0^\infty d\alpha_n F(\alpha_1, \dots, \alpha_n), \tag{24}$$

where F represents the whole structure of the Feynman diagram, including (23). A FORM [57] code is used to treat symbolic expressions; in addition to computing traces, it is also used to repeatedly perform chain rule application in (23) and arrive at an explicit formula with no differential operators. The implementation of the infrared confinement, as expressed by (10), is the last step before the numerical integration.

3. Leptonic Decays of B Mesons

3.1. Overview

A large mass difference between heavy mesons and leptons implies, by phase-space arguments, small branching fractions of pure and radiative leptonic decays. Some of these are further suppressed by CKM elements or helicity. Thus, for most leptonic decays, only limits have been measured.

At the usual 95% confidence level, a branching fraction measurement is available only for $B_s^0 \rightarrow 2\mu$ [58–61] and $B^\pm \rightarrow \tau^\pm \nu_\tau$ [62–65]. If the criteria are loosened to (at least) one sigma significance, additional results can be cited: $B^0 \rightarrow 2\mu$ [58], $B^+ \rightarrow \mu^+ \nu_\mu$ [66,67] and $B^+ \rightarrow \ell^+ \nu_\ell \gamma$ [68]. The limits are settled [23] for $B^+ \rightarrow e^+ \nu_e$, $B^+ \rightarrow e^+ \nu_e \gamma$, $B^+ \rightarrow \mu^+ \nu_\mu \gamma$, $B^+ \rightarrow \mu^+ \mu^- \mu^+ \nu_\mu$, $B^0 \rightarrow e^+ e^-$, $B^0 \rightarrow e^+ e^- \gamma$, $B^0 \rightarrow \mu^+ \mu^- \gamma$, $B^0 \rightarrow \mu^+ \mu^- \mu^+ \mu^-$, $B^0 \rightarrow \tau^+ \tau^-$, $B_s^0 \rightarrow e^+ e^-$, $B_s^0 \rightarrow \tau^+ \tau^-$ and $B_s^0 \rightarrow \mu^+ \mu^- \mu^+ \mu^-$.

These experimental results motivate various analyses. Pure leptonic decays are considered as theoretically clean, with the main source of uncertainty represented by the hadronic effects of the initial state, which are contained in the leptonic decay constant of the hadron. The neutrino production process corresponds, in the leading order, to the annihilation of the constituent quarks into a virtual W meson, which subsequently decays. The branching fraction is given by

$$\mathcal{B}(B^+ \rightarrow \ell^+ \nu) = \frac{G_F^2 m_B m_\ell^2}{8\pi} \left(1 - \frac{m_\ell^2}{m_B^2}\right)^2 f_B^2 |V_{ub}|^2 \tau_{B^+}, \quad (25)$$

where G_F is the Fermi coupling constant, V_{ij} is the CKM matrix element and τ_P is the lifetime of particle P .

General information about B leptonic decays is contained in several reviews. In addition to [32], a more specific focus on processes with charged pseudoscalar mesons is given in [69] and a summary concerning, specifically, B decays (leptonic and semileptonic) is provided in [70]. The existing theoretical approaches follow two directions. One focuses on the SM contributions at different precision levels; the other is concerned with NP beyond the SM.

Dilepton final states are produced in one-loop through box and penguin diagrams. The cross-section formula can be found, e.g., in [71], Equation (4.10). The leptonic decay constants of B (and D) mesons were determined in a model-independent way using lattice calculations in [72]. The SM treatment of dilepton decays includes the computation of three-loop QCD corrections [73], the evaluation of the electroweak contributions at the two-loop level [74] and further improvements of theoretical predictions reached by combining additional EM and strong corrections [75]. The authors of [76] investigated the effect of the virtual photon exchange from scales below the bottom-quark mass and found a dynamical enhancement of the amplitude at the 1% level. The soft-collinear effective theory approach was used in [77] to evaluate the power-enhanced leading-logarithmic QED corrections.

The radiative processes have the advantage of not being helicity-suppressed, at the price of one additional α_{EM} factor. A larger number of results can be cited for radiative dilepton production. An evaluation within a constituent quark model was performed in [78] to estimate branching fractions; the same observables were predicted by the authors of [79,80] using the light-cone QCD sum rules and by those of [81] using the light-front model. Universal form factors related to the light cone wave function of the B_s meson allowed the authors to make estimates in [82]. Interesting results were given in [83], where it was shown that the gauge invariance and other considerations allow significant constraint of the form factor behavior, and also in [84], where the authors demonstrated that the non-perturbative hadronic effects largely cancel out in amplitude ratios of pure leptonic and radiative decays. The impact of the light meson resonances on long-distance QCD effects was studied in [85]. In [86], the authors identified the effective $B \rightarrow \mu\mu\gamma$ lifetime, and a related CP-phase sensitive observable, as appropriate quantities to study the existing B decay discrepancies.

Furthermore, for decays $B \rightarrow \gamma l\nu_l$, several studies can be cited. The work [87] was concerned with photon spectrum and the decay rates of the process. The authors of [88] used the HQET to predict form factors and, in [89], the heavy-quark expansion and soft-collinear effective theory were applied to evaluate the soft-overlap contribution to the photon. The process was also studied in [90]. There, assuming an energetic photon, the authors aimed to quantify the leading power-suppressed corrections in $1/E_\gamma$ and $1/m_b$ from higher-twist B meson light-cone distribution amplitudes. The soft-collinear effective theory was the approach adopted in [91,92].

A recent publication [93] focused on four-body leptonic B decays: off-shell photon form factors were computed within the QCD factorization formalism and predictions for differential distribution of various observables were presented. Similar processes were addressed also in [94–96].

Although the most tensions with the SM are seen in the semileptonic sector, the pure leptonic decays are of concern too. The summary papers [35,97] mention two tensions. The first is related to the combined likelihood for B^0 and B_s^0 decays to $\mu^+\mu^-$ where the theory–measurement difference reaches 2.3σ . The other concerns the branching fraction ratio for the $B_s^0 \rightarrow \mu^+\mu^-$ reaction $R = \mathcal{B}_{\text{exp}}/\mathcal{B}_{\text{SM}}$ which deviates from 1 by 2.4σ . In [98], the difference between the theory and the experiment for the dimuon B_s decay is quantified to be 2.2σ .

The possible NP contributions are usually assessed by introducing new, beyond SM four-fermion contact operators and the corresponding Wilson coefficients. Once evaluated in the appropriate NP approach, it is possible to conclude about their effect on the theory–experiment discrepancy, see, e.g., [99].

An overview of various flavor-violating extensions of the SM, also with relation to $B \rightarrow \ell\ell$ decay, was presented in [100]. In [101], the B_s dimuon decay was considered and it was argued that the decay width difference between the light and heavy B_s mass eigenstates is a well-suited observable for the detection of NP. The work [37] pointed to the ambiguity in choice of the NP operators that might play a role in explaining the tensions in the B semileptonic decays. They show that this ambiguity can be lifted by analyzing the longitudinal polarization asymmetry of the muons in $B_s^* \rightarrow \mu\mu$. Various discrepancies in measured data are addressed in [102]; also among them are dimuon branching fractions. The attempt to explain them is based on lepton-flavored gauge extensions of the SM, a specific construction with a massive gauge boson X_μ and “muoquark” S_3 is presented. Several texts are interested in decays with tau lepton in the final state. In [103–105], these decays were studied in relation to various alternative scenarios of the Higgs boson model and, in [106], they are analyzed in the context of non-universal left–right models.

3.2. Radiative Leptonic Decay $B_s \rightarrow \ell^+\ell^-\gamma$ in CCQM

Before reviewing other CCQM results on leptonic B decays, we present, in more detail, the evaluation of the branching fraction for $B_s \rightarrow \ell^+\ell^-\gamma$ [107]. The computations are, in many ways, similar to those of other cases and provide an insight into how leptonic and radiative decays are treated within the CCQM. Since B_s is the only hadron, one needs to extend the set of parameters (5) by only one number, i.e., $\Lambda_{B_s} = 2.05 \text{ GeV}$, which was settled in previous works. The values of the remaining parameters are identical to (5) (see Equation (8) in [107]). Two explicit forms of the effective Hamiltonian (1) are considered:

$$\mathcal{H}_{\text{eff}}^{b \rightarrow s\ell^+\ell^-} = \frac{G_F \alpha_{\text{EM}}}{2\sqrt{2}\pi} V_{tb} V_{ts}^* \left[C_9^{\text{eff}} \{ \bar{s}\gamma^\mu (1 - \gamma^5)b \} (\bar{\ell}\gamma_\mu \ell) - \frac{2\tilde{m}_b}{q^2} C_7^{\text{eff}} \{ \bar{s}i\sigma^{\mu\nu} q_\nu (1 + \gamma_5)b \} (\bar{\ell}\gamma_\mu \ell) + C_{10} \{ \bar{s}\gamma^\mu (1 - \gamma_5)b \} (\bar{\ell}\gamma_\mu \gamma_5 \ell) \right], \tag{26}$$

$$\mathcal{H}_{\text{eff}}^{b \rightarrow s\gamma} = - \frac{G_F}{\sqrt{2}} V_{tb} V_{ts}^* C_7^{\text{eff}} \frac{e\tilde{m}_b}{8\pi^2} [\bar{s}\sigma_{\mu\nu} (1 + \gamma_5)b] F^{\mu\nu}, \tag{27}$$

where $\sigma_{\mu\nu} = i[\gamma_\mu, \gamma_\nu]$ and $F^{\mu\nu}$ is the EM field tensor. In (26), the dilepton is produced from the weak b – s transition (Figure 2); in (27), the weak transition gives birth to a real photon (Figure 3). An additional set of diagrams depicted in Figure 4 is considered too, where the real photon is emitted as the final-state radiation (FSR).

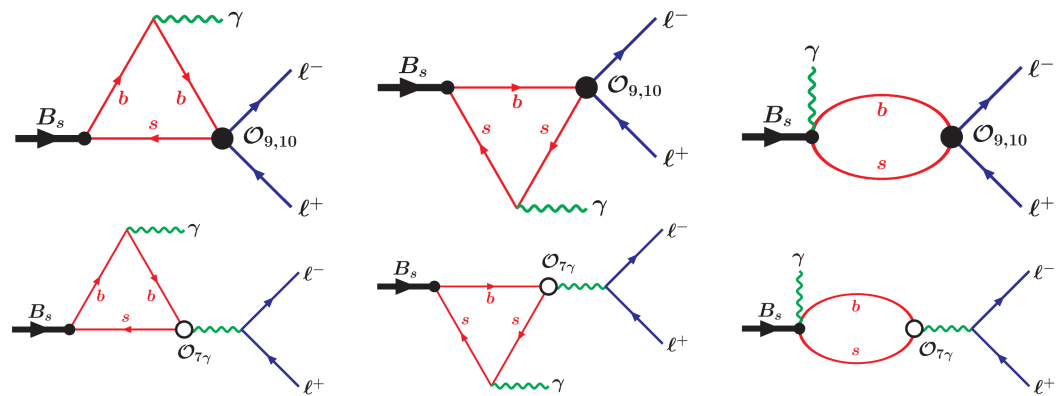


Figure 2. Diagrams with the dilepton produced from the b - s transition. Figures were originally published in [107].

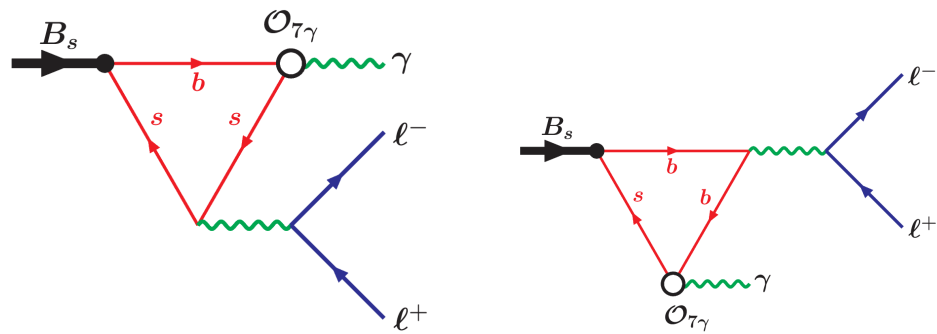


Figure 3. Diagrams with a real photon produced from the b - s transition. Figures were originally published in [107].

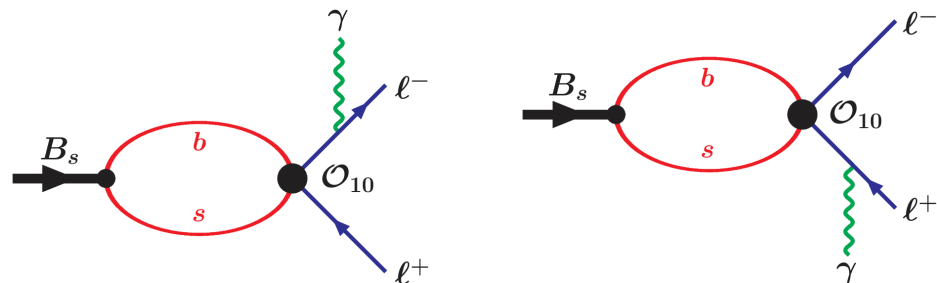


Figure 4. Final-state radiation diagrams. Figures were originally published in [107].

The tilde notation in (26) and (27) indicates the QCD quark mass (different from (5)), which is $\tilde{m}_b = 4.68 \pm 0.03 \text{ GeV}$ [108]. The values of scale-dependent Wilson coefficients were determined in [109] at the matching scale $\mu_0 = 2m_W$ and run according to the hadronic scale $\mu_b = 4.8 \text{ GeV}$. The effective operators are defined through the standard SM operators as follows:

$$\begin{aligned}
 C_7^{\text{eff}} &= C_7 - C_5/3 - C_6, \\
 C_9^{\text{eff}} &= C_9 + C_0[h(\tilde{m}_c, s) + \Omega] - \frac{1}{2}h(1, s)(4C_3 + 4C_4 + 3C_5 + C_6) \\
 &\quad - \frac{1}{2}h(0, s)(C_3 + 3C_4) + \frac{2}{9}(3C_3 + C_4 + 3C_5 + C_6),
 \end{aligned}
 \tag{28}$$

where

$$\begin{aligned}
C_0 &= 3C_1 + C_2 + 3C_3 + C_4 + 3C_5 + C_6, \quad \Omega = \frac{3\pi}{\alpha^2} \kappa \sum_{V_i=\Psi(1s),\Psi(2s)} \frac{\Gamma(V_i \rightarrow \ell^+ \ell^-) m_{V_i}}{m_{V_i}^2 - q^2 - im_{V_i} \Gamma_{V_i}}, \\
\hat{m}_c &= \tilde{m}_c / m_{B_s}, \quad \tilde{m}_c = 1.27 \pm 0.03 \text{ GeV}, \quad s = q^2 / m_{B_s}^2, \quad \kappa = 1 / C_0, \\
h(0, s) &= \frac{8}{27} - \frac{8}{9} \ln \frac{\tilde{m}_b}{\mu} - \frac{4}{9} \ln s + \frac{4}{9} i\pi, \\
h(\hat{m}_c, s) &= -\frac{8}{9} \left[\ln \frac{\tilde{m}_b}{\mu} + \ln \hat{m}_c - \frac{1}{3} - \frac{x}{2} \right] - \frac{2}{9} (2+x) \sqrt{|1-x|} \Theta(x), \\
\Theta(x)|_{x<1} &= \ln \left| \frac{\sqrt{1-x}+1}{\sqrt{1-x}-1} \right| - i\pi, \quad \Theta(x)|_{x>1} = 2 \arctan \frac{1}{\sqrt{x-1}}, \quad x = \frac{4\hat{m}_c^2}{s}.
\end{aligned} \tag{29}$$

The Ω function in C_9^{eff} parameterizes, in the standard Breit–Wigner form, the resonant contributions from $\Psi(1s)$ and $\Psi(2s)$ charmonia states.

Amplitudes given by the diagrams in Figures 2 and 3, where the photon originates from the intermediate QCD-generated states, are labeled as structure-dependent and can be described by four $B_s \rightarrow \gamma$ transition form factors (see, e.g., [85]). Defining momenta as $B_s(p_1) \rightarrow \gamma(p_2) \ell^+(k_+) \ell^-(k_-)$, $q = p_1 - p_2$, with $p_1^2 = m_{B_s}^2$, $p_2^2 = 0$, $\epsilon_2^\dagger \cdot p_2 = 0$ and $k_\pm^2 = m_\ell^2$, one has

$$\begin{aligned}
\langle \gamma(p_2, \epsilon_2) | \bar{s} \gamma^\mu b | B_s(p_1) \rangle &= e(\epsilon_2^\dagger)_\alpha \epsilon^{\mu\alpha\beta\delta} (p_1)_\beta (p_2)_\delta F_V(q^2) / m_{B_s}, \\
\langle \gamma(p_2, \epsilon_2) | \bar{s} \gamma^\mu \gamma_5 b | B_s(p_1) \rangle &= ie(\epsilon_2^\dagger)_\alpha (g^{\mu\alpha} p_1 p_2 - p_1^\alpha p_2^\mu) F_A(q^2) / m_{B_s}, \\
\langle \gamma(p_2, \epsilon_2) | \bar{s} \sigma^{\mu\beta} q_\beta b | B_s(p_1) \rangle &= ie(\epsilon_2^\dagger)_\alpha \epsilon^{\mu\alpha\beta\delta} (p_1)_\beta (p_2)_\delta F_{TV}(q^2), \\
\langle \gamma(p_2, \epsilon_2) | \bar{s} \sigma^{\mu\beta} q_\beta \gamma_5 b | B_s(p_1) \rangle &= e(\epsilon_2^\dagger)_\alpha (g^{\mu\alpha} p_1 p_2 - p_1^\alpha p_2^\mu) F_{TA}(q^2),
\end{aligned} \tag{30}$$

where ϵ is the polarization vector. Each of the four introduced form factors can be expressed as a sum of contributions from the particular Feynman graphs in Figures 2 and 3. One has

$$\begin{aligned}
F_V &= m_{B_s} (e_b \tilde{F}_V^{b\gamma b} + e_s \tilde{F}_V^{s\gamma s}), \\
F_A &= m_{B_s} (e_b \tilde{F}_A^{b\gamma b} + e_s \tilde{F}_A^{s\gamma s} + e_b \tilde{F}_A^{\text{bubble}-b} + e_s \tilde{F}_A^{\text{bubble}-s}), \\
F_{TV} &= e_b \tilde{F}_{TV}^{b\gamma b} + e_s \tilde{F}_{TV}^{s\gamma s} + e_b \tilde{F}_{TV}^{b(\bar{\ell}\ell)b} + e_s \tilde{F}_{TV}^{s(\bar{\ell}\ell)s}, \\
F_{TA} &= e_b \tilde{F}_{TA}^{b\gamma b} + e_s \tilde{F}_{TA}^{s\gamma s} + e_b \tilde{F}_{TA}^{\text{bubble}-b} + e_s \tilde{F}_{TA}^{\text{bubble}-s} + e_b \tilde{F}_{TA}^{b(\bar{\ell}\ell)b} + e_s \tilde{F}_{TA}^{s(\bar{\ell}\ell)s},
\end{aligned} \tag{31}$$

where the “ $q\gamma q$ ” superscript refers to a real photon emission from the quark line, “*bubble*” refers to the real photon emission from the non-local hadron-quark vertex and “ $q(\bar{\ell}\ell)q$ ” corresponds to the virtual photon emission from the quark line.

The branch point at $q^2 = 4m_s^2$, corresponding to the virtual photon emission from the s quark (left in Figure 3), is situated well inside the accessible physical q^2 region. This leads to the appearance of light vector meson resonance, which prevents us from computing the corresponding form factors within the CCQM. An approach inspired by [110] is adopted and a gauge-invariant vector-meson dominance model is used to express the form factors in question:

$$\tilde{F}_{TV,TA}^{s(\bar{\ell}\ell)s} = \tilde{F}_{TA}^{s(\bar{\ell}\ell)s}(0) - \sum_V 2f_V^{EM} G_1^T(0) \frac{q^2 / M_V}{q^2 - M_V^2 + iM_V \Gamma_V}, \tag{32}$$

$$\begin{aligned}
G_1^T &: \langle V(p_2, \epsilon_2) | \bar{s} \sigma^{\mu\nu} b | B_s(p_1) \rangle \\
&= (\epsilon_2^\dagger)_\alpha \left[\epsilon^{\beta\mu\nu\alpha} P_\beta G_1^T(q^2) + \epsilon^{\beta\mu\nu\alpha} q_\beta G_2^T(q^2) + \epsilon^{\alpha\beta\mu\nu} P_\alpha q_\beta \frac{G_0^T(q^2)}{(m_{B_s} + M_V)^2} \right],
\end{aligned} \tag{33}$$

where $P = p_1 + p_2$. With all these objects defined, one can write down the amplitude for the structure-dependent part:

$$\begin{aligned} \mathcal{M}_{SD} = & \frac{G_F}{\sqrt{2}} \frac{\alpha_{EM} V_{tb} V_{ts}^*}{2\pi} e(\epsilon_2^*)_\alpha \left\{ \left[\epsilon^{\mu\alpha\nu\beta} (p_1)_\nu (p_2)_\beta \frac{F_V(q^2)}{m_{B_s}} - iT_1^{\mu\alpha} \frac{F_A(q^2)}{m_{B_s}} \right] \times (C_9^{\text{eff}} \bar{\ell} \gamma_\mu \ell \right. \\ & \left. + C_{10} \bar{\ell} \gamma_\mu \gamma_5 \ell) + \left[\epsilon^{\mu\alpha\nu\beta} (p_1)_\nu (p_2)_\beta F_{TV}(q^2) - iT_1^{\mu\alpha} F_{TA}(q^2) \right] \frac{3\tilde{m}_b}{q^2} C_7^{\text{eff}} \bar{\ell} \gamma_\mu \ell, \right. \end{aligned} \quad (34)$$

where $T_1^{\mu\alpha} = [g^{\mu\alpha} p_1 p_2 - (p_1)^\alpha (p_2)^\mu]$. The structure-independent *bremsstrahlung* (Figure 4) amplitude takes the form:

$$\mathcal{M}_{BR} = -i \frac{G_F}{\sqrt{2}} \frac{\alpha_{EM} V_{tb} V_{ts}^*}{2\pi} e(\epsilon_2^*)_\alpha (2m_\ell f_{B_s} C_{10}) \bar{u}(k_-) \left[\frac{\gamma^\alpha \not{p}_1}{t - m_\ell^2} - \frac{\not{p}_1 \gamma^\alpha}{u - m_\ell^2} \right] \gamma_5 v(k_+). \quad (35)$$

Here, $t = (p_2 + k_-)^2$ and $u = (p_2 + k_+)^2$. To avoid infrared divergences in (35), a lower boundary on the photon energy has to be introduced, i.e., $E_\gamma > E_{\gamma \text{min}}$ (set later), in numerical computations (Table 1), to 20 MeV.

The differential branching fraction in t and $s \equiv q^2$ has a general expression

$$\frac{d\Gamma}{ds dt} = \frac{1}{2^8 \pi^3 m_{B_s}^3} \sum_{\text{pol.}} |\mathcal{M}_{SD} + \mathcal{M}_{BR}|^2, \quad (36)$$

where one sums over the polarization of photons and leptons, $4m_\ell^2 \leq s \leq m_{B_s}^2$, $t_- \leq t \leq t_+$, with $t_\pm = m_\ell^2 + (m_{B_s}^2 - s)[1 \pm \sqrt{1 - 4m_\ell^2/s}]/2$. The explicit formulas for double and single differential distributions we omit here because of their complexity; they are stated in Equations (32)–(38) of [107].

The form factors predicted by the CCQM model are shown in Figure 5. For $F_{TV/TA}$, the form factors for two scenarios are presented; by including the VMD component (32), these form factors become complex and thus their norm is shown. Alternatively, they can be shown without the VMD component as real functions:

$$\tilde{F}_{TV,TA} \equiv F_{TV} - e_s \tilde{F}_{TV,TA}^{s(\bar{\ell}\ell)} \quad (37)$$

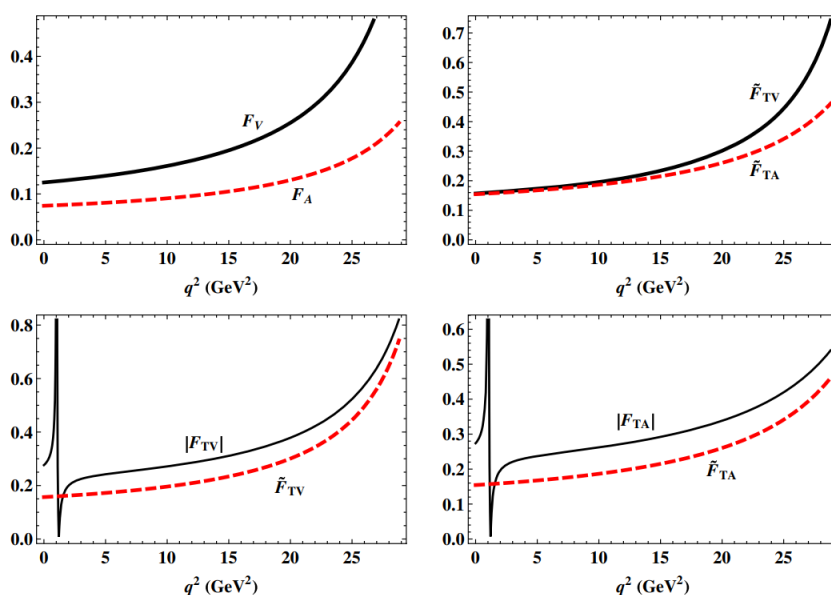


Figure 5. Transition form factors $B_s \rightarrow \gamma$, as defined by (31) and (37). Figures were originally published in [107].

The form factors were also compared to those determined in [110], with which they agreed well. The differential branching fractions shown as a function of dimensionless variable $\hat{s} = q^2/m_{B_s}$ are, together with the branching fraction ratio,

$$r_\gamma(\hat{s}) \equiv \frac{d\mathcal{B}(B_s \rightarrow \gamma\mu^+\mu^-)/d\hat{s}}{d\mathcal{B}(B_s \rightarrow \gamma e^+e^-)/d\hat{s}} \tag{38}$$

as depicted in Figure 6.

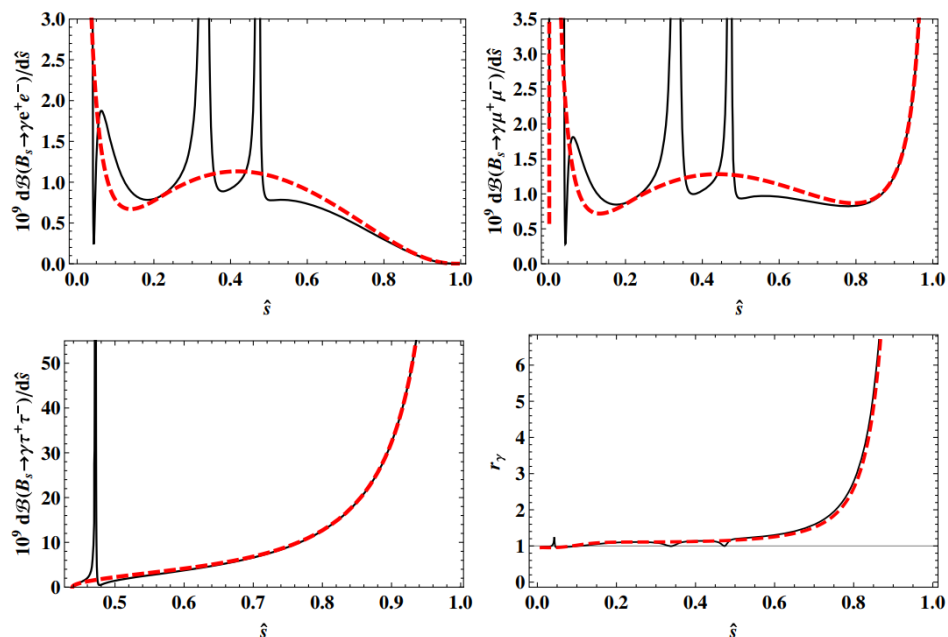


Figure 6. Differential decay rates for $B_s \rightarrow \ell^+ \ell^- \gamma$ and the ratio \hat{r} (38), with long-distant contributions included (solid line) and excluded (dashed line). Figures were originally published in [107].

The total branching fractions for the three lepton flavors are presented in Table 1.

Table 1. Branching fractions for the three lepton flavors. Values in brackets take into account long-distance contributions. Table was originally published in [107].

	Struct. Dep.	Bremst.	Interf.	Sum
$10^9 \mathcal{B}(B_s \rightarrow \gamma e^+ e^-)$	3.05 (15.9)	3.2×10^{-5}	$-4.8 (-9.5) \times 10^{-6}$	3.05 (15.9)
$10^9 \mathcal{B}(B_s \rightarrow \gamma \mu^+ \mu^-)$	1.16 (10.0)	0.53	$-7.4 (-14.4) \times 10^{-3}$	1.7 (10.5)
$10^9 \mathcal{B}(B_s \rightarrow \gamma \tau^+ \tau^-)$	0.10 (0.05)	13.4	0.30 (0.18)	13.8 (13.7)

The numbers in brackets indicate the results of computations with long-distance contributions included (but one excludes the region of the two low-lying charmonia $0.33 \leq \hat{s} \leq 0.55$). Results without the long distance contributions correspond to $\kappa = 0$ in (29). The comparison with theoretical predictions of other authors is shown in Table 2.

Table 2. Comparison of branching fractions with other theoretical predictions. Table was originally published in [107].

	CCQM	[78]	[79]	[80]	[81]	[82]	[85]	[111]	[112]
electron	15.9	6.2	2.35	-	7.1	20.0	24.6	18.4	17.4
muon	10.5	4.6	1.9	-	8.3	12.0	18.9	11.6	17.4
tau	13.7	-	-	15.2	15.7	-	11.6	-	-

The dominant error source of the results was identified to be the uncertainty in the hadronic form factors and the error on the branching fractions was estimated to reach 30%. One should remark that the resonant peaks induced by light ϕ particles lead to significant enhancement of the branching fraction ($\approx 15\%$).

In summary, in the presented SM computations within the CCQM, the hadronic transition form factors and radiative leptonic branching fractions of the B_s meson were evaluated. The form factors are in very good agreement with those presented in [110] and the branching fraction numbers for light leptons agree with [111]. For the tau lepton decay mode, where bremsstrahlung dominates, the presented results agree with all other authors. Together, these results from various authors, with [107] included, reflect our understanding of the SM description of the $B_s \rightarrow \ell^+ \ell^- \gamma$ decay process and provide an estimate of the error in theoretical SM predictions, beyond which one can claim NP manifestations.

3.3. Other CCQM Results on B Leptonic Decay

The CCQM was applied also to the leptonic decays $B \rightarrow \ell^- \bar{\nu}_\ell$ [113] and $B_c^- \rightarrow \tau \bar{\nu}$ [114].

The work [113] provides an SM analysis of pure leptonic and semileptonic decays. Most of the results presented there concern the semileptonic processes, which have richer structure and significant hints for the NP. However, the results for purely leptonic branching fractions were presented too:

$$\mathcal{B}(B^- \rightarrow \ell^- \bar{\nu}_\ell) \quad \begin{matrix} \ell & e & \mu & \tau \\ 1.16 \times 10^{-11} & 0.49 \times 10^{-6} & 1.10 \times 10^{-4} \end{matrix} .$$

These numbers were in good agreement with the experimental values for the tau lepton $(1.090 \pm 0.24) \times 10^{-4}$ [23] and the muon $(0.53 \pm 0.22) \times 10^{-9}$ [67], which have since become more precisely measured, and also with the experimental limit for the electron. The agreement with several theoretical predictions by other authors was shown too. Since the leptonic decay constants are crucial in the description of purely leptonic decays and carry all of the necessary non-perturbative information, their values have also been listed for $B_{(s,c)}^{(*)}$ and $D_{(s)}^{(*)}$ mesons (see Table I in [113]).

In [114], possible NP contributions were evaluated for chosen leptonic and semileptonic decays. It was assumed that these contributions affected only the third generation of leptons and all neutrinos were considered as left-handed. New, beyond SM four-fermion operators were introduced in the Hamiltonian (1):

$$Q_{V_i} = (\bar{q}\gamma^\mu P_i b)(\bar{\tau}\gamma_\mu P_L \nu_\tau), \quad Q_{S_i} = (\bar{q}P_i b)(\bar{\tau}P_L \nu_\tau), \quad Q_{T_L} = (\bar{q}\sigma^{\mu\nu} P_L b)(\bar{\tau}\sigma_{\mu\nu} P_L \nu_\tau) \quad (39)$$

with $\sigma_{\mu\nu} = i[\gamma_\mu, \gamma_\nu]$, $P_{L,R} = (1 \mp \gamma_5)/2$ and $i \in \{L, R\}$ (left, right). Most of the text dealt with semileptonic decays where the $R_{D^{(*)}}$ discrepancy is observed (41). The set of observables was extended to

$$R_{\pi(\rho)} = \frac{\mathcal{B}(\bar{B}^0 \rightarrow \pi(\rho)\tau\bar{\nu})}{\mathcal{B}(\bar{B}^0 \rightarrow \pi(\rho)\mu\bar{\nu})}, \quad R_\tau^u = \frac{\tau_{\bar{B}^0}}{\tau_{\bar{B}^-}} \frac{\mathcal{B}(\bar{B}^- \rightarrow \tau\bar{\nu})}{\mathcal{B}(\bar{B}^0 \rightarrow \pi\mu\bar{\nu})}, \quad R_\tau^c = \frac{\tau_{\bar{B}^0}}{\tau_{\bar{B}_c^-}} \frac{\mathcal{B}(\bar{B}_c^- \rightarrow \tau\bar{\nu})}{\mathcal{B}(\bar{B}^0 \rightarrow D\mu\bar{\nu})}, \quad (40)$$

in which, the first is meant to analyze the R anomaly also for the $b \rightarrow u$ transition and the two others concern leptonic decays. The limits on the Wilson coefficients C_{V_i, S_i, T_i} were extracted by assuming that only one of them was dominant at a time (other than the SM ones). Including in the analysis the leptonic observable R_τ^u (together with $R_{D^{(*)}}$), it was found that no C_{S_R, S_L} values were allowed (within 2σ) and, for C_{V_L, V_R, T_L} , allowed regions were identified in the complex plane (Figure 1 in [114]). Further, the leptonic \bar{B}_c^- branching fractions were evaluated within the SM, $\mathcal{B}(\bar{B}_c^- \rightarrow \tau\bar{\nu}) = 2.85 \times 10^{-2}$, $\mathcal{B}(\bar{B}_c^- \rightarrow \mu\bar{\nu}) = 1.18 \times 10^{-4}$ and observables (40) were predicted for the SM and NP scenarios. In the latter case, the corresponding Wilson coefficient C_i was varied (one at a time) in the allowed region of the complex plain and the impact on the observable was determined. For the leptonic R_τ^c variable, the prediction stands.

$$R_{\tau}^c = \begin{array}{cccc} SM & C_{V_L} & C_{V_R} & C_{T_L} \\ 3.03 & 3.945 \pm 0.735 & 3.925 \pm 0.815 & 3.03. \end{array}$$

In summary, one can say that, within the given scenario, the text translated existing experimental information into the constraints on NP Wilson coefficients. Contributions of some of them (C_{S_R, S_L}) were excluded and some (C_{V_L, V_R, T_L}) were constrained.

4. Semileptonic Decays of B Mesons

4.1. Overview

The experimental information on semileptonic B decays is much larger than on pure leptonic decays. The LHCb experiment alone published, in the past 10 years, more than 35 papers on this topic and the number further increases if other experiments (Belle, BaBar, Belle II) are taken into the account. The same is true for theoretical publications, which are large in quantity. With the aim to provide an overview of the CCQM results, we restrained ourselves only to the most significant experimental measurements and theoretical predictions by other authors.

The focus of the community is predominantly driven by the so-called flavor anomalies. They are often defined as ratios of branching fractions, the most prominent of which are

$$R_{K^{(*)}} = \frac{\mathcal{B}(B \rightarrow K^{(*)} \mu^+ \mu^-)}{\mathcal{B}(B \rightarrow K^{(*)} e^+ e^-)}, \quad R_{D^{(*)}} = \frac{\mathcal{B}(B \rightarrow D^{(*)} \tau \nu_{\tau})}{\mathcal{B}(B \rightarrow D^{(*)} \ell \nu_{\ell})}, \quad R_{J/\Psi} = \frac{\mathcal{B}(B \rightarrow J/\Psi \tau \nu_{\tau})}{\mathcal{B}(B \rightarrow J/\Psi \mu \nu_{\mu})}. \quad (41)$$

The first observable is sensitive to the $b \rightarrow s$ quark transition, while the two others are sensitive to $b \rightarrow c$. Other quantities measured in semileptonic decays of the B meson are listed, for example, in Section VII of [115]. In these and other observables, deviations were seen (see, e.g., Tab XVIII of [116] for a comprehensive review), with some of them reaching up to 4σ , which is naturally interpreted as a significant argument in favor of the NP (see e.g., [117]). The most recent LHCb measurements, nevertheless, weaken some of these observations and imply that the discrepancy with the SM may not be so pronounced after all. In [118], the deviation of correlated observables R_D and R_{D^*} from the SM prediction is 1.9σ and the results for R_K and R_{K^*} given in [119] are in agreement with the SM. However, if one also includes older measurements and measurements from different experiments, the situation seems to not yet to be resolved and discrepancy is still close to 3σ [120].

The LHCb detector was specifically designed for B physics and the experiment successfully reaches its purpose by being the most important source of the experimental information on B decays. The measurements of $B \rightarrow K^* \ell^+ \ell^-$ were presented in works [121–129]. Two of them [126,129] studied the lepton-flavor universality by measuring R_{K^*} , but with no significant deviations from the SM. Most of the remaining works were concerned with angular distributions: the coefficients (noted for a p -wave process, such as $F_L, A_{FB}, S_{3,\dots,9}$) in front of angular terms which appear in the decay width formula are combined into so-called optimized observables $P_i^{(\ell)}$ and, here, some significant tensions are seen (e.g., 3σ in P_2 for q^2 between 6 and 8 GeV^2 [128]).

The semileptonic B decays with the K meson in the final state are addressed in [130–132]. The first publication was concerned with the angular distribution and the differential branching fraction, the two others focused more specifically on the lepton flavor universality question, with an observation of a 2.5σ deviation from the SM in R_K . This was, however, as mentioned earlier, undermined by recent measurements [119] where the deviation is no longer the deviation.

The process $B \rightarrow D^* \ell^+ \ell^-$ was analyzed in [118,133–135] and no deviation of R_{D^*} from the SM greater than 2σ was detected. The same was true for the $R_{J/\Psi}$ observable measured in [136]. The decay of the B_s^0 particle to $\phi \mu^+ \mu^-$ was studied in [137–139], where, in the last analysis, a disagreement with the SM prediction was observed in the differential branching fraction for $1 \text{ GeV}^2 \leq q^2 \leq 6 \text{ GeV}^2$, at the level of 3.6σ .

Various other semileptonic B decays were measured at the LHCb, which we do not mention here. An overview of the lepton flavor universality question in B decays at the LHCb was, in 2022, given in [140].

Additional experimental information on the semileptonic B decays comes from BaBar measurements. Studies of the $B \rightarrow D^{(*)} \ell \nu_\ell$ process were presented in [141–147]. In the first three references, the question of the lepton flavor universality was addressed ($\ell = \tau$) and the measurement of R_D and R_{D^*} was performed. The authors claimed a deviation of 2.0σ for R_D , 2.7σ for R_{D^*} and 3.4σ for their combination. The four latter references present the measurement of the $|V_{cb}|$ element of the CKM matrix and the analysis of corresponding transition form factors.

The decays with the $K^{(*)} \ell^+ \ell^-$ final state were addressed in [148–153]. The texts presented the measurements of branching fractions, the $R_{K^{(*)}}$ observable, the isospin and CP asymmetries, the forward–backward angular asymmetry of the lepton pair and the K^* longitudinal polarization (among others). Overall, the results are in an agreement with the SM expectations; the anomaly observed for isospin asymmetries in both K and K^* channels in [150] was not later confirmed in [151].

The BaBar collaboration also published results on semileptonic B decays into light mesons π and ρ [154,155]. Here, the branching fractions and the $|V_{ub}|$ element were determined and, also, transition form factors were discussed.

Further, BaBar published results on semileptonic decays, where hadronic state X_s containing kaons was produced and corresponding branching fractions were measured [156,157]. One can also mention the measurement of charmless semileptonic decays [158,159] and the measurement with the electron in the final state [160], all of which were used to establish the $|V_{ub}|$ value. In [161], the semileptonic decay, with five particles in the final state $D^{(*)} \pi^+ \pi^- \ell \nu_\ell$, was confirmed.

Important contribution to measurements of semileptonic B decays comes from the Belle and Belle II collaborations.

Analyses [162–166] investigated both D and D^* decay channels (with τ and ν_τ). They measured branching fractions and ratios $R_{D^{(*)}}$, where they did not see significant deviations from the SM expectations. The last work focused also on the extraction of parameters for the Caprini–Lellouch–Neubert form factor parameterization.

Specifically, D^* -containing final states were addressed in [167–172]. Additionally, here, the objects of interest were the branching fractions and the R_{D^*} observable; again, no significant deviations from the SM were seen. Works [168,172] presented, in addition, the measurement of the $|V_{cb}|$ matrix element and form factor analysis; in works [170,171], the τ lepton polarization was measured.

The references [173,174] focused on the $D \ell \nu_\ell$ final state. The first work was concerned with the branching fraction and form factors; in both works, $|V_{cb}|$ was measured. The authors of [175] reported on the first observation of $B \rightarrow \bar{D}_1 \ell \nu_\ell$ decay and measured the branching fractions of $B \rightarrow \bar{D}^{(*)} \pi \ell^+ \nu_\ell$ and $B \rightarrow \bar{D}^{(*)} \pi^+ \pi^- \ell^+ \nu_\ell$ processes.

Production of strange mesons in semileptonic B decays was studied in [176,177] for the K meson, in [178–180] for the K^* meson and in [181] for both, i.e., K and K^* . In addition to branching fractions and $R_{K^{(*)}}$ ratios, some of the works also presented measurements of angular and polarization variables and the isospin asymmetry. In general, all measured values agree well with the SM predictions; some tensions for the subset of the optimized angular observables P_i were reported in [179].

Semileptonic decays to light mesons (π , ρ and η) were described in [182–185]; the works were mostly concerned with the branching fractions and the determination of the $|V_{ub}|$ element of the CKM matrix.

The Belle(II) collaboration also published articles on semileptonic B decays to a general hadronic state X containing the s quark, X_s [186,187], the u quark, X_u [188–190] and the c quark, X_c [191,192]. The main objects of interest were branching fractions, CKM elements $|V_{ub}|$ and $|V_{cb}|$ and the first four moments of the lepton mass squared (for X_c). The question

of the lepton flavor universality in semileptonic decays to a general hadronic state X was addressed in [193].

Other results from different experiments could be cited in the domain of semileptonic B decays, yet the measurements of the above-mentioned B factories represent the most important data from both the quantity and quality perspectives.

The large number of theoretical works implies strong selection criteria, which we base on the impact of the work, with some preference for review and pedagogical texts. We have already mentioned thorough reviews [32,33,35,70,116] which cover (also) the semileptonic B decays. Further survey papers include [194], where the SM theory and appropriate observables are presented, a pedagogically written article [195], which focuses on the charged lepton flavour violation and, also, generally-oriented texts [196,197]. One can, in addition mention [198], in which B flavor anomalies were discussed, and also the similarly oriented recent text [199].

Reliable SM predictions are the starting point for assessing various anomalies. Already, decades ago, a quark potential model was used to make predictions for semileptonic B and D decays [200] with an update several years later [201]. Decays to $D^{(*)}$ mesons were addressed in [202]; the analyticity and dispersion relations were used to produce parametrizations of the QCD form factors with small model dependence. The same authors later published QCD two-loop level computations [203], including lepton mass effect, higher resonances and heavy quark symmetry, which further improved the theoretical precision. The heavy quark spin symmetry was used in [204] to derive dispersive constraints on $B \rightarrow D^{(*)}$ form factors and implications for the determination of $|V_{cb}|$. Semileptonic decays to light mesons ρ , ω , K^* and ϕ were discussed in [205] in the framework of light-cone sum rules; the authors claimed 10% precision at zero momentum transfer. The angular analysis of the process $\bar{B} \rightarrow \bar{K} \ell^+ \ell^-$ was presented in [206]. The work was based on the QCD factorization and large recoil symmetry relations and, in addition to angular coefficients, it also gave a prediction of R_K and explored the potential of the introduced observables to reach the NP. Additionally taking into the consideration the excited state K^* , the publication [207] was dedicated to the charm-loop effect. The results were derived using QCD light-cone sum rules and hadronic dispersion relations and the evaluated charm loop effect, which was claimed to reach up to 20%, was represented as a contribution to the C_9 Wilson coefficient. Lattice QCD was used in [208–210] to predict form factors and matrix elements for processes with $D^{(*)}$ mesons. In [211], the lattice form factors were used as input and allowed to determine CKM matrix elements, or, alternatively, constrain the real part of the Wilson coefficients C_9 and C_{10} . The CKM matrix was also the subject of the work [212], where $|V_{cb}|$ was extracted using the OPE, the expansion in powers of the heavy quark mass and constraints derived from the experimental values on the normalized lepton energy moments. A process with a vector meson particle production $B \rightarrow V \ell^+ \ell^-$ was considered in [213], where the authors used light-cone sum rules to predict form factors. The paper [214] has a partial review character: it presented three common form factor parameterizations, summarized the data and the available lattice information (as of 2016) and gave a special emphasis on the unitarity constraints. Then, it presented fits to experimental points and to the lattice numbers from which the results on R_D and $|V_{cb}|$ were extracted. Radiative corrections to the $R_{K^{(*)}}$ observables were of concern to the authors of [215]; their thorough analysis indicated that these observables were indeed well suited to be a probe of NP. Similar questions related to the same observables were addressed in [216]. Still, the same observables were, together with the angular observables P_i , discussed in a pedagogical way in [217], with special emphasis on the hadronic uncertainties. Coming back to D particles and works published within the few years after the first measurements indicating a possible lepton-flavor violation, one can mention [218], where the coefficients of the Boyd–Grinstein–Lebed form factor parameterization were constrained by analyzing the form factor ratios and their uncertainties in the heavy quark limit. With this knowledge, fits to experimental data were performed and R_{D^*} computed. In [219], two different form factor parameterizations were used to predict R_{D^*} and $|V_{cb}|$. The approach used, in

addition to data, inputs from the light-cone sum rules and lattice, as well as the relations between form factors, as given by HQET. To mention more recent theoretical works, one can point to, e.g., [220,221], where QED corrections and non-local matrix elements were discussed for B decays to dilepton and a kaon. The status of the $b \rightarrow c\tau\nu$ anomalies, as of 2022, was summarized in [222], where the models for global fits were based mostly on the HQET and lattice results. The latter were also reviewed in Section 8 of [18].

The number of NP papers progressively grew as the evidence for tensions and anomalies became more and more convincing, with the first hints appearing at the beginning of the new millennium. Often, the NP is theoretically addressed by non-SM operators appearing in the effective Hamiltonian. This was performed in [223], where the approach was applied to the $b \rightarrow s$ process. No strong claims were given there, but it was shown that the evaluated NP effects can reach up to 13% for R_{K^*} . The same effective-operator approach was applied in [224] to $b \rightarrow c$ transition and the impact of the NP on $B \rightarrow D^*\tau\bar{\nu}_\tau$ observables was evaluated. The authors demonstrated that it is significant, i.e., the sensitivity of the process was high enough for the NP to be detected. Effective operators were also used in [225], where, after the NP operator contributions were discussed, two leptoquark models were proposed to explain two out of three possible scenarios which led to the observed R_K value. Leptoquarks—vector and scalar—were also considered in [226,227], respectively; both works claimed that their theory allowed them to simultaneously resolve discrepancies appearing in $b \rightarrow s$ and $b \rightarrow c$ transitions. Still related to leptoquarks, the authors of [228] investigated single-leptoquark extensions of the SM with $1 \text{ TeV} \lesssim m_{LQ} \lesssim 2 \text{ TeV}$, concluding that no such scalar leptoquark can exist, i.e., a vector particle is the only option. The work [229] used scenarios with light right-handed neutrinos appearing in low-scale seesaw models as the NP framework for analyzing the lepton flavor violation. Among other results, the authors proposed observables, i.e., properly chosen branching fraction ratios, which could discriminate between supersymmetric (SUSY) and non-SUSY NP realizations. Further works which analyze the R_K and R_{K^*} anomalies are [230,231]; the former assumed a composite Higgs model, while the latter used a two-Higgs-doublet model. Finally, we mention a set of more generally oriented works [97,98,232–235], which focused mainly on $b \rightarrow s\ell^+\ell^-$ and which aimed to provide model-independent or theoretically clean conclusions. By different approaches, they investigated the space for NP parameters and most of them presented arguments in favor of some NP scenario.

4.2. Semileptonic and Radiative Decays $B_s \rightarrow \phi\ell^+\ell^-$ and $B_s \rightarrow \phi\gamma$ in CCQM

The $B_s \rightarrow \phi\ell^+\ell^-$ and $B_s \rightarrow \phi\gamma$ decays were within the CCQM analyzed in [236]. The analysis was performed in light of the LHCb measurements [137,138], where the second one was recent at that time. The measurement focused on angular observables and the branching fraction distribution reported on a deviation from the SM in the latter, exceeding 3σ for $1 \text{ GeV}^2 \leq q^2 \leq 6 \text{ GeV}^2$. Several years later, two new measurements were performed. The work [237] addressed the angular distribution, where no significant tensions with the SM were observed; [139], however, confirmed the discrepancy from the previous branching fraction measurement. One may put this observation in relation with R_K and R_{K^*} anomalies, which also happen for the $b \rightarrow s$ transition, from where we derived the motivation to study this process in more detail.

In [236], the authors analyzed both the angular coefficients and the differential decay rate distribution. In addition to (5), the necessary model inputs are

$$\Lambda_{B_s} = 2.05 \text{ GeV} \quad \text{and} \quad \Lambda_\phi = 0.88 \text{ GeV} \quad (42)$$

as determined in prior works. The transition is expressed through two matrix elements:

$$M_1^\mu = \langle \phi(p_2, \epsilon) | \bar{s} O^\mu b | B_s(p_1) \rangle, \quad M_2^\mu = \langle \phi(p_2, \epsilon) | \bar{s} [\sigma^{\mu\nu} q_\nu (1 + \gamma^5)] b | B_s(p_1) \rangle, \quad (43)$$

where $O^\mu = \gamma^\mu(1 - \gamma^5)$ and p_i are momenta, with $q = p_1 - p_2$ and $P = p_1 + p_2$. The variables satisfy $p_1^2 = m_{B_s}^2 \equiv m_1^2$, $p_2^2 = m_\phi^2 \equiv m_2^2$ and $\epsilon_2^\dagger \cdot p_2 = 0$. In total, seven invariant

form factors, defined as coefficient functions in front of the Lorentz structures, are necessary to parameterize them:

$$M_1^\mu = \frac{\epsilon_\nu^\dagger}{m_1 + m_2} \left[-g^{\mu\nu} P \cdot q A_0(q^2) + P^\mu P^\nu A_+(q^2) + q^\mu P^\nu A_-(q^2) + i\epsilon^{\mu\nu\alpha\beta} P_\alpha q_\beta V(q^2) \right], \tag{44}$$

$$M_2^\mu = \epsilon_\nu^\dagger \left[-\left(g^{\mu\nu} - \frac{q^\mu q^\nu}{q^2} \right) P \cdot q a_0(q^2) + \left(P^\mu P^\nu - q^\mu P^\nu \frac{P \cdot q}{q^2} \right) a_+(q^2) + i\epsilon^{\mu\nu\alpha\beta} P_\alpha q_\beta g(q^2) \right]. \tag{45}$$

The same amplitudes can be expressed in the CCQM:

$$M_{1,2}^\mu = N_c g_{B_s} g_\phi \int \frac{d^4 k}{i(2\pi)^4} \tilde{\Phi}_{B_s}(-[k + w_{13} p_1]^2) \tilde{\Phi}_\phi(-[k + w_{23} p_2]^2) \times T_{1,2}, \tag{46}$$

$$T_1 = \text{tr}[O^\mu S_b(k_1 + p_1) \gamma^5 S_s(k) \not{\epsilon}_2^\dagger S_s(k + p_2)], \tag{47}$$

$$T_2 = \text{tr}[\sigma^{\mu\nu} q_\nu (1 + \gamma^5) S_b(k_1 + p_1) \gamma^5 S_s(k) \not{\epsilon}_2^\dagger S_s(k + p_2)], \tag{48}$$

with S_i being quark propagators and N_c being the number of colors. The origins of various terms in (46)–(48) are schematically represented in Figure 7. Once the model expression (46) is evaluated to the level of invariant Lorentz structures, it can be compared to (44) and (45) and the form factor expressions can be read out. Their behavior is shown in Figure 8; they determine the necessary model input and complete the model-dependent part of the calculation.

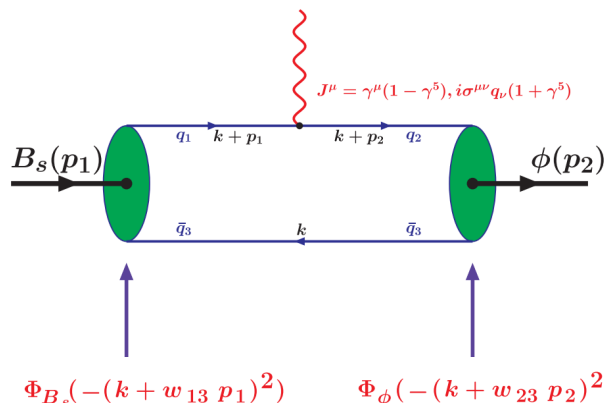


Figure 7. $B_s \rightarrow \phi$ transition in the CCQM. Figure was originally published in [236].

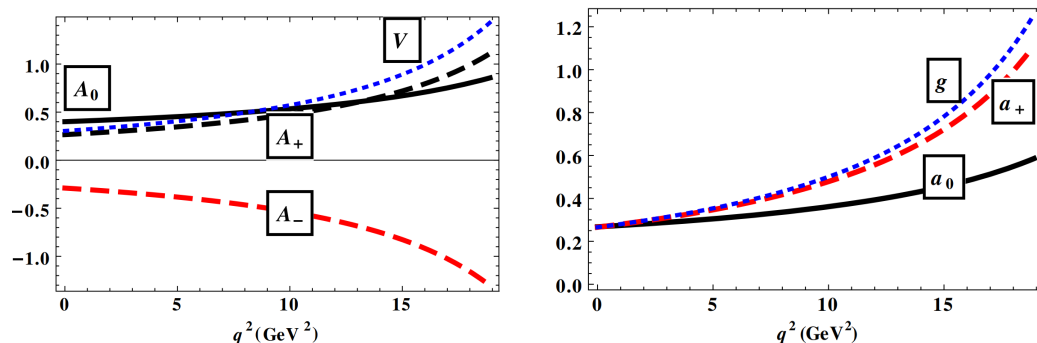


Figure 8. Vector and tensor form factors for the $B_s \rightarrow \phi$ transition, as predicted by the CCQM. Figures were originally published in [236].

Let us also briefly review the remaining steps to reach observable quantities. The set of the SM four-fermion operators is written as

$$\begin{aligned}
 \mathcal{O}_1 &= (\bar{s}_{a_1} \gamma^\mu P_L c_{a_2})(\bar{c}_{a_2} \gamma_\mu P_L b_{a_1}), & \mathcal{O}_2 &= (\bar{s} \gamma^\mu P_L c)(\bar{c} \gamma_\mu P_L b), \\
 \mathcal{O}_3 &= (\bar{s} \gamma^\mu P_L b) \sum_q (\bar{q} \gamma_\mu P_L q), & \mathcal{O}_4 &= (\bar{s}_{a_1} \gamma^\mu P_L b_{a_2}) \sum_q (\bar{q}_{a_2} \gamma_\mu P_L q_{a_1}), \\
 \mathcal{O}_5 &= (\bar{s} \gamma^\mu P_L b) \sum_q (\bar{q} \gamma_\mu P_R q), & \mathcal{O}_6 &= (\bar{s}_{a_1} \gamma^\mu P_L b_{a_2}) \sum_q (\bar{q}_{a_2} \gamma_\mu P_R q_{a_1}), \\
 \mathcal{O}_7 &= \frac{e}{8\pi^2} \tilde{m}_b (\bar{s} \sigma^{\mu\nu} P_R b) F_{\mu\nu}, & \mathcal{O}_8 &= \frac{g_s}{8\pi^2} \tilde{m}_b (\bar{s}_{a_1} \sigma^{\mu\nu} P_R \mathbf{T}_{a_1 a_2} b_{a_2}) \mathbf{G}_{\mu\nu}, \\
 \mathcal{O}_9 &= \frac{e^2}{8\pi^2} (\bar{s} \gamma^\mu P_L b)(\bar{\ell} \gamma_\mu \ell), & \mathcal{O}_{10} &= \frac{e^2}{8\pi^2} (\bar{s} \gamma^\mu P_L b)(\bar{\ell} \gamma_\mu \gamma_5 \ell),
 \end{aligned}
 \tag{49}$$

where $P_{L,R} = (1 \mp \gamma^5)$, a_i are color indices (implicit for color singlet currents), $\mathbf{T}_{a_1 a_2}$ are generators of the $SU(3)$ color group, $\mathbf{G}_{\mu\nu}$ is the gluonic field strength and g_s is the QCD coupling (note: other symbols have meaning as defined before). Operators \mathcal{O}_1 and \mathcal{O}_2 are referred to as current–current operators, $\mathcal{O}_3 - \mathcal{O}_6$ are QCD penguin operators, $\mathcal{O}_{7,8}$ are so-called magnetic penguin operators and \mathcal{O}_8 and \mathcal{O}_9 operators correspond to semileptonic electroweak penguin diagrams. The transition amplitude takes the form

$$\begin{aligned}
 \mathcal{M} &= \frac{G_F}{2\sqrt{2}} \frac{\alpha |V_{tb} V_{ts}^*|}{\pi} \left[C_9^{\text{eff}} \langle \phi | \bar{s} \gamma^\mu P_L b | B_s \rangle (\bar{\ell} \gamma_\mu \ell) - \frac{2\tilde{m}_b}{q^2} C_7^{\text{eff}} \langle \phi | \bar{s} i \sigma^{\mu\nu} q_\nu P_R b | B_s \rangle (\bar{\ell} \gamma_\mu \ell) \right. \\
 &\quad \left. + C_{10} \langle \phi | \bar{s} \gamma^\mu P_L b | B_s \rangle (\bar{\ell} \gamma_\mu \gamma_5 \ell) \right].
 \end{aligned}
 \tag{50}$$

The Wilson coefficients $C_1 - C_6$ are absorbed into the effective coefficients C_7^{eff} and C_9^{eff} ; $C_7^{\text{eff}} = C_7 - C_5/3 - C_6$ and C_9^{eff} is defined by (28) and (29), where, again, the \bar{c} resonances appear in the Breit–Wigner form and one drops them by setting $\kappa = 0$. The renormalization scale is set to $\mu = \tilde{m}_{b, \text{pole}}$. Numerical values of Wilson coefficients were taken from [109], as we described already in Section 3.2. Furthermore, the QCD quark masses are the same as in the leptonic-decay section. In addition to the charm loop contribution, one takes into the consideration the two loop effects, as computed in [238,239]. These modify the effective coefficients

$$C_7^{\text{eff}} \rightarrow C_7^{\text{eff}} - \frac{\alpha_s}{4\pi} (C_1 F_1^{(7)} + C_2 F_2^{(7)}), \quad C_9^{\text{eff}} \rightarrow C_9^{\text{eff}} - \frac{\alpha_s}{4\pi} (C_1 F_1^{(9)} + C_2 F_2^{(9)}),
 \tag{51}$$

where the functions $F_{1,2}^{(7,9)}$ were made publicly available by the authors of [239] as *Wolfram Mathematica* code.

The differential decay rate is then expressed as

$$\frac{d\Gamma(B_s \rightarrow \phi \ell \ell)}{dq^2} = \frac{G_F^2}{(2\pi)^3} \left(\frac{\alpha |V_{tb} V_{ts}^*|}{2\pi} \right)^2 \frac{|\mathbf{p}_2| q^2 \beta_\ell}{12m_1^2} \mathcal{H}_{\text{tot}},
 \tag{52}$$

$$\mathcal{H}_{\text{tot}} = \frac{1}{2} \left(\mathcal{H}_U^{11} + \mathcal{H}_U^{22} + \mathcal{H}_L^{11} + \mathcal{H}_L^{22} \right) + \delta_{\ell\ell} \left(\frac{\mathcal{H}_U^{11}}{2} - \mathcal{H}_U^{22} + \frac{\mathcal{H}_L^{11}}{2} - \mathcal{H}_L^{22} + \frac{3\mathcal{H}_S^{22}}{2} \right),
 \tag{53}$$

where $\delta_{\ell\ell} = 2m_\ell^2/q^2$, $\beta_\ell = \sqrt{1 - 2\delta_{\ell\ell}}$ and $|\mathbf{p}_2| = \sqrt{\lambda^{\text{Källén}}(m_1^2, m_2^2, q^2)}/(2m_1)$ is the momentum of the ϕ meson in the B_s rest frame. The objects \mathcal{H}_X^{ii} represent bilinear combinations of the helicity amplitudes:

$$\mathcal{H}_U^{ii} = |H_{++}^i|^2 + |H_{--}^i|^2, \quad \mathcal{H}_L^{ii} = |H_{00}^i|^2, \quad \mathcal{H}_S^{ii} = |H_{i0}^i|^2,
 \tag{54}$$

which are related to the invariant form factors through intermediate functions $A_{+,-,0}^i$ and V^i :

$$H_{t0}^i = \frac{1}{m_1 + m_2} \frac{m_1 |\mathbf{p}_2|}{m_2 \sqrt{q^2}} \{Pq(-A_0^i + A_+^i) + q^2 A_-^i\}, \tag{55}$$

$$H_{\pm\pm}^i = \frac{1}{m_1 + m_2} (-Pq A_0^i \pm 2m_1 |\mathbf{p}_2| V^i), \tag{56}$$

$$H_{00}^i = \frac{1}{m_1 + m_2} \frac{1}{2m_2 \sqrt{q^2}} \{-Pq(m_1^2 - m_2^2 - q^2) A_0^i + 4m_1^2 |\mathbf{p}_2|^2 A_+^i\}, \tag{57}$$

with

$$V^1 = C_9^{\text{eff}} V + C_7^{\text{eff}} \chi g, \tag{58}$$

$$A_+^1 = C_9^{\text{eff}} A_+ + C_7^{\text{eff}} \chi a_+, \tag{59}$$

$$A_-^1 = C_9^{\text{eff}} A_- + C_7^{\text{eff}} \chi Pq(a_0 - a_+)/q^2, \tag{60}$$

$$A_0^2 = C_{10} A_0, \tag{61}$$

where $\chi = 2\tilde{m}_b(m_1 + m_2)/q^2$.

The full description of the $B_s \rightarrow \phi \ell \ell$ decay requires, other than the q^2 , three additional angles; see, for example, Equation (2.1) in [240], where a completely analogous formula is written for the fully differential decay rate of $B_d \rightarrow K^* \mu^+ \mu^-$. The advantage of the helicity formalism is that the angular observables, i.e., the coefficients in front of various angular terms, have simple expressions. For the longitudinal polarization fraction F_L and the forward-backward asymmetry A_{FB} , they are

$$F_L = \frac{1}{2} \beta_\ell^2 \frac{\mathcal{H}_L^{11} + \mathcal{H}_L^{22}}{\mathcal{H}_{\text{tot}}}, \quad A_{\text{FB}} = -\frac{3}{4} \beta_\ell \frac{\mathcal{H}_P^{12}}{\mathcal{H}_{\text{tot}}}, \tag{62}$$

$$\text{where } \mathcal{H}_P^{12} = \text{Re} [H_{++}^1 (H_{++}^2)^\dagger] - \text{Re} [H_{--}^1 (H_{--}^2)^\dagger]. \tag{63}$$

The CCQM-predicted behavior of the branching fraction and of the two angular observables F_L and A_{FB} is, as a function of q^2 , are shown in Figure 9.

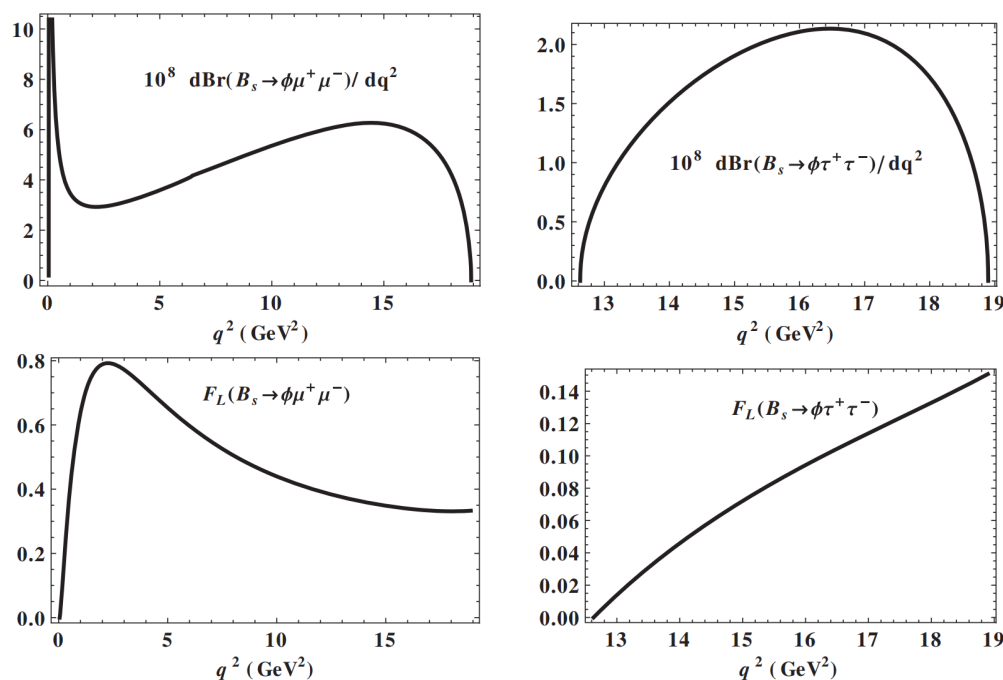


Figure 9. Cont.

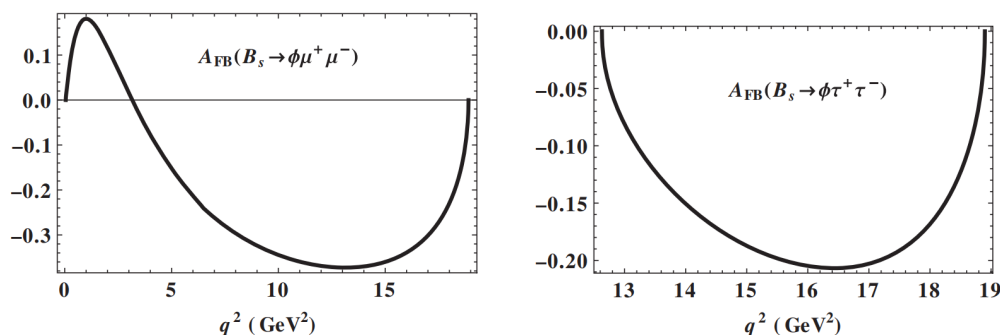


Figure 9. Branching fraction, F_L and A_{FB} as functions of q^2 for μ and τ in the final state. Figures were originally published in [236].

The q^2 -averaged numbers were computed for F_L , A_{FB} , additional angular observables S_3 , S_4 and also for optimized observables P_1 and P'_4 , from which we derive $P_1 = 2S_3/(1 - F_L)$, $P'_4 = S_4/\sqrt{F_L(1 - F_L)}$. The results are presented in Table 3.

Table 3. Total branching fractions and averaged angular observables of selected decay channels for the whole kinematic region. Table contains data originally published in [236].

	$B_s \rightarrow \phi\mu^+\mu^-$	$B_s \rightarrow \phi\tau^+\tau^-$	$B_s \rightarrow \phi\nu\bar{\nu}$
\mathcal{B}_{tot}	$(9.11 \pm 1.82) \times 10^{-7}$	$(1.03 \pm 0.20) \times 10^{-7}$	$(0.84 \pm 0.16) \times 10^{-5}$
$\langle A_{FB} \rangle$	-0.24 ± 0.05	-0.18 ± 0.04	.
$\langle F_L \rangle$	0.45 ± 0.09	0.09 ± 0.02	.
$\langle P_1 \rangle$	-0.52 ± 0.1	-0.76 ± 0.15	.
$\langle P'_4 \rangle$	1.05 ± 0.21	1.33 ± 0.27	.
$\langle S_3 \rangle$	-0.14 ± 0.03	-0.067 ± 0.013	.
$\langle S_4 \rangle$	0.26 ± 0.05	0.083 ± 0.017	.

The table also shows the branching fraction for $B_s \rightarrow \phi\nu\bar{\nu}$; the corresponding decay formula is indicated in Equations (34)–(36) of [236]. The text [236] also contains predictions for the radiative decay to $\phi\gamma$ and non-leptonic decay to $\phi J/\Psi$ (Formulas (37) and (38) therein):

$$\mathcal{B}(B_s \rightarrow \phi\gamma) = (2.39 \pm 0.48) \times 10^{-5}, \quad \mathcal{B}(B_s \rightarrow \phi J/\Psi) = (1.6 \pm 0.3) \times 10^{-3}. \quad (64)$$

The results can be compared to actual experimental numbers [23]:

$$\mathcal{B}(B_s \rightarrow \phi\mu^+\mu^-) = (8.4 \pm 0.4) \times 10^{-7}, \quad \mathcal{B}(B_s \rightarrow \phi\nu\bar{\nu}) < 540 \times 10^{-5}, \quad (65)$$

$$\mathcal{B}(B_s \rightarrow \phi\gamma) = (3.4 \pm 0.4) \times 10^{-5}, \quad \mathcal{B}(B_s \rightarrow \phi J/\Psi) = (1.04 \pm 0.04) \times 10^{-3}. \quad (66)$$

The branching fraction to $\phi\mu^+\mu^-$ is in good agreement with the SM; in fact, the experimental numbers measured after publication moved closer to the published CCQM value. The same is also true for the two non-leptonic decay channels, yet a discrepancy on the order of 2σ remains.

Coming back to the semileptonic decays, detailed interval values were presented in Table VI in [236] for $B_s \rightarrow \phi\mu^+\mu^-$. They mimic the way the experimental measurements are performed and they are of interest because the largest discrepancy observed by [138,139] was the branching fraction on the q^2 interval of 1–6 GeV². (In [139,237], the lower interval limit was 1.1 GeV²; this effect was considered as negligible because the measured quantities are intensive (not additive), e.g., the branching fraction measurement is q^2 -averaged (the number of entries in the interval is divided by the integral length.)) Moreover, the table presents the effect of the two-loop contributions by giving the numbers with and without them. We do not reproduce here all of them but focus only on the interval $1 \text{ GeV}^2 \leq q^2 \leq 6 \text{ GeV}^2$ and observables measured on this interval (see Table 4).

Table 4. Branching fraction and selected angular observables on the interval $1 \text{ GeV}^2 \leq q^2 \leq 6 \text{ GeV}^2$ for $B_s \rightarrow \phi \mu^+ \mu^-$. Indicated are the CCQM predictions with and without 2-loop contributions and the experimental value. Table contains a subset of data originally published in [236].

	CCQM, 2-Loop	CCQM, 1-Loop	Experiment [138,139,237]
$10^7 \mathcal{B}_{\text{tot.}}$	1.56 ± 0.31	1.64 ± 0.33	1.41 ± 0.11 (1.29)
F_L	0.69 ± 0.14	0.71 ± 0.14	0.715 ± 0.036 (0.63)
S_3	-0.034 ± 0.007	-0.039 ± 0.008	-0.083 ± 0.047 (-0.02)
S_4	0.17 ± 0.03	0.19 ± 0.04	0.155 ± 0.058 (0.19)
S_7	0.0065 ± 0.0013	0	0.020 ± 0.059 (-0.03)

In the table, older measurements are also indicated in brackets and one sees that, for all indicated observables except S_3 , the new measurement brings the experimental value closer to the theoretical one. The large error in the S_3 measurement implies that both CCQM predictions (one-loop and two-loop) do not exceed 1σ deviation by much. Considering the two-loop results, one observes that no significant deviations from the experiment are observed; especially, in the branching fraction case, they bring the value closer to the measurement (w.r.t. one-loop calculations).

In summary, we can conclude that the interesting decay channel $B_s \rightarrow \phi \ell^+ \ell^-$ was addressed in the framework of the CCQM. Already at the time of the publication, the comparison with the LHCb numbers did not allow us to claim NP presence: the major discrepancy in the branching fraction on the $1\text{--}6 \text{ GeV}^2$ interval was reduced significantly by the CCQM prediction. This was also true for other discrepancies (F_L, S_4) seen on other intervals. The new data further decreased the branching fraction discrepancy and, with results of the CCQM, one can no longer talk about a discrepancy.

4.3. Other CCQM Results on Semileptonic B Decays

Quite a few papers were dedicated to the study of semileptonic B decays in the framework of the CCQM. We did not include in this overview older texts where an earlier version of the model was used [54,241–248].

The first text we mention [43] was already cited several times here. It is a generally oriented text, focusing mostly on the model itself and presenting its various aspects, including, for the first time, the infrared confinement of quarks. A global fit on basic experimental quantities, such as weak leptonic decay constants, was performed in order to determine universal and hadron-specific model parameters. These parameters were used in the same text to predict weak leptonic decay constants (including for B mesons) and Dalitz decays of several light mesons. The results were encouraging: most of the predictions were in quite good agreement with measured data.

The paper [249] is dedicated to various $B_{(s)}$ decays with, however, emphasis on the nonleptonic processes. In the first part of the text, the global fits were refined and the model parameters were updated. Then, the semileptonic decays were addressed, but only in the context of the universal transition form factors to several final-state mesons (pseudoscalar and vector). The results on form factors were given in the form of plots and the comparison with seven other authors based on the value at $q^2 = 0$ was shown in Table III.

Somewhat similar treatment of the semileptonic decays was given in [250]. Here again, the emphasis was on exotic and nonleptonic decays. The semileptonic decays were addressed in the context of transition form factors, similarly to the previous text.

The publication [251] focused on the semileptonic decays of $B_{(s)}$ to scalar mesons with light masses (below 1 GeV) in the context of the $B \rightarrow K^*(\rightarrow K\pi)\mu^+\mu^-$ decay. The CCQM form factors F_{\pm} and F_T were predicted for the range $0.8 \text{ GeV} \leq \Lambda_S \leq 1.5 \text{ GeV}$ of scalar vector model parameters for the $b \rightarrow u$, $b \rightarrow d$ and $b \rightarrow s$ transitions. The predictions were approximated for $\Lambda_S = 0.8 \text{ GeV}$ and $\Lambda_S = 1.5 \text{ GeV}$ by a simplified parameterization which depended on three numbers. They are given in Table II of the text, so as to make the results available to other authors. Branching fractions ($\Lambda_S = 1.5 \text{ GeV}$) for various

semileptonic decays $B_{(s)} \rightarrow S\ell\ell$, $B_{(s)} \rightarrow S\ell\nu_\ell$ are shown in Table IV of their work. The text then briefly discussed the role of the scalar $K_0^*(800)$ particle in the cascade decay of the B meson, pointing out the fact that the narrow-width approximation is not appropriate, and estimating the S-wave pollution in the $B \rightarrow K^*\ell^+\ell^-$ decay to 6%.

The leptonic and semileptonic processes $B \rightarrow \ell\bar{\nu}$ and $B \rightarrow D^{(*)}\ell^-\bar{\nu}$ were investigated in [113] to address the question of the lepton flavor universality. We have already commented before on the leptonic results; they were entirely linked to the weak decay constant which is, for various B and D mesons, computed in Table I. Semileptonic decays are more demanding and the usual steps are taken: the SM CCQM form factors were determined (additionally, the simplified parameterization was provided) and were used in a helicity formulation to predict the full four-dimensional differential distribution for the decay rate and various q^2 -dependent distributions for angular and polarization observables. By integration, one geobtains total branching fractions, shown in Tables III and IV of their publication, and their ratios R_D and R_{D^*} (in Table V). The results are favorable to the NP presence: the deviation in $R_{D^{(*)}}$ is not smaller than seen by other authors at that time.

An analogous process with the K^* meson in the final state was the subject of the analysis in [49]. The text followed the same logic as the previous one: the model was used to predict form factors and then the helicity formalism was employed to derive various differential distributions. Further to the branching fraction, the emphasis was on the angular coefficients A_{FB} , F_L and $P_i^{(\prime)}$, $i = 1 - 5, 8$ depicted in Figures 7–11 of their publication. The numbers were given for integrated or averaged variables over the whole kinematical range (Tables 5 and 6) and also for various intervals (i.e., bins, Tables 7 and 8). The predicted branching fraction exceeded the measured values,; reliable conclusions as to the angular observables require more precise experimental data.

The article [252] analyzed possible NP scenarios for $\bar{B}^0 \rightarrow D^{(*)}\tau^-\bar{\nu}_\tau$ and, in this way, differed from the previous ones. The analysis relied on the usual effective Hamiltonian approach, where beyond SM four-fermion operators are introduced with the definition analogous to (39), where $q \rightarrow c$. It was assumed that the NP affects only the leptons of the third generation and the effect of each NP operator was studied separately, with no other NP operator interfering. The form factors were computed in the CCQM framework, from where observables quantities were obtained. By the fit to the $R_{D^{(*)}}$ ratios, allowed regions of the complex plane for the Wilson coefficients $V_{L,R}$, S_L and T_L were identified (Figure 2 of their text). No room was found for the S_R coefficient to explain the observed ratio and, thus, the corresponding operator was removed from further considerations. Next, full four-fold differential distribution was derived and various q^2 -differential distributions analyzed: the NP Wilson coefficient was perturbed on the 2σ level from the central value and the effect on a given distribution was depicted as a gray band around the central line (Figures 4–9). Depending on what distributions future measurements will provide, the presented results can serve to identify which NP Wilson coefficients play a role.

The same process was also considered in [253], once again in the NP scenario based on the SM-extended effective Hamiltonian. Here, the main topic were the longitudinal, transverse and normal polarization components of the tau lepton and their high sensitivity to NP effects. Using a model-independent approach and the experimental data, constraints for various NP scenarios were derived and their effect on the polarization observables was investigated. To obtain numerical results, the CCQM form factors were used. The acquired knowledge about the dependence of polarization observables on the NP Wilson coefficients may be useful in future data analysis as a guiding rule to differentiate between various NP scenarios.

Very similar analysis was performed in [114] but for different decays. The text focused on the processes with light mesons in the final state $\bar{B}^0 \rightarrow \pi\tau\bar{\nu}$, $\bar{B}^0 \rightarrow \rho\tau\bar{\nu}$ and on the leptonic decay $B_c \rightarrow \tau\bar{\nu}$, assuming an SM-extended set of four-fermion operators. They used the observables (40), defined already in the leptonic section, and the CCQM-predicted form factors to constrain the introduced NP Wilson coefficients. The effect of their variation on (40) and on selected angular observables was analyzed.

Yet another publication which follows the same logic was [254], focusing this time on the decays $B_c \rightarrow J/\psi \tau \nu$ and $B_c \rightarrow \eta_c \tau \nu$. The observables used to constrain the NP Wilson coefficients were $R_D, R_{D^*}, R_{J/\psi}$ and $\mathcal{B}(B_c \rightarrow \tau \nu)$. With form factors derived in the CCQM by assuming the NP, the impact of variation in these coefficients on other branching fraction ratios and angular observables was evaluated. The work provided a detailed comparison of the CCQM form factors with form factors from different approaches.

The work [255] was interested in $B_c \rightarrow J/\psi \bar{\ell} \nu \ell$ and in the hadronic decay $B_c \rightarrow J/\psi \pi(K)$. This time, an SM calculation was presented; the agreement with the SM was assessed through comparison of measured and predicted values for $R_{J/\psi}$ and two additional observables:

$$R_{\pi^+/\mu^+ \nu} = \mathcal{B}(B_c^+ \rightarrow J/\psi \pi^+)/\mathcal{B}(B_c^+ \rightarrow J/\psi \mu^+ \nu_\mu), \quad (67)$$

$$R_{K^+/\pi^+} = \mathcal{B}(B_c^+ \rightarrow J/\psi K^+)/\mathcal{B}(B_c^+ \rightarrow J/\psi \pi^+). \quad (68)$$

The form factors were evaluated in the CCQM framework and results for a set of semileptonic decays with J/ψ or η in the final state were presented (Table 2 therein). The conclusion regarding the ratios was that an agreement with the SM was reached for $R_{\pi^+/\mu^+ \nu}$ and R_{K^+/π^+} , but the theoretical prediction for $R_{J/\psi}$ was too low with respect to data.

The semileptonic decays $B \rightarrow K^* \mu \mu, B_s^0 \rightarrow \phi \mu \mu$ and the leptonic decay $B_s \rightarrow \mu^+ \mu^-$ were addressed in [256]. This brief text summarized selected results and referred to previous papers.

The next paper dedicated to semileptonic decays was [257]. It analyzed the $B \rightarrow K^{(*)} \nu \bar{\nu}$ process, where the current experimental limits on the branching fraction are expected to not be very far from the central value predicted by theory (i.e., the central value may be measured in the future). The CCQM was used to predict hadronic form factors, which were then used in the helicity framework to predict branching fractions. The results agree with the experimental limits and also with most other authors. Approximately, the value of limits were only four times higher than the central values predicted by theory.

5. Nonleptonic Decays of B Mesons

5.1. Overview

The number of experimental measurements concerning nonleptonic (or hadronic) B decays is even larger than for semileptonic ones. Again, we briefly review the LHCb results and the results of the two B factories, BaBar and Belle(II), as the most representative. Nevertheless, we do not provide an exhaustive list but mention only works with larger impact.

The question of NP is, for hadronic decays, less pronounced than for the semileptonic ones, since these are theoretically less clean. However, the NP is often mentioned and treated together with some of the usual topics such as (exotic) multi-quark states, observations of new decay channels, CP-related measurements, fragmentation fractions or branching fraction determination. In what follows, we try to observe this classification.

The LHCb published several papers reporting the observation of a specific decay channel, some being observed for the first time. This comprises the first observations of $B_s^0 \rightarrow J/\psi f_0(980)$ [258], $B_c^+ \rightarrow J/\psi D_s^+$ and $B_c^+ \rightarrow J/\psi D_s^{*+}$ [259], $B_c^+ \rightarrow B_s^0 \pi^+$ [260], $B^+ \rightarrow D_s^+ D_s^- K^+$ [261], $B_s^0 \rightarrow D^{*+} D^{*-}$ [262], $B^+ \rightarrow J/\psi \eta' K^+$ [263] or $B_s^0 \rightarrow \chi_{c1}(3872) \pi^+ \pi^-$ [264]. For most of these observations, some quantitative numbers are given—usually, branching fraction ratios to a different decay mode (normalization channel).

A special interest is given to the observation of "resonant structures", i.e., observation of possible exotic multi-quark states, which are sometimes seen in invariant mass distributions of particles originating from the B disintegration. An important contribution to the exotic physics was performed in 2013 when the LHCb measured, in the B decay channel, the quantum numbers of the $X(3872)$ resonance [265], previously discovered by Belle. Contemporary texts [266–268] analyze the $\bar{B}_s^0 \rightarrow J/\psi \pi^+ \pi^-$ and $\bar{B}^0 \rightarrow J/\psi \pi^+ \pi^-$ spectra and identify various resonant structures; here, only the usual SM resonances are seen. The

possible tetraquark character of the $f_0(980)$ invoked in the last text has been rejected as inconsistent with data. The situation became different in [269], where four resonant structures, possibly tetraquarks, were observed and their quantum numbers were determined. The work [270] reported on two exotic particles having $c\bar{c}u\bar{s}$ quark content, determined with high significance, and also confirmed four previously reported states. The authors of [271] performed an amplitude analysis of the $B^- \rightarrow J/\psi \Lambda \bar{p}$ process, where the $J/\psi \Lambda$ mass spectrum contains a narrow resonance, possibly indicating a strange pentaquark; its quantum numbers were measured. A resonant structure, referred to as $X(3960)$, was also observed in the $B^+ \rightarrow D_s^+ D_s^- K^+$ decay mode, close to the $D_s^+ D_s^-$ production threshold [272]. It was established to be consistent with a four-quark state $c\bar{c}s\bar{s}$, having quantum numbers $J^{PC} = 0^{++}$. The text [273] analyzed the spectrum of $B^+ \rightarrow D^+ D^- K^+$ and advanced a hypothesis of new charm–strange resonances. Another recent text, [274], also saw a new resonance of mass 4337 MeV in the $J/\psi p$ ($J/\psi \bar{p}$) spectrum of the $B_s^0 \rightarrow J/\psi p \bar{p}$ decay. A very recent analysis [275] was concerned with decays of the B mesons to $J/\psi \phi K_S^0$ and presented evidence for the $T_{\psi s 1}^0$ state in the $J/\psi K_S^0$ -invariant spectrum (presumably a tetraquark).

In addition to direct investigations of the invariant mass spectrum, many LHCb publications rely, in order to identify resonant components, on the Dalitz plot and amplitude analysis, where further resonances are identified—see [276–282]. The hadronic B decays are also often studied in the context of the CP analysis and weak parameter determination [283–296]. Various topics were addressed in these works: observation of the CP violation in a specific decay, measurement of the CP-violating phase, $B_{(s)}^0 - \bar{B}_{(s)}^0$ oscillations and determination of the CKM angles. The B decay measurements were also used to determine basic particle quantities, such as production cross-sections, branching ratios or fragmentation fractions [297–306].

The publications of the BaBar experiment fall into similar categories. We choose to mention, in more detail, the CP-related results which had, in the domain of nonleptonic B decays, the most significant impact. Namely, the violation of the CP symmetry was, before the BaBar measurement [307], only observed for kaons. The measurement was performed for several decay modes of the B^0 particle; for each decay, the CP asymmetry A_{CP} was measured. The latter was defined in terms of a decay-time distribution $f_{\pm}(\Delta t)$ for B and \bar{B} , decaying into the common final state. The results were derived for the $\sin(2\beta)$ quantity, where β is an angle of the unitarity triangle, constructed from the CKM matrix elements, and its deviation from zero measures the CP violation. The significance of the measurement reached 4σ level. The CP-violation topic was then discussed in further publications for the neutral [308–316] and also charged B meson [317–320]. Both indirect (i.e., involving particle–antiparticle oscillations) and direct CP violations were seen with relevant significance. Several texts present measurements where the branching fraction and the CP asymmetries were addressed at the same time [321–326]. In addition to the direct CP violation measurements, the closely related measurements of the CKM angles α and γ were presented in [327–330].

The BaBar collaboration also investigated, in a variety of publications [331–342], the usual quantities which characterize decays, i.e., branching fractions and angular observables. The related topics of resonances and exotic states were subjected to numerous analyses. The resonances were investigated by invariant mass spectra or the Dalitz plot method, as presented in [343–345]. Concerning exotic states, most of the BaBar results were related to the $X(3872)$ particle [346–354] and present related searches, observations and measurements in various decay modes. The state $Y(3940)$, first discovered at Belle, was also observed (as a product of a B decay) and its mass and width were determined.

The Belle experiment was very successful in the search for various exotic states, tetraquarks and pentaquarks. Not all were related to hadronic decays of the B meson, but the most-cited result [355] was. It presented the discovery of the $X(3872)$ particle seen in the $\pi^+ \pi^- J/\psi$ spectrum of $B^{\pm} \rightarrow K^{\pm} \pi^+ \pi^- J/\psi$. Other achievements were the detection of tetraquark candidates $Z(4430)$ [356] and $Y(3940)$ [357], both among the decay products

of B. In addition to these, further publications on this topic were issued [358–367], all related to nonleptonic B decays. The physics program, regarding the CP violation, and weak physics in general, is also very present at Belle. One collaboration published the B^0 CP-violation paper [368] only a short time after BaBar did. Notably, it drew a lot of attention as an independent measurement of the $\sin(2\beta)$ parameter. The measurement was updated later in [369]; direct CP violation was reported in [370,371]. Many additional papers were published by Belle, where various CP parameters (CKM angles) and weak physics-related processes were studied [372–392].

Naturally, the research at Belle is also devoted to branching fraction measurements of different B decay modes [393–402], observation and analysis of new decay channels [403–411], polarization studies [412,413] and photon energy spectra analysis in radiative events [414,415].

The large amount of data on hadronic B decays motivates theorists to describe observations and prove our understanding of the underlying physics to be correct. The exotic multi-quark states have a specific character from the perspective of B physics: as a matter of fact, many of them originate from nonleptonic B decays, yet these decays, seen as exotic production processes, are not addressed very frequently. They often have a larger number of hadrons in the final state (three or more) and, thus, large phase space and technically complicated description. The exotic particles are usually treated in the scenario where they represent the initial state (for the CCQM model, see [48]) and, thus, are not in the scope of this text (i.e., they are not B mesons). The emphasis of the theoretical overview is, therefore, on the remaining topics: branching fractions and weak-interaction physics.

The theoretical grounds to describe (not only) hadronic B decays were laid decades ago. The CP violation in the SM stems from flavor mixing through the CKM matrix which has an irreducible complex phase, as formulated in the pioneering works [416,417]. This rapidly led to the first theoretical predictions. In [418], the expectation of a small but measurable CP non-invariance in B meson decays was expressed. The authors of [419] argued, studying the on-shell transitions in heavy meson cascade decays, that the effect may not be so small after all and proposed methods to detect the CP violation in the B sector. The latter topic was also discussed in [420], where mainly the non-leptonic decay modes were addressed.

In parallel, the issues related to the asymptotic behavior and quark interactions were considered. The review [421] addressed the question of the power behavior of amplitudes and its relation to mesonic wave functions and quantum numbers. As results, quantitative conclusions were made for hadronic form factors, large-angle scattering processes and other related quantities. The highly cited paper [422] presented a relativistic extension of the quark model, based on one-gluon exchange and a linear-confining quark potential. This was used to describe mesons—their spectroscopy and decays—and succeeded to large extent. The work [423] studied (among others) B decays in the framework of the valence quark model; the model assumes factorization and good results were obtained, especially for nonleptonic processes. The following works further sharpened the QCD SM prediction; the next-to-leading QCD corrections were computed in [424], the implications of the heavy quark symmetry were analyzed in [425], the generalized factorization hypothesis and its impact on the structure of non-factorizable corrections were presented in [426] and three-loop anomalous dimensions at the next-to-leading order in α_s for weak radiative B decays were computed in [427]. The role of the charm penguin diagrams in the B decay to pions was evaluated by the authors of [428] and a next-to-leading order evaluation of the branching fraction and photon spectrum of the $B \rightarrow X_s + \gamma$ process was presented in [429].

Coming back to the CP symmetry, one can mention the publication [430], where large time-dependent CP asymmetries in the $B^0 - \bar{B}^0$ system were predicted, or [431], where it was shown that the theoretical uncertainty associated with penguin diagrams in the $B^0 \rightarrow \pi\pi$ decay can be reduced by considering isospin relations.

An important issue addressed by various authors is the factorization validity, often assumed for hadronic matrix elements of the four-fermion operators. In [432], a theoretical investigation of B branching fractions was undertaken and branching fraction ratios of

selected two-body hadronic B decays were proposed as factorization experimental tests. The article [433] was focused on the factorization for heavy-light final states. Such decays were treated in the heavy quark limit and the validity of the factorization ansatz was, in this scenario, proven at the two-loop order. In a similar context, the authors of [434] studied processes with two light mesons (K, π) in the final state. They argued that, in the heavy quark limit, the hadronic matrix elements of nonleptonic B meson decays can be computed from first principles, which helps to reduce the errors on the weak phases α and γ . The paper [435] was oriented very similarly, wherein the proof of the factorization was provided for $B^- \rightarrow D^0 \pi^-$ and $B^0 \rightarrow D^+ \pi^-$. The topic of the factorization was further treated in [436], where decays $B \rightarrow PP$ and $B \rightarrow PV$ were addressed, and also in [437], where soft-collinear effective theory was used to prove factorization for B decaying to two light particles (π, K, ρ, K^*).

One should also mention new physics searches. The paper [438] studied the $B \rightarrow \pi\pi$ process, from which it extracted relevant hadronic parameters. These were then used, under plausible assumptions, to predict $B \rightarrow \pi K$. Those observables (for the latter process) which have small EW penguin contributions seem to agree with the experiments; those with significant contributions do not. This might indicate NP in the W penguin sector. Similar ideas were also developed in [439]. A related topic, the final state interactions in hadronic B decays, was treated in [440]. Indeed, when considering the B decays to light mesons, there are, generally speaking, some difficulties in describing the data. To disentangle possible NP, all SM effects need to be considered, rescattering included. Here, The latter is treated in a phenomenological way in terms of off-shell meson exchange.

We now briefly mention other works of interest: papers [205,441] applied the light-cone sum rules to tackle B decays to light vector and pseudoscalar mesons, respectively, the authors of [442] computed, at next-to-next-to-leading order of QCD, the effective Hamiltonian for non-leptonic $|\Delta F| = 1$ decays and the text [443] focused on the B decays to two vector particles in the framework of the QCD factorization. Finally, we mention the paper [444], which summarized the status of our CKM matrix knowledge based on a global fit to various (leptonic, semileptonic, hadronic) data.

5.2. Nonleptonic B Decays in CCQM

5.2.1. Decay $B_s \rightarrow J/\psi \eta^{(\prime)}$

We have chosen to demonstrate the CCQM approach on two hadronic processes, to point out various aspects of the model application. The first one is $B_s \rightarrow J/\psi \eta^{(\prime)}$ [445], where a fit to the data was performed, so as to determine the model input parameters. The $\eta^{(\prime)}$ mesons are described as a superposition of light ($q = u, d$) and strange components, $\eta = -\sin \delta(\bar{q}q) - \cos \delta(\bar{s}s)$ and $\eta' = \cos \delta(\bar{q}q) - \sin \delta(\bar{s}s)$, where $\delta = \varphi_P - \pi/2$, $\varphi_P = 41.4^\circ$ [446]. The considered decay was treated within the naïve factorization picture in the leading order, meaning it was described as a $B_s \rightarrow \eta^{(\prime)}$ transition, where only the $\bar{s}s$ component of the latter was taken into the account (see Figure 10).

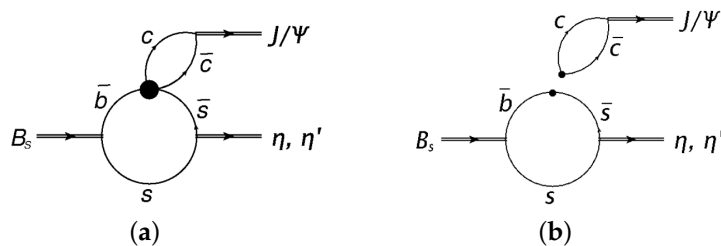


Figure 10. The $B_s \rightarrow \eta^{(\prime)} J/\psi$ decay as a B_s transition to the $\bar{s}s$ component of $\eta^{(\prime)}$ (a), in the factorization picture (b). Figure was originally published in [445].

The necessary inputs for the decay width formula ($P = \eta, \eta'$),

$$\Gamma(B_s \rightarrow J/\Psi + P) = \frac{G_F^2}{4\pi} |V_{cb}V_{cs}^*| C_W^2 f_{J/\Psi}^2 |\mathbf{q}_P|^3 \zeta_P^2 [F_+^{B_s\eta^{(\prime)}}(m_{J/\Psi}^2)]^2, \quad \zeta_\eta = \cos \delta, \quad \zeta_{\eta'} = \sin \delta \quad (69)$$

are the leptonic decay constants $f_{J/\Psi} \equiv f_V$ and the transition form factor F_+ :

$$m_V f_V \epsilon_V^\mu = N_c g_V \int \frac{d^4k}{(2\pi)^4 i} \tilde{\Phi}(-k^2) \text{tr}[O^\mu S_1(k + w_1 p) \not{\epsilon}_V S_2(k - w_2 p)], \quad p^2 = m_V^2, \quad (70)$$

$$\begin{aligned} \langle P_{q_1, q_3}(p_2) | \bar{q}_2 O^\mu q_1 | B_{\bar{q}_3, q_2}(p_1) \rangle &= F_+(q^2) P^\mu + F_-(q^2) q^\mu, \\ &= N_c g_B g_P \int \frac{d^4k}{(2\pi)^4 i} \tilde{\Phi}_B(-[k + w_{13} p_1]^2) \tilde{\Phi}_P(-[k + w_{23} p_2]^2) \\ &\quad \times \text{tr}[O^\mu S_1(k + p_1) \gamma^5 S_3(k) \gamma^5 S_2(k + p_2)], \end{aligned} \quad (71)$$

where the Wilson coefficient is given by $C_W = C_1 + C_2/N_c + C_3 + C_4/N_c + C_5 + C_6/N_c$ and the meaning of other symbols is analogous to Sections 3.2 and 4.2. The results are derived in the large N_c limit: $N_c \rightarrow \infty$. To obtain the form factor and the decay constants, one needs to know the model Λ parameters $\Lambda_{\eta}^{\bar{q}q}$, $\Lambda_{\eta}^{\bar{s}s}$, $\Lambda_{\eta'}^{\bar{q}q}$ and $\Lambda_{\eta'}^{\bar{s}s}$ —four in total, if one treats q and s components as independent. They can be derived from various processes where they play a role, so, in addition to the two studied decay channels, also $\eta \rightarrow \gamma\gamma$, $\eta' \rightarrow \gamma\gamma$, $\varphi \rightarrow \eta\gamma$, $\varphi \rightarrow \eta'\gamma$, $\rho^0 \rightarrow \eta\gamma$, $\omega \rightarrow \eta\gamma$, $\eta' \rightarrow \omega\gamma$, $B_d \rightarrow J/\Psi + \eta$ and $B_d \rightarrow J/\Psi + \eta'$ have been chosen. Fitting together all 11 processes, the optimal fit parameters were determined:

$$\Lambda_{\eta}^{\bar{q}q} = 0.881 \text{ GeV}, \quad \Lambda_{\eta}^{\bar{s}s} = 1.973 \text{ GeV}, \quad \Lambda_{\eta'}^{\bar{q}q} = 0.257 \text{ GeV}, \quad \Lambda_{\eta'}^{\bar{s}s} = 2.797 \text{ GeV}. \quad (72)$$

Other model parameters were taken from previous works, namely, $\Lambda_{B_s} = 1.95 \text{ GeV}$, $\Lambda_{B_d} = 1.88 \text{ GeV}$ and $\Lambda_{J/\Psi} = 1.48 \text{ GeV}$. Moreover, hadron-independent parameters (5) were tuned to different values (see Equation (6) in [445]). With these in hand, one computes results, as shown in Table 5.

Table 5. Decay widths and branching fractions for various processes with η and η' mesons, as predicted by the CCQM. Table contains a subset of data originally published in [445].

Observable	CCQM	Exp. [23]
$\Gamma(\eta \rightarrow \gamma\gamma)$	0.380 keV	$0.515 \pm 0.020 \text{ keV}$
$\Gamma(\eta' \rightarrow \gamma\gamma)$	3.74 keV	$4.34 \pm 0.14 \text{ keV}$
$\Gamma(\eta' \rightarrow \omega\gamma)$	9.49 keV	$4.74 \pm 0.15 \text{ keV}$
$\Gamma(\rho \rightarrow \eta\gamma)$	53.07 keV	$44.22 \pm 0.24 \text{ keV}$
$\Gamma(\omega \rightarrow \eta\gamma)$	6.21 keV	$3.91 \pm 0.06 \text{ keV}$
$\Gamma(\varphi \rightarrow \eta\gamma)$	42.59 keV	$55.28 \pm 0.17 \text{ keV}$
$\Gamma(\varphi \rightarrow \eta'\gamma)$	0.276 keV	$0.26 \pm 0.001 \text{ keV}$
$\mathcal{B}(B_d \rightarrow J/\Psi + \eta)$	16.5×10^{-6}	$(10.8 \pm 2.3) \times 10^{-6}$
$\mathcal{B}(B_d \rightarrow J/\Psi + \eta')$	12.2×10^{-6}	$(7.6 \pm 2.4) \times 10^{-6}$
$\mathcal{B}(B_s \rightarrow J/\Psi + \eta)$	4.67×10^{-4}	$(4.0 \pm 0.7) \times 10^{-4}$
$\mathcal{B}(B_s \rightarrow J/\Psi + \eta')$	4.04×10^{-4}	$(3.3 \pm 0.4) \times 10^{-4}$

Generally speaking, the discrepancies in terms of standard deviations are rather large, yet the model roughly (within a factor of 2) reproduces the data. There might be reasons for the differences that require understanding, e.g., a gluonic contribution to the η' state [446] could weaken the largest disagreement for $\Gamma(\eta' \rightarrow \omega\gamma)$. As pointed out in [445], other models on the market do not seem to perform better than ours.

The Belle and LHCb collaborations also measured the ratio [447,448]

$$R = \frac{\mathcal{B}(B_s \rightarrow J/\Psi + \eta')}{\mathcal{B}(B_s \rightarrow J/\Psi + \eta)} = \begin{cases} 0.73 \pm 0.14, & \text{Belle} \\ 0.90 \pm 0.1, & \text{LHCb} \\ 0.86, & \text{CCQM} \end{cases} \quad (73)$$

Here, the CCQM number reproduces the measurements well and, through the predicted form factors, adds a non-trivial factor 0.83 to the model-independent part of the calculation:

$$R^{\text{theor}} = \left(\frac{|\mathbf{q}_{\eta'}|^3}{|\mathbf{q}_{\eta}|^3} \tan^2(\delta) \right) \times \left(\frac{F_+^{B_s \eta'}}{F_+^{B_s \eta}} \right)^2 = 1.04 \dots \times 0.83 \dots \approx 0.86. \quad (74)$$

The overall precision of results is not fully satisfactory and further efforts may be performed to investigate the discrepancies. Nevertheless, in addition to the results themselves that we wanted, in this subsection, we also to point to the methodology we adopted in the CCQM for determining the model inputs.

5.2.2. Decay $B \rightarrow D_{(s)}^{(*)}h, (h = \pi, \rho)$

The second process we want to review is the B_d decay to a D meson and a light particle [449]. The interest here comes from the observation c(onfirmed by other authors too) that the predictions systematically overshoot the data, which might indicate the NP.

The processes are described in the leading order and naïve factorization framework. These decays correspond to a rich set of various spin states and diagram topologies, as is summarized in Figure 11 and Table 6. One labels, by $D_{1,2,3}$, the diagram structure (color favored, color suppressed and their interference), where, within each group, various spin configurations are present (labeled A, \dots, D).

Table 6. Studied decays arranged with respect to the spin structure and diagram topology. Underlined parts correspond to the transition of the spectator quark (in the case of D_3 , refer to the first diagram in Figure 11c). Table was originally published in [449].

Spin Structure	D_1 Diagram	D_2 Diagram	D_3 Diagram
(A) <u>$PS \rightarrow PS + PS$</u>	$B^0 \rightarrow D^- + \pi^+$ $B^0 \rightarrow \pi^- + D^+$ $B^0 \rightarrow \pi^- + D_s^+$ $B^+ \rightarrow \pi^0 + D_s^+$	$B^0 \rightarrow \pi^0 + \bar{D}^0$	$B^+ \rightarrow \bar{D}^0 + \pi^+$
(B) <u>$PS \rightarrow PS + V$</u>	$B^0 \rightarrow D^- + \rho^+$ $B^0 \rightarrow \pi^- + D_s^{*+}$ $B^+ \rightarrow \pi^0 + D_s^{*+}$ $B^+ \rightarrow \pi^0 + D_s^{*+}$	$B^0 \rightarrow \pi^0 + \bar{D}^{*0}$	$B^+ \rightarrow \bar{D}^0 + \rho^+$
(C) <u>$PS \rightarrow V + PS$</u>	$B^0 \rightarrow D^{*-} + \pi^+$ $B^0 \rightarrow \rho^- + D_s^+$ $B^+ \rightarrow \rho^0 + D_s^+$	$B^0 \rightarrow \rho^0 + \bar{D}^0$	$B^+ \rightarrow \bar{D}^{*0} + \pi^+$
(D) <u>$PS \rightarrow V + V$</u>	$B^0 \rightarrow D^{*-} + \rho^+$ $B^0 \rightarrow \rho^- + D_s^{*+}$ $B^+ \rightarrow \rho^0 + D_s^{*+}$	$B^0 \rightarrow \rho^0 + \bar{D}^{*0}$	$B^+ \rightarrow \bar{D}^{*0} + \rho^+$

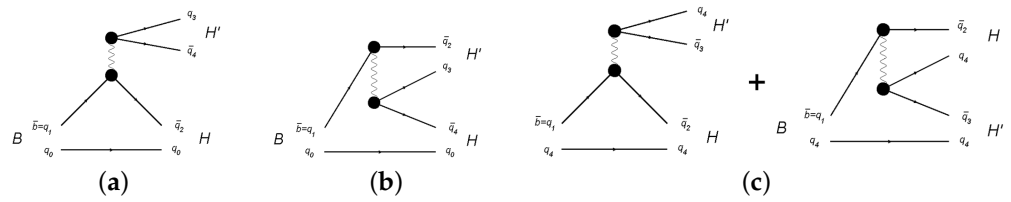


Figure 11. B decays to two hadrons: color-favored D_1 (a), color-suppressed D_2 (b) and their interference D_3 (c). Figures were originally published in [449].

Using the leading order operators,

$$Q_1 = [(\bar{q}_1)_{i_1}(q_2)_{i_2}]_{V-A}[(\bar{q}_3)_{i_2}(q_4)_{i_1}]_{V-A}, \quad Q_2 = [(\bar{q}_1)_{i_1}(q_2)_{i_1}]_{V-A}[(\bar{q}_3)_{i_2}(q_4)_{i_2}]_{V-A}, \quad (75)$$

where i_j are color indices and $[q_1q_2]_{V-A} = \bar{q}_1\gamma^\mu(1 - \gamma^5)q_2$, one can derive form factors. In the case of the scalar-to-scalar transition given by (71), they are, for the scalar-to-vector form factor, the expression

$$\begin{aligned} \langle V_{q_3,q_2}(p_2, \epsilon) | \bar{q}_1 O^\mu q_2 | B_{q_3,q_1}(p_1) \rangle = & \quad (76) \\ = \frac{\epsilon_V^\dagger}{m_B + m_V} \left[-g^{\mu\nu} P \cdot q A_0(q^2) + P^\mu P^\nu A_+(q^2) + q^\mu P^\nu A_-(q^2) + \epsilon^{\mu\nu\alpha\beta} P_\alpha q_\beta V(q^2) \right]. \end{aligned}$$

The obtained form factors are shown in Figure 12; the hadron-specific and universal CCQM parameters used in their prediction are summarized in Table II in [449].

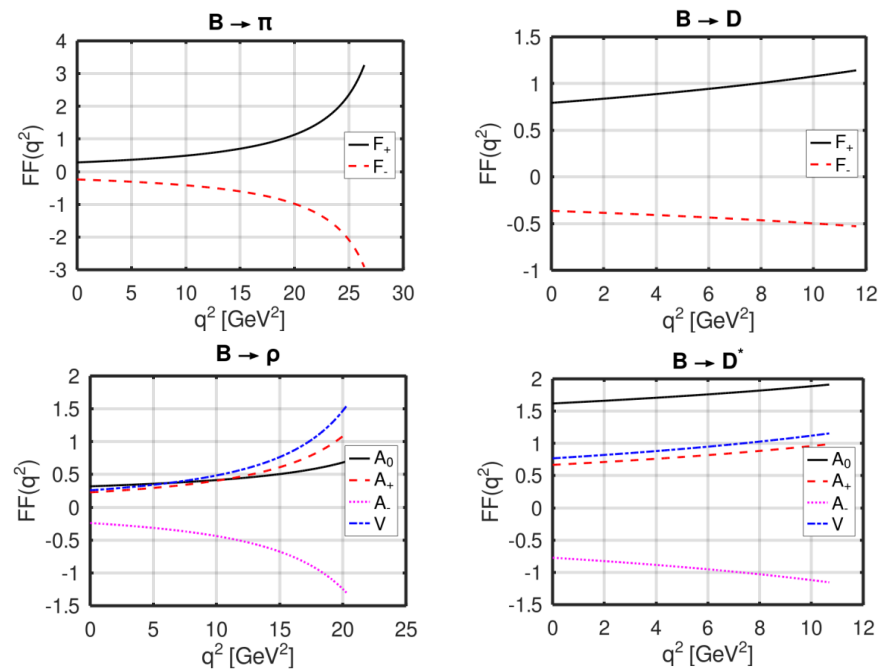


Figure 12. Transition form factors, as predicted by the CCQM. Figures were originally published in [449].

The corresponding decay-width formulas (see [449], page 3) then allow one to obtain the results summarized in Table 7.

Table 7. CCQM branching fractions compared to data. Table was originally published in [449].

	Process	Diagram	$\mathcal{B}_{\text{CCQM}}/E$	$\mathcal{B}_{\text{PDG}}/E$	E
1	$B^0 \rightarrow D^- + \pi^+$	D_1	5.34 ± 0.27	2.52 ± 0.13	10^{-3}
2	$B^0 \rightarrow \pi^- + D^+$	D_1	11.19 ± 0.56	7.4 ± 1.3	10^{-7}
3	$B^0 \rightarrow \pi^- + D_s^+$	D_1	3.48 ± 0.17	2.16 ± 0.26	10^{-5}
4	$B^+ \rightarrow \pi^0 + D_s^+$	D_1	1.88 ± 0.09	1.6 ± 0.5	10^{-5}
5	$B^0 \rightarrow D^- + \rho^+$	D_1	14.06 ± 0.70	7.6 ± 1.2	10^{-3}
6	$B^0 \rightarrow \pi^- + D_s^{*+}$	D_1	3.66 ± 0.18	2.1 ± 0.4	10^{-5}
7	$B^+ \rightarrow \pi^0 + D_s^{*+}$	D_1	0.804 ± 0.04	<3.6	10^{-6}
8	$B^+ \rightarrow \pi^0 + D_s^{*+}$	D_1	0.197 ± 0.01	<2.6	10^{-4}
9	$B^0 \rightarrow D^{*-} + \pi^+$	D_1	4.74 ± 0.24	2.74 ± 0.13	10^{-3}
10	$B^0 \rightarrow \rho^- + D_s^+$	D_1	2.76 ± 0.14	<2.4	10^{-5}
11	$B^+ \rightarrow \rho^0 + D_s^+$	D_1	0.149 ± 0.01	<3.0	10^{-4}
12	$B^0 \rightarrow D^{*-} + \rho^+$	D_1	14.58 ± 0.73	6.8 ± 0.9	10^{-3}
13	$B^0 \rightarrow \rho^- + D_s^{*+}$	D_1	5.09 ± 0.25	4.1 ± 1.3	10^{-5}
14	$B^+ \rightarrow \rho^0 + D_s^{*+}$	D_1	0.275 ± 0.01	<4.0	10^{-4}
15	$B^0 \rightarrow \pi^0 + \bar{D}^0$	D_2	0.085 ± 0.00	2.63 ± 0.14	10^{-4}
16	$B^0 \rightarrow \pi^0 + \bar{D}^{*0}$	D_2	1.13 ± 0.06	2.2 ± 0.6	10^{-4}
17	$B^0 \rightarrow \rho^0 + \bar{D}^0$	D_2	0.675 ± 0.03	3.21 ± 0.21	10^{-4}
18	$B^0 \rightarrow \rho^0 + \bar{D}^{*0}$	D_2	1.50 ± 0.08	<5.1	10^{-4}
19	$B^+ \rightarrow \bar{D}^0 + \pi^+$	D_3	3.89 ± 0.19	4.68 ± 0.13	10^{-3}
20	$B^+ \rightarrow \bar{D}^0 + \rho^+$	D_3	1.83 ± 0.09	1.34 ± 0.18	10^{-2}
21	$B^+ \rightarrow \bar{D}^{*0} + \pi^+$	D_3	7.60 ± 0.38	4.9 ± 0.17	10^{-3}
22	$B^+ \rightarrow \bar{D}^{*0} + \rho^+$	D_3	11.75 ± 0.59	9.8 ± 1.7	10^{-3}

The level of agreement between the model and the data can be visually estimated by looking at Figure 13.

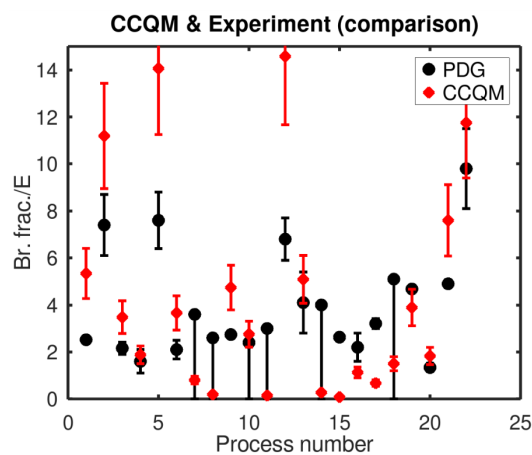


Figure 13. The comparison of CCQM predictions and data. Processes are numbered as in Table 7. Figure was originally published in [449].

Generally speaking, the description of data is not satisfactory. The agreement within error is only reached for measurements where limits are given but for few other cases. This might be expected for a subset of the processes, since the factorization assumption is not supposed to hold in the scenario where the spectator quark enters the light meson (see [433]). Still, one sees an overall overestimation, including decays with the spectator quark entering the D meson. This observation joins similar observations made by other authors [42,450–452], i.e., it is seen across various approaches, which naturally raises ques-

tions about the NP. The authors of [452] talked about a “novel puzzle” and NP scenarios were advanced to explain it in [42,452].

5.3. Other CCQM Results on Nonleptonic B Decays

The CCQM was also applied to other hadronic decay processes of B mesons. Skipping older publications [248,453] with an earlier version of the model, we can mention again the generally oriented text [249], where decay width for B_s progressing to $D_s^- + D_s^{(*)+}$, $D_s^{*-} + D_s^{(*)+}$ and $J/\Psi + \Phi$ were computed. They were determined within the effective Hamiltonian approach using the helicity formalism from the CCQM-predicted form factors. The numbers were in fair agreement with experimental measurements. The same results were reviewed in paper [250], which, in addition, treated the exotic state $X(3872)$ as a tetraquark and evaluated its selected branching fractions.

The work [454] dealt with double-heavy B_c particles and their decays to charmonia and various D mesons. Two diagrams contributed in the leading order; in one, the B_c spectator quark \bar{c} goes to the charmonium state, while, in the other, it forms the D meson. One thus needs to evaluate form factors of six transitions $B_c \rightarrow D, D_s, \eta_c, D^*, D_s^*, J/\Psi$; their behavior is shown in Figure 2 of the work and their values at zero are also presented. Next, helicity amplitudes were constructed and branching fractions calculated for, in total, eight processes $B_s \rightarrow \eta_c + D_{(s)}^{(*)}$ and $B_s \rightarrow J/\Psi + D_{(s)}^{(*)}$ (all combinations of brackets). Comparison with the experiment was based on branching fraction ratios $\mathcal{R}(D_s^+/\pi^+)$, $\mathcal{R}(D_s^{*+}/\pi^+)$, $\mathcal{R}(D_s^+/D_s^+)$ and also Γ_{++}/Γ measured by Atlas [455] and LHCb [259]. Here,

$$\mathcal{R}(A/B) = \frac{\mathcal{B}(B_c^+ \rightarrow J/\Psi A)}{\mathcal{B}(B_c^+ \rightarrow J/\Psi B)} \tag{77}$$

and Γ_{++}/Γ is the transverse polarization fraction in the $B_c^+ \rightarrow J/\Psi + D_s^{*+}$ decay. The results were presented in the Table VIII of [454] with no significant deviations from the SM. However, as two different sets of Wilson coefficients were investigated, it turned out that the results were quite sensitive to their choice.

Similar processes were addressed in [255], though with π or K in the final state instead of D . Consequently, only one diagram contributed, which was the one corresponding to the transition to charmonium, since all other π/K production diagrams from B_c were of a higher order. Furthermore, the semileptonic mode to $J/\Psi \mu \nu_\mu$ was investigated, so as to define observables $\mathcal{R}(\pi^+/\mu^+\nu)$, $\mathcal{R}(K^+/\pi^+)$, $\mathcal{R}(J/\Psi)$ and $\mathcal{R}(\eta_c)$ (see (41) and (77)). With the CCQM transition form factors identical to those mentioned previously, one obtains, in total, eight decay widths $B_c^+ \rightarrow \eta_c + h$, $B_c^+ \rightarrow J/\Psi + h$, $h \in \{\pi^+, \rho^+, K^+, K^{*+}\}$ (Table 3 of the publication) and branching fraction ratios, which can be compared to the LHCb numbers (Table 5 of [255]) and also to other theoretical works. The ratios are in agreement with measurements, except for $\mathcal{R}(J/\Psi)$, which deviates by more than 2σ .

Finally, we mention the paper [456], dedicated to vector particles B_s^* and B_s^* and their transition to $B_{(s)}\gamma$ and $D_{(s)}^* + V$, $V \in \{\rho, K^*, D^*, D_s^*\}$. The radiative deexcitation processes use the formalism presented in Section 2.4 to describe the decay: a photon can be radiated from one of the valence quarks or from the non-local quark–hadron vertex. In the latter case, however, it can be shown that the contribution vanishes due to the anomalous nature of the $V \rightarrow P\gamma$ process and so the calculation is simplified. The results on decay widths of B^+ , B^0 and B_s^{*0} , as presented in Table V of their work, depend on radiative decay constants of the particles given in Table IV. As to what concerns the decays to two vector particles, the computation proceeds in a usual way, where the CCQM invariant form factors are combined to helicity amplitudes to give branching fractions. Due to small cross-sections of the studied processes, the experimental numbers were not available and so the CCQM results were compared to other theoretical approaches (Table XII of [456]).

6. Summary and Outlook

We provided, in this text, a review of the results of the covariant confined quark model for B decays, presented together with a survey of selected experimental and theoretical results. Differently from other physics models and their achievements mentioned here, we explained in depth the principles of the CCQM (Section 2) and presented computational details for the chosen processes, namely, $B_s \rightarrow \ell^+ \ell^- \gamma$ (Section 3.2), $B_s \rightarrow \phi \ell^+ \ell^- \gamma$ (Section 4.2), $B \rightarrow D_{(s)}^{(*)} h$, ($h = \pi, \rho$) and $B_s \rightarrow J/\psi \eta^{(\prime)}$ (Section 5.2). For the sake of the review, the decays were divided into three groups: leptonic, semileptonic and non-leptonic. Although somewhat arbitrary, this division allowed us to demonstrate the application of the CCQM in various situations. Generally speaking, despite some studies on NP contributions, the CCQM results do not provide strong indications for NP and suggest that further efforts within the SM may be needed.

One should also recall that we presented only a small section of what the CCQM can provide: it was, in many papers, successfully applied to describe baryon, tetraquark and other mesonic states. The quality of the CCQM is also confirmed by the interest of other authors. Narrowing the large number of citations to those related to B decays and referring to the recent version of the model (2010 and later, without conference papers), one sees that the model was noticed by large collaborations (LHCb [58,457], ATLAS [458]).

The ongoing physics program on existing and future high-luminosity machines implies that the CCQM may also, in the future, be an appropriate theoretical tool which will contribute to unraveling the questions brought by experiments about the presence of NP or the nature of various (exotic) states. Together with other approaches, it may help to understand model-related uncertainties beyond which new physics observations can be claimed.

Author Contributions: S.D. and A.Z.D.: methodology, supervision; M.A.I.: methodology, software, review and editing, supervision; A.L.: software, original draft preparation, review and editing. All authors have read and agreed to the published version of the manuscript.

Funding: S.D., A.Z.D. and A.L. acknowledge the support of the Slovak Grant Agency for Sciences VEGA, grant no. 2/0105/21.

Data Availability Statement: No specific data are associated with this work.

Conflicts of Interest: The authors declare no conflict of interest.

References

- Weinberg, S. Phenomenological Lagrangians. *Physica A* **1979**, *96*, 327–340. [[CrossRef](#)]
- Gasser, J.; Leutwyler, H. Chiral Perturbation Theory to One Loop. *Ann. Phys.* **1984**, *158*, 142. [[CrossRef](#)]
- Gasser, J.; Leutwyler, H. Chiral Perturbation Theory: Expansions in the Mass of the Strange Quark. *Nucl. Phys. B* **1985**, *250*, 465–516. [[CrossRef](#)]
- Scherer, S. Chiral perturbation theory: Success and challenge. *Eur. Phys. J. A* **2006**, *28*, 59–70. [[CrossRef](#)]
- MacHleidt, R.; Sammarruca, F. Chiral EFT based nuclear forces: Achievements and challenges. *Phys. Scr.* **2016**, *91*, 83007. [[CrossRef](#)]
- Dyson, F.J. The S Matrix in Quantum Electrodynamics. *Phys. Rev.* **1949**, *75*, 1736–1755. [[CrossRef](#)]
- Schwinger, J.S. On the Green's functions of quantized fields. 1. *Proc. Nat. Acad. Sci. USA* **1951**, *37*, 452–455. [[CrossRef](#)]
- Schwinger, J.S. On the Green's functions of quantized fields. 2. *Proc. Nat. Acad. Sci. USA* **1951**, *37*, 455–459. [[CrossRef](#)]
- Roberts, C.D.; Williams, A.G. Dyson-Schwinger equations and their application to hadronic physics. *Prog. Part. Nucl. Phys.* **1994**, *33*, 477–575. [[CrossRef](#)]
- Ivanov, M.A.; Kalinovsky, Y.L.; Roberts, C.D. Survey of heavy meson observables. *Phys. Rev. D* **1999**, *60*, 034018. [[CrossRef](#)]
- Shifman, M.A.; Vainshtein, A.I.; Zakharov, V.I. QCD and Resonance Physics. Theoretical Foundations. *Nucl. Phys. B* **1979**, *147*, 385–447. [[CrossRef](#)]
- Shifman, M.A.; Vainshtein, A.I.; Zakharov, V.I. QCD and Resonance Physics: Applications. *Nucl. Phys. B* **1979**, *147*, 448–518. [[CrossRef](#)]
- de Rafael, E. An Introduction to sum rules in QCD: Course. In Proceedings of the Les Houches Summer School in Theoretical Physics, Session 68: Probing the Standard Model of Particle Interactions, Les Houches, France, 28 July–5 September 1997; pp. 1171–1218.

14. Colangelo, P.; Khodjamirian, A. QCD sum rules, a modern perspective. In *At the Frontier of Particle Physics: Handbook of QCD*; World Scientific: Singapore, 2000; pp. 1495–1576. [[CrossRef](#)]
15. Isgur, N.; Wise, M.B. Weak Decays of Heavy Mesons in the Static Quark Approximation. *Phys. Lett. B* **1989**, *232*, 113–117. [[CrossRef](#)]
16. Isgur, N.; Wise, M.B. Weak transition form-factors between heavy mesons. *Phys. Lett. B* **1990**, *237*, 527–530. [[CrossRef](#)]
17. Neubert, M. Heavy quark symmetry. *Phys. Rep.* **1994**, *245*, 259–396. [[CrossRef](#)]
18. Aoki, Y.; Blum, T.; Colangelo, G.; Collins, S.; Morte, M.D.; Dimopoulos, P.; Dürr, S.; Feng, X.; Fukaya, H.; Golterman, M.; et al. FLAG Review 2021. *Eur. Phys. J. C* **2022**, *82*, 869. [[CrossRef](#)]
19. Gambino, P.; Hashimoto, S. Inclusive Semileptonic Decays from Lattice QCD. *Phys. Rev. Lett.* **2020**, *125*, 032001. [[CrossRef](#)]
20. Desiderio, A.; Frezzotti, R.; Garofalo, M.; Giusti, D.; Hansen, M.; Lubicz, V.; Martinelli, G.; Sachrajda, C.T.; Sanfilippo, F.; Simula, S.; et al. First lattice calculation of radiative leptonic decay rates of pseudoscalar mesons. *Phys. Rev. D* **2021**, *103*, 014502. [[CrossRef](#)]
21. Boyle, P.A.; Chakraborty, B.; Davies, C.T.; DeGrand, T.; DeTar, C.; Del Debbio, L.; El-Khadra, A.X.; Erben, F.; Flynn, J.M.; Gámiz, E.; et al. A lattice QCD perspective on weak decays of b and c quarks Snowmass 2022 White Paper. *arXiv* **2022**, arXiv:2205.15373.
22. Gambino, P.; Hashimoto, S.; Mächler, S.; Panero, M.; Sanfilippo, F.; Simula, S.; Smecca, A.; Tantalo, N. Lattice QCD study of inclusive semileptonic decays of heavy mesons. *J. High Energy Phys.* **2022**, *7*, 83. [[CrossRef](#)]
23. Particle Data Group; Workman, R.L.; Burkert, V.D.; Crede, V.; Klempt, E.; Thoma, U.; Tiator, L.; Agashe, K.; Aielli, G.; Allanach, B.C.; et al. Review of Particle Physics. *PTEP* **2022**, *2022*, 083C01. [[CrossRef](#)]
24. Ebert, D.; Galkin, V.O.; Faustov, R.N. Mass spectrum of orbitally and radially excited heavy—Light mesons in the relativistic quark model. *Phys. Rev. D* **1998**, *57*, 5663–5669; Erratum in *Phys. Rev. D* **1999**, *59*, 019902. [[CrossRef](#)]
25. Ebert, D.; Faustov, R.N.; Galkin, V.O. Properties of heavy quarkonia and B_c mesons in the relativistic quark model. *Phys. Rev. D* **2003**, *67*, 014027. [[CrossRef](#)]
26. Nambu, Y.; Jona-Lasinio, G. Dynamical Model of Elementary Particles Based on an Analogy with Superconductivity. 1. *Phys. Rev.* **1961**, *122*, 345–358. [[CrossRef](#)]
27. Nambu, Y.; Jona-Lasinio, G. Dynamical model of elementary particles based on an analogy with superconductivity. II. *Phys. Rev.* **1961**, *124*, 246–254. [[CrossRef](#)]
28. Klevansky, S.P. The Nambu-Jona-Lasinio model of quantum chromodynamics. *Rev. Mod. Phys.* **1992**, *64*, 649–708. [[CrossRef](#)]
29. Guo, X.Y.; Chen, X.L.; Deng, W.Z. The Heavy mesons in Nambu-Jona-Lasinio model. *Chin. Phys. C* **2013**, *37*, 033102. [[CrossRef](#)]
30. Luan, Y.L.; Chen, X.L.; Deng, W.Z. Meson electro-magnetic form factors in an extended Nambu–Jona-Lasinio model including heavy quark flavors. *Chin. Phys. C* **2015**, *39*, 113103. [[CrossRef](#)]
31. Anikin, I.V.; Ivanov, M.A.; Kulimanova, N.B.; Lyubovitskij, V.E. The Extended Nambu-Jona-Lasinio model with separable interaction: Low-energy pion physics and pion nucleon form-factor. *Z. Phys. C* **1995**, *65*, 681–690. [[CrossRef](#)]
32. Buchalla, G.; Buras, A.J.; Lautenbacher, M.E. Weak decays beyond leading logarithms. *Rev. Mod. Phys.* **1996**, *68*, 1125–1144. [[CrossRef](#)]
33. Bevan, A.J.; Golob, B.; Mannel, Th.; Prell, S.; Yabsley, B.D.; Aihara, H.; Anulli, F.; Arnaud, N.; Aushev, T.; Beneke, M.; et al. The Physics of the B Factories. *Eur. Phys. J. C* **2014**, *74*, 3026. [[CrossRef](#)]
34. Artuso, M.; Isidori, G.; Stone, S. *New Physics in b Decays*; World Scientific: Singapore, 2022. [[CrossRef](#)]
35. Altmannshofer, W.; Stangl, P. New physics in rare B decays after Moriond 2021. *Eur. Phys. J. C* **2021**, *81*, 952. [[CrossRef](#)]
36. Jäger, S.; Kirk, M.; Lenz, A.; Leslie, K. Charming new physics in rare B-decays and mixing? *Phys. Rev. D* **2018**, *97*, 015021. [[CrossRef](#)]
37. Kumbhakar, S.; Saini, J. New physics effects in purely leptonic B_s^* decays. *Eur. Phys. J. C* **2019**, *79*, 394. [[CrossRef](#)]
38. Chala, M.; Egede, U.; Spannowsky, M. Searching new physics in rare B -meson decays into multiple muons. *Eur. Phys. J. C* **2019**, *79*, 431. [[CrossRef](#)]
39. Coy, R.; Frigerio, M.; Mescia, F.; Sumensari, O. New physics in $b \rightarrow s\ell\ell$ transitions at one loop. *Eur. Phys. J. C* **2020**, *80*, 52. [[CrossRef](#)]
40. Charles, J.; Descotes-Genon, S.; Ligeti, Z.; Monteil, S.; Papucci, M.; Trabelsi, K.; Vale Silva, L. New physics in B meson mixing: future sensitivity and limitations. *Phys. Rev. D* **2020**, *102*, 056023. [[CrossRef](#)]
41. Bhutta, F.M.; Huang, Z.R.; Lü, C.D.; Ali Paracha, M.; Wang, W. New physics in $b \rightarrow s\ell\ell$ anomalies and its implications for the complementary neutral current decays. *Nucl. Phys. B* **2022**, *979*, 115763. [[CrossRef](#)]
42. Cai, F.M.; Deng, W.J.; Li, X.Q.; Yang, Y.D. Probing new physics in class-I B-meson decays into heavy-light final states. *J. High Energy Phys.* **2021**, *10*, 235. [[CrossRef](#)]
43. Branz, T.; Faessler, A.; Gutsche, T.; Ivanov, M.A.; Körner, J.G.; Lyubovitskij, V.E. Relativistic constituent quark model with infrared confinement. *Phys. Rev. D* **2010**, *81*, 034010. [[CrossRef](#)]
44. Ganbold, G.; Gutsche, T.; Ivanov, M.A.; Lyubovitskij, V.E. On the meson mass spectrum in the covariant confined quark model. *J. Phys. G* **2015**, *42*, 075002. [[CrossRef](#)]
45. Gutsche, T.; Ivanov, M.A.; Körner, J.G.; Lyubovitskij, V.E.; Santorelli, P.; Habel, N. Semileptonic decay $\Lambda_b \rightarrow \Lambda_c + \tau^- + \bar{\nu}_\tau$ in the covariant confined quark model. *Phys. Rev. D* **2015**, *91*, 074001; Erratum in *Phys. Rev. D* **2015**, *91*, 119907. [[CrossRef](#)]
46. Gutsche, T.; Ivanov, M.A.; Körner, J.G.; Lyubovitskij, V.E.; Santorelli, P. Heavy-to-light semileptonic decays of Λ_b and Λ_c baryons in the covariant confined quark model. *Phys. Rev. D* **2014**, *90*, 114033; Erratum in *Phys. Rev. D* **2016**, *94*, 059902. [[CrossRef](#)]

47. Ivanov, M.A. Nonleptonic Decays of Doubly Charmed Baryons. *Particles* **2020**, *3*, 123–144. [[CrossRef](#)]
48. Dubnička, S.; Dubničková, A.Z.; Ivanov, M.A.; Liptaj, A. Dynamical Approach to Decays of XYZ States. *Symmetry* **2020**, *12*, 884. [[CrossRef](#)]
49. Dubnička, S.; Dubničková, A.Z.; Habył, N.; Ivanov, M.A.; Liptaj, A.; Nurbakova, G.S. Decay $B \rightarrow K^*(\rightarrow K\pi)\ell^+\ell^-$ in covariant quark model. *Few Body Syst.* **2016**, *57*, 121–143. [[CrossRef](#)]
50. Jouvett, B. On the meaning of Fermi coupling. *Nuovo Cim.* **1956**, *3*, 1133–1135. [[CrossRef](#)]
51. Salam, A. Lagrangian theory of composite particles. *Nuovo Cim.* **1962**, *25*, 224–227. [[CrossRef](#)]
52. Weinberg, S. Elementary particle theory of composite particles. *Phys. Rev.* **1963**, *130*, 776–783. [[CrossRef](#)]
53. Hayashi, K.; Hirayama, M.; Muta, T.; Seto, N.; Shirafuji, T. Compositeness criteria of particles in quantum field theory and S-matrix theory. *Fortschritte Phys.* **1967**, *15*, 625–660. [[CrossRef](#)]
54. Faessler, A.; Gutsche, T.; Ivanov, M.A.; Korner, J.G.; Lyubovitskij, V.E. The Exclusive rare decays $B \rightarrow K(K^*)\bar{\ell}\ell$ and $B_c \rightarrow D(D^*)\bar{\ell}\ell$ in a relativistic quark model. *Eur. Phys. J. Direct* **2002**, *4*, 18. [[CrossRef](#)]
55. Branz, T.; Faessler, A.; Gutsche, T.; Ivanov, M.A.; Korner, J.G.; Lyubovitskij, V.E.; Oexl, B. Radiative decays of double heavy baryons in a relativistic constituent three-quark model including hyperfine mixing. *Phys. Rev. D* **2010**, *81*, 114036. [[CrossRef](#)]
56. Terning, J. Gauging nonlocal Lagrangians. *Phys. Rev. D* **1991**, *44*, 887–897. [[CrossRef](#)]
57. Ruijl, B.; Ueda, T.; Vermaseren, J.A.M. Forcer, a FORM program for the parametric reduction of four-loop massless propagator diagrams. *Comput. Phys. Commun.* **2020**, *253*, 107198. [[CrossRef](#)]
58. Aaij, R.; Abellán Beteta, C.; Ackernley, T.; Adeva, B.; Adinolfi, M.; Afsharnia, H.; Aidala, C.A.; Aiola, S.; Ajaltouni, Z.; Akar, S.; et al. Analysis of Neutral B-Meson Decays into Two Muons. *Phys. Rev. Lett.* **2022**, *128*, 041801. [[CrossRef](#)] [[PubMed](#)]
59. Aaboud, M.; Aad, G.; Abbott, B.; Abbott, D.C.; Abdinov, O.; Abeloos, B.; Abhayasinghe, D.K.; Abidi, S.H.; AbouZeid, O.S.; Abraham, N.L.; et al. Study of the rare decays of B_s^0 and B^0 mesons into muon pairs using data collected during 2015 and 2016 with the ATLAS detector. *J. High Energy Phys.* **2019**, *04*, 098. [[CrossRef](#)]
60. Sirunyan, A.M.; Tumasyan, A.; Adam, W.; Ambrogio, F.; Bergauer, T.; Brandstetter, J.; Dragicevic, M.; Erö, J.; Escalante Del Valle, A.; Flechl, M.; Frühwirth, R.; et al. Measurement of properties of $B_s^0 \rightarrow \mu^+\mu^-$ decays and search for $B^0 \rightarrow \mu^+\mu^-$ with the CMS experiment. *J. High Energy Phys.* **2020**, *04*, 188. [[CrossRef](#)]
61. Langenegger, U. Recent results on $B \rightarrow \mu^+\mu^-$ decays with the CMS experiment. *Mod. Phys. Lett. A* **2020**, *35*, 2030017. [[CrossRef](#)]
62. Kronenbitter, B.; Heck, M.; Goldenzweig, P.; Kuhr, T.; Abdesselam, A.; Adachi, I.; Aihara, H.; Said, S.I.; Arinstein, K.; Asner, D.M.; et al. Measurement of the branching fraction of $B^+ \rightarrow \tau^+\nu_\tau$ decays with the semileptonic tagging method. *Phys. Rev. D* **2015**, *92*, 051102. [[CrossRef](#)]
63. Hara, K.; Horii, Y.; Iijima, T.; Adachi, I.; Aihara, H.; Asner, D.M.; Aushev, T.; Aziz, T.; Bakich, A.M.; Barrett, M.; et al. Evidence for $B^- \rightarrow \tau^-\bar{\nu}_\tau$ with a Hadronic Tagging Method Using the Full Data Sample of Belle. *Phys. Rev. Lett.* **2013**, *110*, 131801. [[CrossRef](#)]
64. Lees, J.P.; Poireau, V.; Tisserand, V.; Garra Tico, J.; Grauges, E.; Palano, A.; Eigen, G.; Stugu, B.; Brown, D.N.; Kerth, L.T.; et al. Evidence of $B^+ \rightarrow \tau^+\nu$ decays with hadronic B tags. *Phys. Rev. D* **2013**, *88*, 031102. [[CrossRef](#)]
65. Aubert, B.; Karyotakis, Y.; Lees, J.P.; Poireau, V.; Principe, E.; Prudent, X.; Tisserand, V.; Garra Tico, J.; Grauges, E.; Martinelliab, M.; et al. A Search for $B^+ \rightarrow \ell^+\nu_\ell$ Recoiling Against $B^- \rightarrow D^0\ell^-\bar{\nu}X$. *Phys. Rev. D* **2010**, *81*, 051101. [[CrossRef](#)]
66. Sibidanov, A.; Varvell, K.E.; Adachi, I.; Aihara, H.; Said, S. Al.; Asner, D.M.; Aushev, T.; Ayad, R.; Babu, V.; Badhrees, I.; et al. Search for $B^- \rightarrow \mu^-\bar{\nu}_\mu$ Decays at the Belle Experiment. *Phys. Rev. Lett.* **2018**, *121*, 031801. [[CrossRef](#)] [[PubMed](#)]
67. Prim, M.T.; Bernlochner, F.U.; Goldenzweig, P.; Heck, M.; Adachi, I.; Adamczyk, K.; Aihara, H.; Al Said, S.; Asner, D.M.; Atmacan, H.; et al. Search for $B^+ \rightarrow \mu^+\nu_\mu$ and $B^+ \rightarrow \mu^+N$ with inclusive tagging. *Phys. Rev. D* **2020**, *101*, 032007. [[CrossRef](#)]
68. Gelb, M.; Bernlochner, F.U.; Goldenzweig, P.; Metzner, F.; Adachi, I.; Aihara, H.; Al Said, S.; Asner, D.M.; Atmacan, H.; Aushev, T.; et al. Search for the rare decay of $B^+ \rightarrow \ell^+\nu_\ell\gamma$ with improved hadronic tagging. *Phys. Rev. D* **2018**, *98*, 112016. [[CrossRef](#)]
69. Rosner, J.L.; Stone, S.; Van de Water, R.S. Leptonic Decays of Charged Pseudoscalar Mesons-2015. *arXiv* **2015**, arXiv:1509.02220.
70. Dingfelder, J.; Mannel, T. Leptonic and semileptonic decays of B mesons. *Rev. Mod. Phys.* **2016**, *88*, 035008. [[CrossRef](#)]
71. Buchalla, G.; Buras, A.J. QCD corrections to rare K and B decays for arbitrary top quark mass. *Nucl. Phys. B* **1993**, *400*, 225–239. [[CrossRef](#)]
72. Bazavov, A.; Bernard, C.; Brown, N.; DeTar, C.; El-Khadra, A.X.; Gámiz, E.; Gottlieb, Steven; Heller, U.M.; Komijani, J.; Kronfeld, A.S.; et al. B- and D-meson leptonic decay constants from four-flavor lattice QCD. *Phys. Rev. D* **2018**, *98*, 074512. [[CrossRef](#)]
73. Hermann, T.; Misiak, M.; Steinhauser, M. Three-loop QCD corrections to $B_s \rightarrow \mu^+\mu^-$. *J. High Energy Phys.* **2013**, *12*, 097. [[CrossRef](#)]
74. Bobeth, C.; Gorbahn, M.; Stamou, E. Electroweak Corrections to $B_{s,d} \rightarrow \ell^+\ell^-$. *Phys. Rev. D* **2014**, *89*, 034023. [[CrossRef](#)]
75. Bobeth, C.; Gorbahn, M.; Hermann, T.; Misiak, M.; Stamou, E.; Steinhauser, M. $B_{s,d} \rightarrow l^+l^-$ in the Standard Model with Reduced Theoretical Uncertainty. *Phys. Rev. Lett.* **2014**, *112*, 101801. [[CrossRef](#)] [[PubMed](#)]
76. Beneke, M.; Bobeth, C.; Szafron, R. Enhanced electromagnetic correction to the rare B-meson decay $B_{s,d} \rightarrow \mu^+\mu^-$. *Phys. Rev. Lett.* **2018**, *120*, 011801. [[CrossRef](#)] [[PubMed](#)]
77. Beneke, M.; Bobeth, C.; Szafron, R. Power-enhanced leading-logarithmic QED corrections to $B_q \rightarrow \mu^+\mu^-$. *J. High Energy Phys.* **2019**, *10*, 232; Erratum in *J. High Energy Phys.* **2022**, *11*, 099. [[CrossRef](#)]
78. Eilam, G.; Lu, C.D.; Zhang, D.X. Radiative dileptonic decays of B mesons. *Phys. Lett. B* **1997**, *391*, 461–464. [[CrossRef](#)]
79. Aliev, T.M.; Ozpineci, A.; Savci, M. $B(q) \rightarrow \text{lepton}^+ \text{lepton}^- \text{gamma}$ decays in light cone QCD. *Phys. Rev. D* **1997**, *55*, 7059–7066. [[CrossRef](#)]

80. Aliev, T.M.; Pak, N.K.; Savci, M. Rare radiative $B \rightarrow \tau^+ \tau^- \gamma$ decay. *Phys. Lett. B* **1998**, *424*, 175–184. [[CrossRef](#)]
81. Geng, C.Q.; Lih, C.C.; Zhang, W.M. Study of $B(s,d) \rightarrow l^+ l^- \gamma$ decays. *Phys. Rev. D* **2000**, *62*, 074017. [[CrossRef](#)]
82. Dincer, Y.; Sehgal, L.M. Charge asymmetry and photon energy spectrum in the decay $B(s) \rightarrow l^+ l^- \gamma$. *Phys. Lett. B* **2001**, *521*, 7–14. [[CrossRef](#)]
83. Kruger, F.; Melikhov, D. Gauge invariance and form-factors for the decay $B \rightarrow \gamma l^+ l^-$. *Phys. Rev. D* **2003**, *67*, 034002. [[CrossRef](#)]
84. Descotes-Genon, S.; Sachrajda, C.T. Universality of nonperturbative QCD effects in radiative B decays. *Phys. Lett. B* **2003**, *557*, 213–223. [[CrossRef](#)]
85. Melikhov, D.; Nikitin, N. Rare radiative leptonic decays $B(d,s) \rightarrow l^+ l^- \gamma$. *Phys. Rev. D* **2004**, *70*, 114028. [[CrossRef](#)]
86. Carvunis, A.; Dettori, F.; Gangal, S.; Guadagnoli, D.; Normand, C. On the effective lifetime of $B_s \rightarrow \mu \mu \gamma$. *J. High Energy Phys.* **2021**, *12*, 078. [[CrossRef](#)]
87. Burdman, G.; Goldman, J.T.; Wyler, D. Radiative leptonic decays of heavy mesons. *Phys. Rev. D* **1995**, *51*, 111–117. [[CrossRef](#)]
88. Korchemsky, G.P.; Pirjol, D.; Yan, T.M. Radiative leptonic decays of B mesons in QCD. *Phys. Rev. D* **2000**, *61*, 114510. [[CrossRef](#)]
89. Braun, V.M.; Khodjamirian, A. Soft contribution to $B \rightarrow \gamma l \nu_\ell$ and the B-meson distribution amplitude. *Phys. Lett. B* **2013**, *718*, 1014–1019. [[CrossRef](#)]
90. Beneke, M.; Braun, V.M.; Ji, Y.; Wei, Y.B. Radiative leptonic decay $B \rightarrow \gamma l \nu_\ell$ with subleading power corrections. *J. High Energy Phys.* **2018**, *07*, 154. [[CrossRef](#)]
91. Lunghi, E.; Pirjol, D.; Wyler, D. Factorization in leptonic radiative $B \rightarrow \gamma e \nu$ decays. *Nucl. Phys. B* **2003**, *649*, 349–364. [[CrossRef](#)]
92. Bosch, S.W.; Hill, R.J.; Lange, B.O.; Neubert, M. Factorization and Sudakov resummation in leptonic radiative B decay. *Phys. Rev. D* **2003**, *67*, 094014. [[CrossRef](#)]
93. Wang, C.; Wang, Y.M.; Wei, Y.B. QCD factorization for the four-body leptonic B-meson decays. *J. High Energy Phys.* **2022**, *2*, 141. [[CrossRef](#)]
94. Danilina, A.; Nikitin, N.; Toms, K. Decays of charged B-mesons into three charged leptons and a neutrino. *Phys. Rev. D* **2020**, *101*, 096007. [[CrossRef](#)]
95. Ivanov, M.A.; Melikhov, D. Theoretical analysis of the leptonic decays $B \rightarrow \ell \ell \nu \ell$: Identical leptons in the final state. *Phys. Rev. D* **2022**, *105*, 094038. [[CrossRef](#)]
96. Ivanov, M.A.; Melikhov, D. Theoretical analysis of the leptonic decays $B \rightarrow \ell \ell \bar{\nu}_\ell$. *Phys. Rev. D* **2022**, *105*, 014028; Erratum in *Phys. Rev. D* **2022**, *106*, 119901. [[CrossRef](#)]
97. Geng, L.S.; Grinstein, B.; Jäger, S.; Li, S.Y.; Martin Camalich, J.; Shi, R.X. Implications of new evidence for lepton-universality violation in $b \rightarrow s \ell + \ell^-$ decays. *Phys. Rev. D* **2021**, *104*, 035029. [[CrossRef](#)]
98. Algueró, M.; Capdevila, B.; Descotes-Genon, S.; Matias, J.; Novoa-Brunet, M. $b \rightarrow s \ell^+ \ell^-$ global fits after R_{K_S} and $R_{K^{*+}}$. *Eur. Phys. J. C* **2022**, *82*, 326. [[CrossRef](#)]
99. Fleischer, R.; Jaarsma, R.; Tetlalmatzi-Xolocotzi, G. Mapping out the space for new physics with leptonic and semileptonic $B_{(c)}$ decays. *Eur. Phys. J. C* **2021**, *81*, 658. [[CrossRef](#)]
100. D'Ambrosio, G.; Giudice, G.F.; Isidori, G.; Strumia, A. Minimal flavor violation: An Effective field theory approach. *Nucl. Phys. B* **2002**, *645*, 155–187. [[CrossRef](#)]
101. De Bruyn, K.; Fleischer, R.; Kneijens, R.; Koppenburg, P.; Merk, M.; Pellegrino, A.; Tuning, N. Probing New Physics via the $B_s^0 \rightarrow \mu^+ \mu^-$ Effective Lifetime. *Phys. Rev. Lett.* **2012**, *109*, 041801. [[CrossRef](#)]
102. Greljo, A.; Soreq, Y.; Stangl, P.; Thomsen, A.E.; Zupan, J. Muonic force behind flavor anomalies. *J. High Energy Phys.* **2022**, *04*, 151. [[CrossRef](#)]
103. Hou, W.S. Enhanced charged Higgs boson effects in $B \rightarrow \tau$ anti-neutrino, μ anti-neutrino and $b \rightarrow \tau$ anti-neutrino + X. *Phys. Rev. D* **1993**, *48*, 2342–2344. [[CrossRef](#)]
104. Akeroyd, A.G.; Recksiegel, S. The Effect of H^{\pm} on $B^{\pm} \rightarrow \tau^{\pm} \nu(\tau)$ and $B^{\pm} \rightarrow \mu^{\pm} \nu$ muon neutrino. *J. Phys. G* **2003**, *29*, 2311–2317. [[CrossRef](#)]
105. Crivellin, A.; Greub, C.; Kokulu, A. Explaining $B \rightarrow D \tau \nu$, $B \rightarrow D^* \tau \nu$ and $B \rightarrow \tau \nu$ in a 2HDM of type III. *Phys. Rev. D* **2012**, *86*, 054014. [[CrossRef](#)]
106. He, X.G.; Valencia, G. B decays with τ leptons in nonuniversal left-right models. *Phys. Rev. D* **2013**, *87*, 014014. [[CrossRef](#)]
107. Dubnička, S.; Dubničková, A.Z.; Ivanov, M.A.; Liptaj, A.; Santorelli, P.; Tran, C.T. Study of $B_s \rightarrow \ell^+ \ell^- \gamma$ decays in covariant quark model. *Phys. Rev. D* **2019**, *99*, 014042. [[CrossRef](#)]
108. Bauer, C.W.; Ligeti, Z.; Luke, M.; Manohar, A.V.; Trott, M. Global analysis of inclusive B decays. *Phys. Rev. D* **2004**, *70*, 094017. [[CrossRef](#)]
109. Descotes-Genon, S.; Hurth, T.; Matias, J.; Virto, J. Optimizing the basis of $B \rightarrow K^* l l$ observables in the full kinematic range. *J. High Energy Phys.* **2013**, *5*, 137. [[CrossRef](#)]
110. Kozachuk, A.; Melikhov, D.; Nikitin, N. Rare FCNC radiative leptonic $B_{s,d} \rightarrow \gamma l^+ l^-$ decays in the standard model. *Phys. Rev. D* **2018**, *97*, 053007. [[CrossRef](#)]
111. Melikhov, D.; Kozachuk, A.; Nikitin, N. Rare FCNF radiative leptonic decays $B \rightarrow \gamma \ell^+ \ell^-$. *PoS* **2017**, *EPS-HEP2017*, 314. [[CrossRef](#)]
112. Wang, W.Y.; Xiong, Z.H.; Zhou, S.H. Complete Analyses on the Short-Distance Contribution of $B_s \rightarrow \ell^+ \ell^- \gamma$ in the Standard Model. *Chin. Phys. Lett.* **2013**, *30*, 111202. [[CrossRef](#)]

113. Ivanov, M.A.; Körner, J.G.; Tran, C.T. Exclusive decays $B \rightarrow \ell^- \bar{\nu}$ and $B \rightarrow D^{(*)} \ell^- \bar{\nu}$ in the covariant quark model. *Phys. Rev. D* **2015**, *92*, 114022. [[CrossRef](#)]
114. Ivanov, M.A.; Körner, J.G.; Tran, C.T. Looking for new physics in leptonic and semileptonic decays of B-meson. *Phys. Part. Nucl. Lett.* **2017**, *14*, 669–676. [[CrossRef](#)]
115. Amhis, Y.; Banerjee, Sw.; Ben-Haim, E.; Bertholet, E.; Bernlochner, F.U.; Bona, M.; Bozek, A.; Bozzi, C.; Brodzicka, J.; Chobanova, V.; et al. Averages of b-hadron, c-hadron, and τ -lepton properties as of 2021. *Phys. Rev. D* **2023**, *107*, 052008. [[CrossRef](#)]
116. Bernlochner, F.U.; Sevilla, M.F.; Robinson, D.J.; Wormser, G. Semitauonic b-hadron decays: A lepton flavor universality laboratory. *Rev. Mod. Phys.* **2022**, *94*, 015003. [[CrossRef](#)]
117. Crivellin, A.; Greub, C.; Müller, D.; Saturnino, F. Importance of Loop Effects in Explaining the Accumulated Evidence for New Physics in B Decays with a Vector Leptoquark. *Phys. Rev. Lett.* **2019**, *122*, 011805. [[CrossRef](#)] [[PubMed](#)]
118. LHCb Collaboration. Measurement of the Ratios of Branching Fractions $\mathcal{R}(D^*)$ and $\mathcal{R}(D^0)$. *arXiv* **2023**, arXiv:2302.02886.
119. LHCb Collaboration. Test of Lepton Universality in $b \rightarrow s \ell^+ \ell^-$ decays. *arXiv* **2022**, arXiv:2212.09152.
120. Puthumanai, R. Measurement of $R(D^*)$ with Hadronic τ^+ Decays at $\sqrt{s} = 13\text{TeV}$ TeV by the LHCb Collaboration (CERN Seminar). Available online: <https://indico.cern.ch/event/1231797/> (accessed on 21 March 2023).
121. Aaij, R.; Beteta, C. Abellán ; Adeva, B.; Adinolfi, M.; Adrover, C.; Affolder, A.; Ajaltouni, Z.; Albrecht, J.; Alessio, F.; Alexander, M.; et al. Differential branching fraction and angular analysis of the decay $B^0 \rightarrow K^{*0} \mu^+ \mu^-$. *J. High Energy Phys.* **2013**, *8*, 131. [[CrossRef](#)]
122. Aaij, R.; Adeva, B.; Adinolfi, M.; Adrover, C.; Affolder, A.; Ajaltouni, Z.; Albrecht, J.; Alessio, F.; Alexander, M.; Ali, S.; Alkhazov, G.; et al. Measurement of Form-Factor-Independent Observables in the Decay $B^0 \rightarrow K^{*0} \mu^+ \mu^-$. *Phys. Rev. Lett.* **2013**, *111*, 191801. [[CrossRef](#)]
123. Aaij, R.; Adeva, B.; Adinolfi, M.; Affolder, A.; Ajaltouni, Z.; Albrecht, J.; Alessio, F.; Alexander, M.; Ali, S.; Alkhazov, G.; et al. Differential branching fractions and isospin asymmetries of $B \rightarrow K^{(*)} \mu^+ \mu^-$ decays. *J. High Energy Phys.* **2014**, *6*, 133. [[CrossRef](#)]
124. Aaij, R.; Adeva, B.; Adinolfi, M.; Affolder, A.; Ajaltouni, Z.; Akar, S.; Albrecht, J.; Alessio, F.; Alexander, M.; Ali, S.; et al. Angular analysis of the $B^0 \rightarrow K^{*0} e^+ e^-$ decay in the low- q^2 region. *J. High Energy Phys.* **2015**, *4*, 64. [[CrossRef](#)]
125. Aaij, R.; Abellán Beteta, C.; Adeva, B.; Adinolfi, M.; Affolder, A.; Ajaltouni, Z.; Akar, S.; Albrecht, J.; Alessio, F.; Alexander, M.; et al. Angular analysis of the $B^0 \rightarrow K^{*0} \mu^+ \mu^-$ decay using 3 fb^{-1} of integrated luminosity. *J. High Energy Phys.* **2016**, *2*, 104. [[CrossRef](#)]
126. Aaij, R.; Adeva, B.; Adinolfi, M.; Ajaltouni, Z.; Akar, S.; Albrecht, J.; Alessio, F.; Alexander, M.; Ali, S.; Alkhazov, G.; et al. Test of lepton universality with $B^0 \rightarrow K^{*0} \ell^+ \ell^-$ decays. *J. High Energy Phys.* **2017**, *8*, 055. [[CrossRef](#)]
127. Aaij, R.; Abellán Beteta, C.; Ackernley, T.; Adeva, B.; Adinolfi, M.; Afsharnia, H.; Aidala, C.A.; Aiola, S.; Ajaltouni, Z.; Akar, S.; et al. Measurement of CP -Averaged Observables in the $B^0 \rightarrow K^{*0} \mu^+ \mu^-$ Decay. *Phys. Rev. Lett.* **2020**, *125*, 011802. [[CrossRef](#)]
128. Aaij, R.; Beteta, C. Abellán ; Ackernley, T.; Adeva, B.; Adinolfi, M.; Afsharnia, H.; Aidala, C.A.; Aiola, S.; Ajaltouni, Z.; Akar, S.; et al. Angular Analysis of the $B^+ \rightarrow K^{*+} \mu^+ \mu^-$ Decay. *Phys. Rev. Lett.* **2021**, *126*, 161802. [[CrossRef](#)]
129. Aaij, R.; Abdemottaleb, A. S.W.; Abellán Beteta, C.; Abudinén, F.; Ackernley, T.; Adeva, B.; Adinolfi, M.; Afsharnia, H.; Agapopoulou, C.; Aidala, C.A.; et al. Tests of lepton universality using $B^0 \rightarrow K_S^0 \ell^+ \ell^-$ and $B^+ \rightarrow K^{*+} \ell^+ \ell^-$ decays. *Phys. Rev. Lett.* **2022**, *128*, 191802. [[CrossRef](#)]
130. Aaij, R.; Beteta, C. Abellán ; Adametz, A.; Adeva, B.; Adinolfi, M.; Adrover, C.; Affolder, A.; Ajaltouni, Z.; Albrecht, J.; Alessio, F.; et al. Differential branching fraction and angular analysis of the $B^+ \rightarrow K^+ \mu^+ \mu^-$ decay. *J. High Energy Phys.* **2013**, *2*, 105. [[CrossRef](#)]
131. Aaij, R.; Adeva, B.; Adinolfi, M.; Affolder, A.; Ajaltouni, Z.; Akar, S.; Albrecht, J.; Alessio, F.; Alexander, M.; Ali, S.; et al. Test of lepton universality using $B^+ \rightarrow K^+ \ell^+ \ell^-$ decays. *Phys. Rev. Lett.* **2014**, *113*, 151601. [[CrossRef](#)] [[PubMed](#)]
132. Aaij, R.; Abellán Beteta, C.; Adeva, B.; Adinolfi, M.; Aidala, C.A.; Ajaltouni, Z.; Akar, S.; Albicocco, P.; Albrecht, J.; Alessio, F.; et al. Search for lepton-universality violation in $B^+ \rightarrow K^+ \ell^+ \ell^-$ decays. *Phys. Rev. Lett.* **2019**, *122*, 191801. [[CrossRef](#)]
133. Aaij, R.; Adeva, B.; Adinolfi, M.; Affolder, A.; Ajaltouni, Z.; Akar, S.; Albrecht, J.; Alessio, F.; Alexander, M.; Ali, S.; Alkhazov, G.; et al. Measurement of the ratio of branching fractions $\mathcal{B}(\bar{B}^0 \rightarrow D^{*+} \tau^- \bar{\nu}_\tau) / \mathcal{B}(\bar{B}^0 \rightarrow D^{*+} \mu^- \bar{\nu}_\mu)$. *Phys. Rev. Lett.* **2015**, *115*, 111803; Erratum in *Phys. Rev. Lett.* **2015**, *115*, 159901. [[CrossRef](#)]
134. Aaij, R.; Adeva, B.; Adinolfi, M.; Ajaltouni, Z.; Akar, S.; Albrecht, J.; Alessio, F.; Alexander, M.; Albero, A. Alfonso ; Ali, S.; et al. Measurement of the ratio of the $B^0 \rightarrow D^{*-} \tau^+ \nu_\tau$ and $B^0 \rightarrow D^{*-} \mu^+ \nu_\mu$ branching fractions using three-prong τ -lepton decays. *Phys. Rev. Lett.* **2018**, *120*, 171802. [[CrossRef](#)]
135. Aaij, R.; Adeva, B.; Adinolfi, M.; Ajaltouni, Z.; Akar, S.; Albrecht, J.; Alessio, F.; Alexander, M.; Albero, A. Alfonso ; Ali, S.; et al. Test of Lepton Flavor Universality by the measurement of the $B^0 \rightarrow D^{*-} \tau^+ \nu_\tau$ branching fraction using three-prong τ decays. *Phys. Rev. D* **2018**, *97*, 072013. [[CrossRef](#)]
136. Aaij, R.; Adeva, B.; Adinolfi, M.; Ajaltouni, Z.; Akar, S.; Albrecht, J.; Alessio, F.; Alexander, M.; Albero, A. Alfonso ; Ali, S.; et al. Measurement of the ratio of branching fractions $\mathcal{B}(B_c^+ \rightarrow J/\psi \tau^+ \nu_\tau) / \mathcal{B}(B_c^+ \rightarrow J/\psi \mu^+ \nu_\mu)$. *Phys. Rev. Lett.* **2018**, *120*, 121801. [[CrossRef](#)] [[PubMed](#)]
137. Aaij, R.; Abellán Beteta, C.; Adeva, B.; Adinolfi, M.; Adrover, C.; Affolder, A.; Ajaltouni, Z.; Albrecht, J.; Alessio, F.; Alexander, M.; et al. Differential branching fraction and angular analysis of the decay $B_s^0 \rightarrow \phi \mu^+ \mu^-$. *J. High Energy Phys.* **2013**, *7*, 84. [[CrossRef](#)]
138. Aaij, R.; Adeva, B.; Adinolfi, M.; Affolder, A.; Ajaltouni, Z.; Akar, S.; Albrecht, J.; Alessio, F.; Alexander, M.; Ali, S.; et al. Angular analysis and differential branching fraction of the decay $B_s^0 \rightarrow \phi \mu^+ \mu^-$. *J. High Energy Phys.* **2015**, *9*, 179. [[CrossRef](#)]

139. Aaij, R.; Abellán Beteta, C.; Ackernley, T.; Adeva, B.; Adinolfi, M.; Afsharnia, H.; Aidala, C.A.; Aiola, S.; Ajaltouni, Z.; Akar, S.; et al. Branching Fraction Measurements of the Rare $B_s^0 \rightarrow \phi\mu^+\mu^-$ and $B_s^0 \rightarrow f_2'(1525)\mu^+\mu^-$ Decays. *Phys. Rev. Lett.* **2021**, *127*, 151801. [[CrossRef](#)]
140. Aaij, R.; Beteta, C. Abellán; Ackernley, T.; Adeva, B.; Adinolfi, M.; Afsharnia, H.; Aidala, C.A.; Aiola, S.; Ajaltouni, Z.; Akar, S.; et al. Test of lepton universality in beauty-quark decays. *Nat. Phys.* **2022**, *18*, 277–282. [[CrossRef](#)]
141. Aubert, B.; Bona, M.; Boutigny, D.; Karyotakis, Y.; Lees, J.P.; Poireau, V.; Prudent, X.; Tisserand, V.; Zghiche, A.; Tico, J.G.; et al. Observation of the semileptonic decays $B \rightarrow D^*\tau^-\bar{\nu}(\tau)$ and evidence for $B \rightarrow D\tau^-\bar{\nu}(\tau)$. *Phys. Rev. Lett.* **2008**, *100*, 021801. [[CrossRef](#)]
142. Lees, J.P.; Poireau, V.; Tisserand, V.; Garra Tico, J.; Grauges, E.; Palano, A.; Eigen, G.; Stugu, B.; Brown, D.N.; Kerth, L.T.; et al. Evidence for an excess of $\bar{B} \rightarrow D^{(*)}\tau^-\bar{\nu}_\tau$ decays. *Phys. Rev. Lett.* **2012**, *109*, 101802. [[CrossRef](#)]
143. Lees, J.P.; Poireau, V.; Tisserand, V.; Grauges, E.; Palano, A.; Eigen, G.; Stugu, B.; Brown, D.N.; Kerth, L.T.; Kolomensky, Yu. G.; et al. Measurement of an Excess of $\bar{B} \rightarrow D^{(*)}\tau^-\bar{\nu}_\tau$ Decays and Implications for Charged Higgs Bosons. *Phys. Rev. D* **2013**, *88*, 072012. [[CrossRef](#)]
144. Aubert, B.; Karyotakis, Y.; Lees, J.P.; Poireau, V.; Principe, E.; Prudent, X.; Tisserand, V.; Tico, J. Garra; Grauges, E.; Martinelli, M.; et al. Measurement of $|V(cb)|$ and the Form-Factor Slope in anti-B \rightarrow D l anti-nu Decays in Events Tagged by a Fully Reconstructed B Meson. *Phys. Rev. Lett.* **2010**, *104*, 011802. [[CrossRef](#)]
145. Aubert, B.; Bona, M.; Boutigny, D.; Karyotakis, Y.; Lees, J.P.; Poireau, V.; Prudent, X.; Tisserand, V.; Zghiche, A.; Tico, J.G.; et al. Determination of the form-factors for the decay $B^0 \rightarrow D^{*-\ell^+\nu_l}$ and of the CKM matrix element $|V_{cb}|$. *Phys. Rev. D* **2008**, *77*, 032002. [[CrossRef](#)]
146. Aubert, B.; Bona, M.; Karyotakis, Y.; Lees, J.P.; Poireau, V.; Principe, E.; Prudent, X.; Tisserand, V.; Tico, J. Garra; Grauges, E.; et al. Measurements of the Semileptonic Decays anti-B \rightarrow D l anti-nu and anti-B \rightarrow D* l anti-nu Using a Global Fit to D X l anti-nu Final States. *Phys. Rev. D* **2009**, *79*, 012002. [[CrossRef](#)]
147. Lees, J.P.; Poireau, V.; Tisserand, V.; Grauges, E.; Palano, A.; Eigen, G.; Brown, D.N.; Kolomensky, Yu. G.; Fritsch, M.; Koch, H.; et al. Extraction of form Factors from a Four-Dimensional Angular Analysis of $\bar{B} \rightarrow D^*\ell^-\bar{\nu}_\ell$. *Phys. Rev. Lett.* **2019**, *123*, 091801. [[CrossRef](#)] [[PubMed](#)]
148. Aubert, B.; Barate, R.; Boutigny, D.; Gaillard, J. -M.; Hicheur, A.; Karyotakis, Y.; Lees, J.P.; Robbe, P.; Tisserand, V.; Zghiche, A.; et al. Evidence for the rare decay $B \rightarrow K^*\ell^+\ell^-$ and measurement of the $B \rightarrow K\ell^+\ell^-$ branching fraction. *Phys. Rev. Lett.* **2003**, *91*, 221802. [[CrossRef](#)] [[PubMed](#)]
149. Aubert, B.; Barate, R.; Bona, M.; Boutigny, D.; Couderc, F.; Karyotakis, Y.; Lees, J.P.; Poireau, V.; Tisserand, V.; Zghiche, A.; et al. Measurements of branching fractions, rate asymmetries, and angular distributions in the rare decays $B \rightarrow K\ell^+\ell^-$ and $B \rightarrow K^*\ell^+\ell^-$. *Phys. Rev. D* **2006**, *73*, 092001. [[CrossRef](#)]
150. Aubert, B.; Bona, M.; Karyotakis, Y.; Lees, J.P.; Poireau, V.; Principe, E.; Prudent, X.; Tisserand, V.; Garra Tico, J.; Grauges, E.; et al. Direct CP, Lepton Flavor and Isospin Asymmetries in the Decays $B \rightarrow K^{(*)}\ell^+\ell^-$. *Phys. Rev. Lett.* **2009**, *102*, 091803. [[CrossRef](#)] [[PubMed](#)]
151. Lees, J.P.; Poireau, V.; Tisserand, V.; Garra Tico, J.; Grauges, E.; Palano, A.; Eigen, G.; Stugu, B.; Brown, D.N.; Kerth, L.T.; et al. Measurement of Branching Fractions and Rate Asymmetries in the Rare Decays $B \rightarrow K^{(*)}l^+l^-$. *Phys. Rev. D* **2012**, *86*, 032012. [[CrossRef](#)]
152. Aubert, B.; Bona, M.; Karyotakis, Y.; Lees, J.P.; Poireau, V.; Prudent, X.; Tisserand, V.; Zghiche, A.; Tico, J. Garra; Grauges, E.; et al. Angular Distributions in the Decays $B \rightarrow K^*l^+l^-$. *Phys. Rev. D* **2009**, *79*, 031102. [[CrossRef](#)]
153. Lees, J.P.; Poireau, V.; Tisserand, V.; Grauges, E.; Palano, A.; Eigen, G.; Stugu, B.; Brown, D.N.; Kerth, L.T.; Kolomensky, Yu. G.; et al. Measurement of angular asymmetries in the decays $B \rightarrow K^*\ell^+\ell^-$. *Phys. Rev. D* **2016**, *93*, 052015. [[CrossRef](#)]
154. Aubert, B.; Bona, M.; Boutigny, D.; Karyotakis, Y.; Lees, J.P.; Poireau, V.; Prudent, X.; Tisserand, V.; Zghiche, A.; Grauges, E.; et al. Measurement of the $B^0 \rightarrow \pi^-\ell^+\nu$ form-factor shape and branching fraction, and determination of $|V_{ub}|$ with a loose neutrino reconstruction technique. *Phys. Rev. Lett.* **2007**, *98*, 091801. [[CrossRef](#)]
155. Del Amo Sanchez, P.; Lees, J.P.; Poireau, V.; Principe, E.; Tisserand, V.; Garra Tico, J.; Grauges, E.; Martinelli, M.; Palano, A.; Pappagallo, M.; et al. Study of $B \rightarrow \pi\ell\nu$ and $B \rightarrow \rho\ell\nu$ Decays and Determination of $|V_{ub}|$. *Phys. Rev. D* **2011**, *83*, 032007. [[CrossRef](#)]
156. Aubert, B.; Barate, R.; Boutigny, D.; Couderc, F.; Gaillard, J. -M.; Hicheur, A.; Karyotakis, Y.; Lees, J.P.; Tisserand, V.; Zghiche, A.; et al. Measurement of the $B \rightarrow X_s\ell^+\ell^-$ branching fraction with a sum over exclusive modes. *Phys. Rev. Lett.* **2004**, *93*, 081802. [[CrossRef](#)] [[PubMed](#)]
157. Lees, J.P.; Poireau, V.; Tisserand, V.; Grauges, E.; Palano, A.; Eigen, G.; Stugu, B.; Brown, D.N.; Kerth, L.T.; Kolomensky, Yu. G.; et al. Measurement of the $B \rightarrow X_s l^+ l^-$ branching fraction and search for direct CP violation from a sum of exclusive final states. *Phys. Rev. Lett.* **2014**, *112*, 211802. [[CrossRef](#)]
158. Aubert, B.; Barate, R.; Boutigny, D.; Gaillard, J. -M.; Hicheur, A.; Karyotakis, Y.; Lees, J.P.; Robbe, P.; Tisserand, V.; Zghiche, A.; et al. Measurement of the inclusive charmless semileptonic branching ratio of B mesons and determination of $|V_{ub}|$. *Phys. Rev. Lett.* **2004**, *92*, 071802. [[CrossRef](#)]
159. Lees, J.P.; Poireau, V.; Tisserand, V.; Garra Tico, J.; Grauges, E.; Palano, A.; Eigen, G.; Stugu, B.; Brown, D.N.; Kerth, L.T.; et al. Branching fraction and form-factor shape measurements of exclusive charmless semileptonic B decays, and determination of $|V_{ub}|$. *Phys. Rev. D* **2012**, *86*, 092004. [[CrossRef](#)]

160. Lees, J.P.; Poireau, V.; Tisserand, V.; Grauges, E.; Palano, A.; Eigen, G.; Brown, D.N.; Kolomensky, Yu. G.; Koch, H.; Schroeder, T.; et al. Measurement of the inclusive electron spectrum from B meson decays and determination of $|V_{ub}|$. *Phys. Rev. D* **2017**, *95*, 072001. [[CrossRef](#)]
161. Lees, J.P.; Poireau, V.; Tisserand, V.; Grauges, E.; Palanoab, A.; Eigen, G.; Stugu, B.; Brown, D. N.; Kerth, L.T.; Kolomensky, Yu. G.; et al. Observation of $\bar{B} \rightarrow D^{(*)}\pi^+\pi^-\ell^-\bar{\nu}$ decays in e^+e^- collisions at the Y(4S) resonance. *Phys. Rev. Lett.* **2016**, *116*, 041801. [[CrossRef](#)]
162. Bozek, A.; Rozanska, M.; Adachi, I.; Aihara, H.; Arinstein, K.; Aulchenko, V.; Aushev, T.; Aziz, T.; Bakich, A.M.; Bhardwaj, V.; et al. Observation of $B^+ \rightarrow \bar{D}^*0\tau^+\nu_\tau$ and Evidence for $B^+ \rightarrow \bar{D}^*0\tau^+\nu_\tau$ at Belle. *Phys. Rev. D* **2010**, *82*, 072005. [[CrossRef](#)]
163. Huschle, M.; Kuhr, T.; Heck, M.; Goldenzweig, P.; Abdesselam, A.; Adachi, I.; Adamczyk, K.; Aihara, H.; Said, S. Al ; Arinstein, K.; et al. Measurement of the branching ratio of $\bar{B} \rightarrow D^{(*)}\tau^-\bar{\nu}_\tau$ relative to $\bar{B} \rightarrow D^{(*)}\ell^-\bar{\nu}_\ell$ decays with hadronic tagging at Belle. *Phys. Rev. D* **2015**, *92*, 072014. [[CrossRef](#)]
164. Abdesselam, A.; Adachi, I.; Adamczyk, K.; Aihara, H.; Said, S.A.; Arinstein, K.; Arita, Y.; Asner, D.M.; Aso, T.; Atmacan, H.; et al. Measurement of $\mathcal{R}(D)$ and $\mathcal{R}(D^*)$ with a semileptonic tagging method. *arXiv* **2019**, arXiv:1904.08794.
165. Caria, G.; Urquijo, P.; Adachi, I.; Aihara, H.; Al Said, S.; Asner, D.M.; Atmacan, H.; Aushev, T.; Babu, V.; Badhrees, I.; et al. Measurement of $\mathcal{R}(D)$ and $\mathcal{R}(D^*)$ with a semileptonic tagging method. *Phys. Rev. Lett.* **2020**, *124*, 161803. [[CrossRef](#)]
166. Abudinén, F.; Adachi, I.; Adamczyk, K.; Aggarwal, L.; Ahlburg, P.; Ahmed, H.; Ahn, J.K.; Aihara, H.; et al. Measurement of the $B^0 \rightarrow D^{*-}\ell^+\nu_\ell$ branching ratio and $|V_{cb}|$ with a fully reconstructed accompanying B meson in 2019–2021 Belle II data. *arXiv* **2023**, arXiv:2301.04716.
167. Matyja, A.; Rozanska, M.; Adachi, I.; Aihara, H.; Aulchenko, V.; Aushev, T.; Bahinipati, S.; Bakich, A.M.; Balagura, V.; Barberio, E.; et al. Observation of $B^0 \rightarrow D^{*-}\tau^+\nu_\tau$ decay at Belle. *Phys. Rev. Lett.* **2007**, *99*, 191807. [[CrossRef](#)] [[PubMed](#)]
168. Dungen, W.; Schwanda, C.; Adachi, I.; Aihara, H.; Aushev, T.; Aziz, T.; Bakich, A.M.; Balagura, V.; Barberio, E.; Bischofberger, M.; et al. Measurement of the form factors of the decay $B^0 \rightarrow D^{*-}\ell^+\nu_\ell$ and determination of the CKM matrix element $|V_{cb}|$. *Phys. Rev. D* **2010**, *82*, 112007. [[CrossRef](#)]
169. Sato, Y.; Iijima, T.; Adamczyk, K.; Aihara, H.; Asner, D.M.; Atmacan, H.; Aushev, T.; Ayad, R.; Aziz, T.; Babu, V.; et al. Measurement of the branching ratio of $\bar{B}^0 \rightarrow D^{*+}\tau^-\bar{\nu}_\tau$ relative to $\bar{B}^0 \rightarrow D^{*+}\ell^-\bar{\nu}_\ell$ decays with a semileptonic tagging method. *Phys. Rev. D* **2016**, *94*, 072007. [[CrossRef](#)]
170. Hirose, S.; Iijima, T.; Adachi, I.; Adamczyk, K.; Aihara, H.; Al Said, S.; Asner, D.M.; Atmacan, H.; Aulchenko, V.; Aushev, T.; et al. Measurement of the τ lepton polarization and $R(D^*)$ in the decay $\bar{B} \rightarrow D^*\tau^-\bar{\nu}_\tau$. *Phys. Rev. Lett.* **2017**, *118*, 211801. [[CrossRef](#)]
171. Hirose, S.; Iijima, T.; Adachi, I.; Adamczyk, K.; Aihara, H.; Al Said, S.; Asner, D.M.; Atmacan, H.; Aushev, T.; Ayad, R.; et al. Measurement of the τ lepton polarization and $R(D^*)$ in the decay $\bar{B} \rightarrow D^*\tau^-\bar{\nu}_\tau$ with one-prong hadronic τ decays at Belle. *Phys. Rev. D* **2018**, *97*, 012004. [[CrossRef](#)]
172. Waheed, E.; Urquijo, P.; Ferlewicz, D.; Adachi, I.; Adamczyk, K.; Aihara, H.; Al Said, S.; Asner, D.M.; Atmacan, H.; Aushev, T.; et al. Measurement of the CKM matrix element $|V_{cb}|$ from $B^0 \rightarrow D^{*-}\ell^+\nu_\ell$ at Belle. *Phys. Rev. D* **2019**, *100*, 052007; Erratum in *Phys. Rev. D* **2021**, *103*, 079901. [[CrossRef](#)]
173. Glattauer, R.; Schwanda, C.; Abdesselam, A.; Adachi, I.; Adamczyk, K.; Aihara, H.; Al Said, S.; Asner, D.M.; Aushev, T.; Ayad, R.; et al. Measurement of the decay $B \rightarrow D\ell\nu_\ell$ in fully reconstructed events and determination of the Cabibbo-Kobayashi-Maskawa matrix element $|V_{cb}|$. *Phys. Rev. D* **2016**, *93*, 032006. [[CrossRef](#)]
174. Abudinén, F.; Adachi, I.; Adamczyk, K.; Aggarwal, L.; Ahlburg, P.; Ahmed, H.; Ahn, J.K.; Aihara, H.; Akopov, N.; Aloisio, A.; et al. Determination of $|V_{cb}|$ from $B \rightarrow D\ell\nu$ decays using 2019–2021 Belle II data. *arXiv* **2022**, arXiv:2210.13143.
175. Meier, F.; Vossen, A.; Adachi, I.; Adamczyk, K.; Aihara, H.; Al Said, S.; Asner, D.M.; Atmacan, H.; Aushev, T.; Ayad, R.; et al. First observation of $B \rightarrow \bar{D}^*(\rightarrow \bar{D}\pi^+\pi^-)\ell^+\nu_\ell$ and measurement of the $B \rightarrow \bar{D}^{(*)}\pi\ell^+\nu_\ell$ and $B \rightarrow \bar{D}^{(*)}\pi^+\pi^-\ell^+\nu_\ell$ branching fractions with hadronic tagging at Belle. *arXiv* **2022**, arXiv:2211.09833.
176. Abe, K.; Abe, K.; Abe, R.; Adachi, I.; Ahn, B.S.; Aihara, H.; Akatsu, M.; Asano, Y.; Aso, T.; Aulchenko, V.; et al. Observation of the decay $B \rightarrow K\ell^+\ell^-$. *Phys. Rev. Lett.* **2002**, *88*, 021801. [[CrossRef](#)] [[PubMed](#)]
177. Choudhury, S.; Sandilya, S.; Trabelsi, K.; Giri, A.; Aihara, H.; Al Said, S.; Asner, D.M.; Atmacan, H.; Aulchenko, V.; Aushev, T.; et al. Test of lepton flavor universality and search for lepton flavor violation in $B \rightarrow K\ell\ell$ decays. *J. High Energy Phys.* **2021**, *03*, 105. [[CrossRef](#)]
178. Ishikawa, A.; Abe, K.; Adachi, I.; Aihara, H.; Anipko, D.; Asano, Y.; Aushev, T.; Bakich, A.M.; Balagura, V.; Barbero, M.; et al. Measurement of Forward-Backward Asymmetry and Wilson Coefficients in $B \rightarrow K^*l^+l^-$. *Phys. Rev. Lett.* **2006**, *96*, 251801. [[CrossRef](#)]
179. Wehle, S.; Niebuhr, C.; Yashchenko, S.; Adachi, I.; Aihara, H.; Said, S. Al ; Asner, D.M.; Aulchenko, V.; Aushev, T.; Ayad, R.; et al. Lepton-Flavor-Dependent Angular Analysis of $B \rightarrow K^*\ell^+\ell^-$. *Phys. Rev. Lett.* **2017**, *118*, 111801. [[CrossRef](#)]
180. Wehle, S.; Adachi, I.; Adamczyk, K.; Aihara, H.; Asner, D.M.; Atmacan, H.; Aulchenko, V.; Aushev, T.; Ayad, R.; Babu, V.; et al. Test of Lepton-Flavor Universality in $B \rightarrow K^*\ell^+\ell^-$ Decays at Belle. *Phys. Rev. Lett.* **2021**, *126*, 161801. [[CrossRef](#)]
181. Wei, J. -T.; Chang, P.; Adachi, I.; Aihara, H.; Aulchenko, V.; Aushev, T.; Bakich, A.M.; Balagura, V.; Barberio, E.; Bondar, A.; et al. Measurement of the Differential Branching Fraction and Forward-Backward Asymmetry for $B \rightarrow K^{(*)}\ell^+\ell^-$. *Phys. Rev. Lett.* **2009**, *103*, 171801. [[CrossRef](#)]
182. Ha, H.; Won, E.; Adachi, I.; Aihara, H.; Aziz, T.; Bakich, A.M.; Balagura, V.; Barberio, E.; Bay, A.; Belous, K.; et al. Measurement of the decay $B^0 \rightarrow \pi^-\ell^+\nu$ and determination of $|V_{ub}|$. *Phys. Rev. D* **2011**, *83*, 071101. [[CrossRef](#)]

183. Adamczyk, K.; Aggarwal, L.; Ahlburg, P.; Ahmed, H.; Ahn, J.K.; Aihara, H.; Akopov, N.; Aloisio, A.; Ameli, F.; Andricek, L.; et al. Determination of $|V_{ub}|$ from untagged $B^0 \rightarrow \pi^- \ell^+ \nu_\ell$ decays using 2019–2021 Belle II data. *arXiv* **2022**, arXiv:2210.04224.
184. Abudinén, F.; Adachi, I.; Adamczyk, K.; Aggarwal, L.; Ahlburg, P.; Ahmed, H.; Ahn, J.K.; Aihara, H.; Akopov, N.; Aloisio, A.; et al. Reconstruction of $B \rightarrow \rho \ell \nu_\ell$ decays identified using hadronic decays of the recoil B meson in 2019–2021 Belle II data. *arXiv* **2022**, arXiv:2211.15270.
185. Gebauer, U.; Beleño, C.; Frey, A.; Adachi, I.; Adamczyk, K.; Aihara, H.; Al Said, S.; Asner, D.M.; Atmacan, H.; Aushev, T.; et al. Measurement of the branching fractions of the $B^+ \rightarrow \eta \ell^+ \nu_\ell$ and $B^+ \rightarrow \eta' \ell^+ \nu_\ell$ decays with signal-side only reconstruction in the full q^2 range. *Phys. Rev. D* **2022**, *106*, 032013. [[CrossRef](#)]
186. Kaneko, J.; Abe, K.; Abe, K.; Abe, T.; Adachi, I.; Ahn, Byoung Sup; Aihara, H.; Akatsu, M.; Asano, Y.; Aso, T.; et al. Measurement of the electroweak penguin process $B \rightarrow X(s) l^+ l^-$. *Phys. Rev. Lett.* **2003**, *90*, 021801. [[CrossRef](#)]
187. Iwasaki, M.; Itoh, K.; Aihara, H.; Abe, K.; Abe, K.; Adachi, I.; Asano, Y.; Aushev, T.; Bahinipati, S.; Bakich, A.M.; et al. Improved measurement of the electroweak penguin process $B \rightarrow X_s l^+ l^-$. *Phys. Rev. D* **2005**, *72*, 092005. [[CrossRef](#)]
188. Cao, L.; Sutcliffe, W.; Van Tonder, R.; Bernlochner, F.U.; Adachi, I.; Aihara, H.; Asner, D.M.; Aushev, T.; Babu, V.; Bahinipati, S.; et al. Measurement of Differential Branching Fractions of Inclusive $B \rightarrow X_u \ell^+ \nu_\ell$ Decays. *Phys. Rev. Lett.* **2021**, *127*, 261801. [[CrossRef](#)] [[PubMed](#)]
189. Cao, L.; Sutcliffe, W.; Van Tonder, R.; Bernlochner, F.U.; Adachi, I.; Aihara, H.; Al Said, S.; Asner, D.M.; Atmacan, H.; Aushev, T.; et al. Measurements of Partial Branching Fractions of Inclusive $B \rightarrow X_u \ell^+ \nu_\ell$ Decays with Hadronic Tagging. *Phys. Rev. D* **2021**, *104*, 012008. [[CrossRef](#)]
190. Sibidanov, A.; Varvell, K.E.; Adachi, I.; Aihara, H.; Asner, D.M.; Aulchenko, V.; Aushev, T.; Bakich, A.M.; Bala, A.; Bozek, A.; et al. Study of Exclusive $B \rightarrow X_u \ell \nu$ Decays and Extraction of $\|V_{ub}\|$ using Full Reconstruction Tagging at the Belle Experiment. *Phys. Rev. D* **2013**, *88*, 032005. [[CrossRef](#)]
191. van Tonder, R.; Cao, L.; Sutcliffe, W.; Welsch, M.; Bernlochner, F.U.; Adachi, I.; Aihara, H.; Asner, D.M.; Aushev, T.; Ayad, R.; et al. Measurements of q^2 Moments of Inclusive $B \rightarrow X_c \ell^+ \nu_\ell$ Decays with Hadronic Tagging. *Phys. Rev. D* **2021**, *104*, 112011. [[CrossRef](#)]
192. Abudinén, F.; Adamczyk, K.; Aggarwal, L.; Ahmed, H.; Aihara, H.; Akopov, N.; Aloisio, A.; Anh Ky, N.; Asner, D.M.; Atmacan, H.; et al. Measurement of lepton mass squared moments in B to $X_c \ell \nu \ell$ decays with the Belle II experiment. *Phys. Rev. D* **2023**, *107*, 072002. [[CrossRef](#)]
193. Aggarwal, L.; Ahmed, H.; Aihara, H.; Akopov, N.; Aloisio, A.; Ky, N.A.; Asner, D.M.; Atmacan, H.; Aushev, T.; Aushev, V.; et al. A test of light-lepton universality in the rates of inclusive semileptonic B -meson decays at Belle II. *arXiv* **2023**, arXiv:2301.08266.
194. Altmannshofer, W.; Ball, P.; Bharucha, A.; Buras, A.J.; Straub, D.M.; Wick, M. Symmetries and Asymmetries of $B \rightarrow K^* \mu^+ \mu^-$ Decays in the Standard Model and Beyond. *J. High Energy Phys.* **2009**, *01*, 019. [[CrossRef](#)]
195. Calibbi, L.; Signorelli, G. Charged Lepton Flavour Violation: An Experimental and Theoretical Introduction. *Riv. Nuovo Cim.* **2018**, *41*, 71–174. [[CrossRef](#)]
196. Blake, T.; Lanfranchi, G.; Straub, D.M. Rare B Decays as Tests of the Standard Model. *Prog. Part. Nucl. Phys.* **2017**, *92*, 50–91. [[CrossRef](#)]
197. Bifani, S.; Descotes-Genon, S.; Romero Vidal, A.; Schune, M.H. Review of Lepton Universality tests in B decays. *J. Phys. G* **2019**, *46*, 023001. [[CrossRef](#)]
198. Cornella, C.; Faroughy, D.A.; Fuentes-Martin, J.; Isidori, G.; Neubert, M. Reading the footprints of the B-meson flavor anomalies. *J. High Energy Phys.* **2021**, *08*, 050. [[CrossRef](#)]
199. London, D.; Matias, J. B Flavour Anomalies: 2021 Theoretical Status Report. *Ann. Rev. Nucl. Part. Sci.* **2022**, *72*, 37–68. [[CrossRef](#)]
200. Isgur, N.; Scora, D.; Grinstein, B.; Wise, M.B. Semileptonic B and D Decays in the Quark Model. *Phys. Rev. D* **1989**, *39*, 799–818. [[CrossRef](#)]
201. Scora, D.; Isgur, N. Semileptonic meson decays in the quark model: An update. *Phys. Rev. D* **1995**, *52*, 2783–2812. [[CrossRef](#)] [[PubMed](#)]
202. Boyd, C.G.; Grinstein, B.; Lebed, R.F. Model independent determinations of anti- $B \rightarrow D$ (lepton), D^* (lepton) anti-neutrino form-factors. *Nucl. Phys. B* **1996**, *461*, 493–511. [[CrossRef](#)]
203. Boyd, C.G.; Grinstein, B.; Lebed, R.F. Precision corrections to dispersive bounds on form-factors. *Phys. Rev. D* **1997**, *56*, 6895–6911. [[CrossRef](#)]
204. Caprini, I.; Lellouch, L.; Neubert, M. Dispersive bounds on the shape of anti- $B \rightarrow D^*$ lepton anti-neutrino form-factors. *Nucl. Phys. B* **1998**, *530*, 153–181. [[CrossRef](#)]
205. Ball, P.; Zwicky, R. $B_{d,s} \rightarrow \rho, \omega, K^*, \phi$ decay form-factors from light-cone sum rules revisited. *Phys. Rev. D* **2005**, *71*, 014029. [[CrossRef](#)]
206. Bobeth, C.; Hiller, G.; Piranishvili, G. Angular distributions of $\bar{B} \rightarrow \bar{K} \ell^+ \ell^-$ decays. *J. High Energy Phys.* **2007**, *12*, 040. [[CrossRef](#)]
207. Khodjamirian, A.; Mannel, T.; Pivovarov, A.A.; Wang, Y.M. Charm-loop effect in $B \rightarrow K^{(*)} \ell^+ \ell^-$ and $B \rightarrow K^* \gamma$. *J. High Energy Phys.* **2010**, *09*, 089. [[CrossRef](#)]
208. Bailey, Jon A.; Bazavov, A.; Bernard, C.; Bouchard, C.M.; DeTar, C.; Du, Daping; El-Khadra, A.X.; Foley, J.; Freeland, E.D.; Gámiz, E.; et al. Update of $|V_{cb}|$ from the $\bar{B} \rightarrow D^* \ell \bar{\nu}$ form factor at zero recoil with three-flavor lattice QCD. *Phys. Rev. D* **2014**, *89*, 114504. [[CrossRef](#)]

209. Na, H.; Bouchard, C.M.; Lepage, G.P.; Monahan, C.; Shigemitsu, J. $B \rightarrow Dlv$ form factors at nonzero recoil and extraction of $|V_{cb}|$. *Phys. Rev. D* **2015**, *92*, 054510; Erratum in *Phys. Rev. D* **2016**, *93*, 119906. [[CrossRef](#)]
210. Harrison, J.; Davies, C.; Wingate, M. Lattice QCD calculation of the $B_{(s)} \rightarrow D_{(s)}^* \ell \nu$ form factors at zero recoil and implications for $|V_{cb}|$. *Phys. Rev. D* **2018**, *97*, 054502. [[CrossRef](#)]
211. Du, D.; El-Khadra, A.X.; Gottlieb, S.; Kronfeld, A.S.; Laiho, J.; Lunghi, E.; Van de Water, R.S.; Zhou, R. Phenomenology of semileptonic B-meson decays with form factors from lattice QCD. *Phys. Rev. D* **2016**, *93*, 034005. [[CrossRef](#)]
212. Alberti, A.; Gambino, P.; Healey, K.J.; Nandi, S. Precision Determination of the Cabibbo-Kobayashi-Maskawa Element V_{cb} . *Phys. Rev. Lett.* **2015**, *114*, 061802. [[CrossRef](#)]
213. Bharucha, A.; Straub, D.M.; Zwicky, R. $B \rightarrow V \ell^+ \ell^-$ in the Standard Model from light-cone sum rules. *J. High Energy Phys.* **2016**, *08*, 098. [[CrossRef](#)]
214. Bigi, D.; Gambino, P. Revisiting $B \rightarrow D \ell \nu$. *Phys. Rev. D* **2016**, *94*, 094008. [[CrossRef](#)]
215. Bordone, M.; Isidori, G.; Pattori, A. On the Standard Model predictions for R_K and R_{K^*} . *Eur. Phys. J. C* **2016**, *76*, 440. [[CrossRef](#)]
216. Jäger, S.; Martin Camalich, J. Reassessing the discovery potential of the $B \rightarrow K^* \ell^+ \ell^-$ decays in the large-recoil region: SM challenges and BSM opportunities. *Phys. Rev. D* **2016**, *93*, 014028. [[CrossRef](#)]
217. Capdevila, B.; Descotes-Genon, S.; Hofer, L.; Matias, J. Hadronic uncertainties in $B \rightarrow K^* \mu^+ \mu^-$: a state-of-the-art analysis. *J. High Energy Phys.* **2017**, *04*, 016. [[CrossRef](#)]
218. Bigi, D.; Gambino, P.; Schacht, S. $R(D^*)$, $|V_{cb}|$, and the Heavy Quark Symmetry relations between form factors. *J. High Energy Phys.* **2017**, *11*, 061. [[CrossRef](#)]
219. Jaiswal, S.; Nandi, S.; Patra, S.K. Extraction of $|V_{cb}|$ from $B \rightarrow D^{(*)} \ell \nu_\ell$ and the Standard Model predictions of $R(D^{(*)})$. *J. High Energy Phys.* **2017**, *12*, 060. [[CrossRef](#)]
220. Isidori, G.; Nabeebaccus, S.; Zwicky, R. QED corrections in $\bar{B} \rightarrow \bar{K} \ell^+ \ell^-$ at the double-differential level. *J. High Energy Phys.* **2020**, *12*, 104. [[CrossRef](#)]
221. Gubernari, N.; van Dyk, D.; Virto, J. Non-local matrix elements in $B_{(s)} \rightarrow \{K^{(*)}, \phi\} \ell^+ \ell^-$. *J. High Energy Phys.* **2021**, *02*, 088. [[CrossRef](#)]
222. Iguro, S.; Kitahara, T.; Watanabe, R. Global fit to $b \rightarrow c \tau \nu$ anomalies 2022 mid-autumn. *arXiv* **2022**, arXiv:2210.10751.
223. Hiller, G.; Kruger, F. More model-independent analysis of $b \rightarrow s$ processes. *Phys. Rev. D* **2004**, *69*, 074020. [[CrossRef](#)]
224. Fajfer, S.; Kamenik, J.F.; Nisandzic, I. On the $B \rightarrow D^* \tau \bar{\nu}_\tau$ Sensitivity to New Physics. *Phys. Rev. D* **2012**, *85*, 094025. [[CrossRef](#)]
225. Hiller, G.; Schmaltz, M. R_K and future $b \rightarrow s \ell \ell$ physics beyond the standard model opportunities. *Phys. Rev. D* **2014**, *90*, 054014. [[CrossRef](#)]
226. Fajfer, S.; Košnik, N. Vector leptoquark resolution of R_K and $R_{D^{(*)}}$ puzzles. *Phys. Lett. B* **2016**, *755*, 270–274. [[CrossRef](#)]
227. Crivellin, A.; Müller, D.; Ota, T. Simultaneous explanation of $R(D^{(*)})$ and $b \rightarrow s \mu^+ \mu^-$: the last scalar leptoquarks standing. *J. High Energy Phys.* **2017**, *09*, 040. [[CrossRef](#)]
228. Angelescu, A.; Bečirević, D.; Faroughy, D.A.; Jaffredo, F.; Sumensari, O. Single leptoquark solutions to the B-physics anomalies. *Phys. Rev. D* **2021**, *104*, 055017. [[CrossRef](#)]
229. Abada, A.; Krauss, M.E.; Porod, W.; Staub, F.; Vicente, A.; Weiland, C. Lepton flavor violation in low-scale seesaw models: SUSY and non-SUSY contributions. *J. High Energy Phys.* **2014**, *11*, 048. [[CrossRef](#)]
230. Gripaos, B.; Nardecchia, M.; Renner, S.A. Composite leptoquarks and anomalies in B-meson decays. *J. High Energy Phys.* **2015**, *05*, 006. [[CrossRef](#)]
231. Crivellin, A.; D'Ambrosio, G.; Heeck, J. Explaining $h \rightarrow \mu^\pm \tau^\mp$, $B \rightarrow K^* \mu^+ \mu^-$ and $B \rightarrow K \mu^+ \mu^- / B \rightarrow K e^+ e^-$ in a two-Higgs-doublet model with gauged $L_\mu - L_\tau$. *Phys. Rev. Lett.* **2015**, *114*, 151801. [[CrossRef](#)]
232. Descotes-Genon, S.; Hofer, L.; Matias, J.; Virto, J. Global analysis of $b \rightarrow s \ell \ell$ anomalies. *J. High Energy Phys.* **2016**, *06*, 092. [[CrossRef](#)]
233. Altmannshofer, W.; Stangl, P.; Straub, D.M. Interpreting Hints for Lepton Flavor Universality Violation. *Phys. Rev. D* **2017**, *96*, 055008. [[CrossRef](#)]
234. Algueró, M.; Capdevila, B.; Crivellin, A.; Descotes-Genon, S.; Masjuan, P.; Matias, J.; Novoa Brunet, M.; Virto, J. Emerging patterns of New Physics with and without Lepton Flavour Universal contributions. *Eur. Phys. J. C* **2019**, *79*, 714; Addendum *Eur. Phys. J. C* **2020**, *80*, 511. [[CrossRef](#)]
235. Hurth, T.; Mahmoudi, F.; Santos, D.M.; Neshatpour, S. More Indications for Lepton Nonuniversality in $b \rightarrow s \ell^+ \ell^-$. *Phys. Lett. B* **2022**, *824*, 136838. [[CrossRef](#)]
236. Dubnička, S.; Dubničková, A.Z.; Issadykov, A.; Ivanov, M.A.; Liptaj, A.; Sakhiyev, S.K. Decay $B_s \rightarrow \phi \ell^+ \ell^-$ in covariant quark model. *Phys. Rev. D* **2016**, *93*, 094022. [[CrossRef](#)]
237. Aaij, R.; Abdelmotteleb, A. S.W.; Abellán Beteta, C.; Ackernley, T.; Adeva, B.; Adinolfi, M.; Afsharnia, H.; Agapopoulou, C.; Aidala, C.A.; Aiola, S.; et al. Angular analysis of the rare decay $B_s^0 \rightarrow \phi \mu^+ \mu^-$. *J. High Energy Phys.* **2021**, *11*, 043. [[CrossRef](#)]
238. Asatryan, H.H.; Asatrian, H.M.; Greub, C.; Walker, M. Calculation of two loop virtual corrections to $b \rightarrow s \ell^+ \ell^-$ in the standard model. *Phys. Rev. D* **2002**, *65*, 074004. [[CrossRef](#)]
239. Greub, C.; Pilipp, V.; Schupbach, C. Analytic calculation of two-loop QCD corrections to $b \rightarrow s \ell^+ \ell^-$ in the high q^2 region. *J. High Energy Phys.* **2008**, *12*, 040. [[CrossRef](#)]

240. Aaboud, M.; Aad, G.; Abbott, B.; Abidinov, O.; Abeloos, B.; Abidi, S.H.; AbouZeid, O.S.; Abraham, N.L.; Abramowicz, H.; Abreu, H.; et al. Angular analysis of $B_d^0 \rightarrow K^* \mu^+ \mu^-$ decays in pp collisions at $\sqrt{s} = 8$ TeV with the ATLAS detector. *J. High Energy Phys.* **2018**, *10*, 047. [[CrossRef](#)]
241. Ivanov, M.A.; Khomutenko, O.E. B and D meson decays with taking into account confinement of light quarks. *Sov. J. Nucl. Phys.* **1991**, *53*, 337–342.
242. Ivanov, M.A.; Khomutenko, O.E.; Mizutani, T. Form-factors of semileptonic decays of heavy mesons in the quark confinement model. *Phys. Rev. D* **1992**, *46*, 3817–3831. [[CrossRef](#)] [[PubMed](#)]
243. Ivanov, M.A.; Santorelli, P. Leptonic and semileptonic decays of pseudoscalar mesons. *Phys. Lett. B* **1999**, *456*, 248–255. [[CrossRef](#)]
244. Ivanov, M.A.; Santorelli, P.; Tancredi, N. The Semileptonic form-factors of B and D mesons in the quark confinement model. *Eur. Phys. J. A* **2000**, *9*, 109–114. [[CrossRef](#)]
245. Ivanov, M.A.; Korner, J.G.; Santorelli, P. The Semileptonic decays of the B_c meson. *Phys. Rev. D* **2001**, *63*, 074010. [[CrossRef](#)]
246. Ivanov, M.A.; Lyubovitskij, V.E. Exclusive rare decays of B and B_c mesons in a relativistic quark model. *Lect. Notes Phys.* **2004**, *647*, 245–263. [[CrossRef](#)]
247. Ivanov, M.A.; Korner, J.G.; Santorelli, P. Semileptonic decays of B_c mesons into charmonium states in a relativistic quark model. *Phys. Rev. D* **2005**, *71*, 094006; Erratum in *Phys. Rev. D* **2007**, *75*, 019901. [[CrossRef](#)]
248. Ivanov, M.A.; Korner, J.G.; Santorelli, P. Exclusive semileptonic and nonleptonic decays of the B_c meson. *Phys. Rev. D* **2006**, *73*, 054024. [[CrossRef](#)]
249. Ivanov, M.A.; Korner, J.G.; Kovalenko, S.G.; Santorelli, P.; Saidullaeva, G.G. Form factors for semileptonic, nonleptonic and rare B (B_s) meson decays. *Phys. Rev. D* **2012**, *85*, 034004. [[CrossRef](#)]
250. Dineykhon, M.; Ivanov, M.A.; Saidullaeva, G.G. Exotic states and rare B/s-decays in the covariant quark model. *Phys. Part. Nucl.* **2012**, *43*, 749–782. [[CrossRef](#)]
251. Issadykov, A.; Ivanov, M.A.; Sakhiyev, S.K. Form factors of the B-S-transitions in the covariant quark model. *Phys. Rev. D* **2015**, *91*, 074007. [[CrossRef](#)]
252. Ivanov, M.A.; Körner, J.G.; Tran, C.T. Analyzing new physics in the decays $\bar{B}^0 \rightarrow D^{(*)} \tau^- \bar{\nu}_\tau$ with form factors obtained from the covariant quark model. *Phys. Rev. D* **2016**, *94*, 094028. [[CrossRef](#)]
253. Ivanov, M.A.; Körner, J.G.; Tran, C.T. Probing new physics in $\bar{B}^0 \rightarrow D^{(*)} \tau^- \bar{\nu}_\tau$ using the longitudinal, transverse, and normal polarization components of the tau lepton. *Phys. Rev. D* **2017**, *95*, 036021. [[CrossRef](#)]
254. Tran, C.T.; Ivanov, M.A.; Körner, J.G.; Santorelli, P. Implications of new physics in the decays $B_c \rightarrow (J/\psi, \eta_c) \tau \nu$. *Phys. Rev. D* **2018**, *97*, 054014. [[CrossRef](#)]
255. Issadykov, A.; Ivanov, M.A. The decays $B_c \rightarrow J/\psi + \bar{\ell} \nu_\ell$ and $B_c \rightarrow J/\psi + \pi(K)$ in covariant confined quark model. *Phys. Lett. B* **2018**, *783*, 178–182. [[CrossRef](#)]
256. Issadykov, A.; Ivanov, M.A. b-s Anomaly Decays in Covariant Quark Model. *Phys. Part. Nucl. Lett.* **2018**, *15*, 393–396. [[CrossRef](#)]
257. Issadykov, A.; Ivanov, M.A. $B \rightarrow K^{(*)} \nu \bar{\nu}$ in covariant confined quark model. *Mod. Phys. Lett. A* **2023**, *38*, 2350006. [[CrossRef](#)]
258. Aaij, R.; Adeva, B.; Adinolfi, M.; Adrover, C.; Affolder, A.; Ajaltouni, Z.; Albrecht, J.; Alessio, F.; Alexander, M.; Alvarez Cartelle, P.; et al. First observation of $B_s^0 \rightarrow J/\psi f_0(980)$ decays. *Phys. Lett. B* **2011**, *698*, 115–122. [[CrossRef](#)]
259. Aaij, R.; Abellan Beteta, C.; Adeva, B.; Adinolfi, M.; Adrover, C.; Affolder, A.; Ajaltouni, Z.; Albrecht, J.; Alessio, F.; Alexander, M.; et al. Observation of $B_c^+ \rightarrow J/\psi D_s^+$ and $B_c^+ \rightarrow J/\psi D_s^{*+}$ decays. *Phys. Rev. D* **2013**, *87*, 112012; Erratum *Phys. Rev. D* **2014**, *89*, 019901. [[CrossRef](#)]
260. Aaij, R.; Adeva, B.; Adinolfi, M.; Adrover, C.; Affolder, A.; Ajaltouni, Z.; Albrecht, J.; Alessio, F.; Alexander, M.; Ali, S.; et al. Observation of the Decay $B_c^+ \rightarrow B_s^0 \pi^+$. *Phys. Rev. Lett.* **2013**, *111*, 181801. [[CrossRef](#)]
261. LHCb Collaboration. First observation of the $B^+ \rightarrow D_s^+ D_s^- K^+$ decay. *arXiv* **2022**, arXiv:2211.05034.
262. LHCb Collaboration. Observation of the $B_s^0 \rightarrow D^{*+} D^{*-}$ decay. *arXiv* **2022**, arXiv:2210.14945.
263. LHCb Collaboration. Observation of the $B^+ \rightarrow J/\psi \eta' K^+$ decay. *arXiv* **2023**, arXiv:2303.09443.
264. LHCb Collaboration. Observation of the $B_s^0 \rightarrow \chi_{c1}(3872) \pi^+ \pi^-$ decay. *arXiv* **2023**, arXiv:2302.10629.
265. Aaij, R.; Abellan Beteta, C.; Adeva, B.; Adinolfi, M.; Adrover, C.; Affolder, A.; Ajaltouni, Z.; Albrecht, J.; Alessio, F.; Alexander, M.; et al. Determination of the X(3872) meson quantum numbers. *Phys. Rev. Lett.* **2013**, *110*, 222001. [[CrossRef](#)]
266. Aaij, R.; Abellan Beteta, C.; Adeva, B.; Adinolfi, M.; Adrover, C.; Affolder, A.; Ajaltouni, Z.; Albrecht, J.; Alessio, F.; Alexander, M.; et al. Analysis of the resonant components in $B_s \rightarrow J/\psi \pi^+ \pi^-$. *Phys. Rev. D* **2012**, *86*, 052006. [[CrossRef](#)]
267. Aaij, R.; Adeva, B.; Adinolfi, M.; Affolder, A.; Ajaltouni, Z.; Albrecht, J.; Alessio, F.; Alexander, M.; Ali, S.; Alkhazov, G.; et al. Measurement of resonant and CP components in $\bar{B}_s^0 \rightarrow J/\psi \pi^+ \pi^-$ decays. *Phys. Rev. D* **2014**, *89*, 092006. [[CrossRef](#)]
268. Aaij, R.; Adeva, B.; Adinolfi, M.; Affolder, A.; Ajaltouni, Z.; Albrecht, J.; Alessio, F.; Alexander, M.; Ali, S.; Alkhazov, G.; et al. Measurement of the resonant and CP components in $\bar{B}^0 \rightarrow J/\psi \pi^+ \pi^-$ decays. *Phys. Rev. D* **2014**, *90*, 012003. [[CrossRef](#)]
269. Aaij, R.; Adeva, B.; Adinolfi, M.; Ajaltouni, Z.; Akar, S.; Albrecht, J.; Alessio, F.; Alexander, M.; Ali, S.; Alkhazov, G.; et al. Observation of $J/\psi \phi$ structures consistent with exotic states from amplitude analysis of $B^+ \rightarrow J/\psi \phi K^+$ decays. *Phys. Rev. Lett.* **2017**, *118*, 022003. [[CrossRef](#)]
270. Aaij, R.; Abellan Beteta, C.; Ackernley, T.; Adeva, B.; Adinolfi, M.; Afsharnia, H.; Aidala, C.A.; Aiola, S.; Ajaltouni, Z.; Akar, S.; et al. Observation of New Resonances Decaying to $J/\psi K^{++}$ and $J/\psi \phi$. *Phys. Rev. Lett.* **2021**, *127*, 082001. [[CrossRef](#)]
271. LHCb Collaboration. Observation of a $J/\psi \Lambda$ resonance consistent with a strange pentaquark candidate in $B^- \rightarrow J/\psi \Lambda \bar{p}$ decays. *arXiv* **2022**, arXiv:2210.10346.

272. LHCb Collaboration. Observation of a resonant structure near the $D_s^+ D_s^-$ threshold in the $B^+ \rightarrow D_s^+ D_s^- K^+$ decay. *arXiv* **2022**, arXiv:2210.15153.
273. Aaij, R.; Abellán Beteta, C.; Ackernley, T.; Adeva, B.; Adinolfi, M.; Afsharnia, H.; Aidala, C.A.; Aiola, S.; Ajaltouni, Z.; Akar, S.; et al. A model-independent study of resonant structure in $B^+ \rightarrow D^+ D^- K^+$ decays. *Phys. Rev. Lett.* **2020**, *125*, 242001. [[CrossRef](#)]
274. Aaij, R.; Abdelmotteleb, A. S.W.; Abellán Beteta, C.; Ackernley, T.; Adeva, B.; Adinolfi, M.; Afsharnia, H.; Aidala, C.A.; Aiola, S.; Ajaltouni, Z.; et al. Evidence for a new structure in the $J/\psi p$ and $J/\psi \bar{p}$ systems in $B_s^0 \rightarrow J/\psi p \bar{p}$ decays. *Phys. Rev. Lett.* **2022**, *128*, 062001. [[CrossRef](#)]
275. LHCb Collaboration. Evidence of a $J/\psi K_S^0$ structure in $B^0 \rightarrow J/\psi K_S^0$ decays. *arXiv* **2023**, arXiv:2301.04899.
276. Aaij, R.; Adeva, B.; Adinolfi, M.; Affolder, A.; Ajaltouni, Z.; Akar, S.; Albrecht, J.; Alessio, F.; Alexander, M.; Ali, S.; et al. Dalitz plot analysis of $B_s^0 \rightarrow \bar{D}^0 K^- \pi^+$ decays. *Phys. Rev. D* **2014**, *90*, 072003. [[CrossRef](#)]
277. Aaij, R.; Adeva, B.; Adinolfi, M.; Affolder, A.; Ajaltouni, Z.; Akar, S.; Albrecht, J.; Alessio, F.; Alexander, M.; Ali, S.; et al. Dalitz plot analysis of $B^0 \rightarrow \bar{D}^0 \pi^+ \pi^-$ decays. *Phys. Rev. D* **2015**, *92*, 032002. [[CrossRef](#)]
278. Aaij, R.; Adeva, B.; Adinolfi, M.; Ajaltouni, Z.; Akar, S.; Albrecht, J.; Alessio, F.; Alexander, M.; Ali, S.; Alkhazov, G.; et al. Amplitude analysis of $B^- \rightarrow D^+ \pi^- \pi^-$ decays. *Phys. Rev. D* **2016**, *94*, 072001. [[CrossRef](#)]
279. Aaij, R.; Adeva, B.; Adinolfi, M.; Ajaltouni, Z.; Akar, S.; Albrecht, J.; Alessio, F.; Alexander, M.; Ali, S.; Alkhazov, G.; et al. Amplitude analysis of $B^+ \rightarrow J/\psi \phi K^+$ decays. *Phys. Rev. D* **2017**, *95*, 012002. [[CrossRef](#)]
280. Aaij, R.; Abellán Beteta, C.; Ackernley, T.; Adeva, B.; Adinolfi, M.; Afsharnia, H.; Aidala, C.A.; Aiola, S.; Ajaltouni, Z.; Akar, S.; et al. Amplitude analysis of the $B^+ \rightarrow D^+ D^- K^+$ decay. *Phys. Rev. D* **2020**, *102*, 112003. [[CrossRef](#)]
281. LHCb Collaboration. Amplitude analysis of the $D_s^+ \rightarrow \pi^- \pi^+ \pi^+$ decay. *arXiv* **2022**, arXiv:2209.09840.
282. LHCb Collaboration. Amplitude analysis of $B^0 \rightarrow \bar{D}^0 D_s^+ \pi^-$ and $B^+ \rightarrow D^- D_s^+ \pi^+$ decays. *arXiv* **2022**, arXiv:2212.02717.
283. Aaij, R.; Abellán Beteta, C.; Adeva, B.; Adinolfi, M.; Adrover, C.; Affolder, A.; Ajaltouni, Z.; Albrecht, J.; Alessio, F.; Alexander, M.; et al. Measurement of the CP-violating phase ϕ_s in the decay $B_s^0 \rightarrow J/\psi \phi$. *Phys. Rev. Lett.* **2012**, *108*, 101803. [[CrossRef](#)]
284. Aaij, R.; Abellán Beteta, C.; Adeva, B.; Adinolfi, M.; Adrover, C.; Affolder, A.; Ajaltouni, Z.; Albrecht, J.; Alessio, F.; Alexander, M.; et al. First evidence of direct CP violation in charmless two-body decays of B_s^0 mesons. *Phys. Rev. Lett.* **2012**, *108*, 201601. [[CrossRef](#)]
285. Aaij, R.; Adeva, B.; Adinolfi, M.; Adrover, C.; Affolder, A.; Ajaltouni, Z.; Albrecht, J.; Alessio, F.; Alexander, M.; Alkhazov, G.; et al. Measurement of the $B_s^0 - \bar{B}_s^0$ oscillation frequency Δm_s in $B_s^0 \rightarrow D_s^- (3)\pi$ decays. *Phys. Lett. B* **2012**, *709*, 177–184. [[CrossRef](#)]
286. Aaij, R.; Adeva, B.; Adinolfi, M.; Adrover, C.; Affolder, A.; Ajaltouni, Z.; Albrecht, J.; Alessio, F.; Alexander, M.; Ali, S.; et al. Measurement of CP violation in the phase space of $B^\pm \rightarrow K^\pm \pi^+ \pi^-$ and $B^\pm \rightarrow K^\pm K^+ K^-$ decays. *Phys. Rev. Lett.* **2013**, *111*, 101801. [[CrossRef](#)]
287. Aaij, R.; Adeva, B.; Adinolfi, M.; Adrover, C.; Affolder, A.; Ajaltouni, Z.; Albrecht, J.; Alessio, F.; Alexander, M.; Ali, S.; et al. Measurement of CP violation in the phase space of $B^\pm \rightarrow K^+ K^- \pi^\pm$ and $B^\pm \rightarrow \pi^+ \pi^- \pi^\pm$ decays. *Phys. Rev. Lett.* **2014**, *112*, 011801. [[CrossRef](#)]
288. Aaij, R.; Abellán Beteta, C.; Adeva, B.; Adinolfi, M.; Adrover, C.; Affolder, A.; Ajaltouni, Z.; Albrecht, J.; Alessio, F.; Alexander, M.; et al. Precision measurement of the $B_s^0 - \bar{B}_s^0$ oscillation frequency with the decay $B_s^0 \rightarrow D_s^- \pi^+$. *New J. Phys.* **2013**, *15*, 053021. [[CrossRef](#)]
289. Aaij, R.; Abellán Beteta, C.; Adeva, B.; Adinolfi, M.; Adrover, C.; Affolder, A.; Ajaltouni, Z.; Albrecht, J.; Alessio, F.; Alexander, M.; et al. Observation of CP violation in $B^\pm \rightarrow DK^\pm$ decays. *Phys. Lett. B* **2012**, *712*, 203–212; Erratum in *Phys. Lett. B* **2012**, *713*, 351. [[CrossRef](#)]
290. Aaij, R.; Abellán Beteta, C.; Adeva, B.; Adinolfi, M.; Adrover, C.; Affolder, A.; Ajaltouni, Z.; Albrecht, J.; Alessio, F.; Alexander, M.; et al. First observation of CP violation in the decays of B_s^0 mesons. *Phys. Rev. Lett.* **2013**, *110*, 221601. [[CrossRef](#)] [[PubMed](#)]
291. Aaij, R.; Abellán Beteta, C.; Adeva, B.; Adinolfi, M.; Adrover, C.; Affolder, A.; Ajaltouni, Z.; Albrecht, J.; Alessio, F.; Alexander, M.; et al. Measurement of CP violation and the B_s^0 meson decay width difference with $B_s^0 \rightarrow J/\psi K^+ K^-$ and $B_s^0 \rightarrow J/\psi \pi^+ \pi^-$ decays. *Phys. Rev. D* **2013**, *87*, 112010. [[CrossRef](#)]
292. Aaij, R.; Adeva, B.; Adinolfi, M.; Affolder, A.; Ajaltouni, Z.; Akar, S.; Albrecht, J.; Alessio, F.; Alexander, M.; Ali, S.; et al. Measurement of the CP-violating phase ϕ_s in $\bar{B}_s^0 \rightarrow J/\psi \pi^+ \pi^-$ decays. *Phys. Lett. B* **2014**, *736*, 186–195. [[CrossRef](#)]
293. Aaij, R.; Adeva, B.; Adinolfi, M.; Affolder, A.; Ajaltouni, Z.; Akar, S.; Albrecht, J.; Alessio, F.; Alexander, M.; Ali, S.; et al. Measurement of CP violation in $B^0 \rightarrow J/\psi K_S^0$ decays. *Phys. Rev. Lett.* **2015**, *115*, 031601. [[CrossRef](#)]
294. Aaij, R.; Adeva, B.; Adinolfi, M.; Affolder, A.; Ajaltouni, Z.; Akar, S.; Albrecht, J.; Alessio, F.; Alexander, M.; Ali, S.; et al. Precision measurement of CP violation in $B_s^0 \rightarrow J/\psi K^+ K^-$ decays. *Phys. Rev. Lett.* **2015**, *114*, 041801. [[CrossRef](#)]
295. LHCb Collaboration. Measurement of the CKM angle γ with $B^\pm \rightarrow D[K^\mp \pi^\pm \pi^\pm \pi^\mp] h^\pm$ decays using a binned phase-space approach. *arXiv* **2022**, arXiv:2209.03692.
296. LHCb Collaboration. A study of CP violation in the decays $B^\pm \rightarrow [K^+ K^- \pi^+ \pi^-]_D h^\pm$ ($h = K, \pi$) and $B^\pm \rightarrow [\pi^+ \pi^- \pi^+ \pi^-]_D h^\pm$. *arXiv* **2023**, arXiv:2301.10328.
297. Aaij, R.; Abellán Beteta, C.; Adametz, A.; Adeva, B.; Adinolfi, M.; Adrover, C.; Affolder, A.; Ajaltouni, Z.; Albrecht, J.; Alessio, F.; et al. Measurements of B_c^+ production and mass with the $B_c^+ \rightarrow J/\psi \pi^+$ decay. *Phys. Rev. Lett.* **2012**, *109*, 232001. [[CrossRef](#)] [[PubMed](#)]

298. Aaij, R.; Abellan Beteta, C.; Adeva, B.; Adinolfi, M.; Adrover, C.; Affolder, A.; Ajaltouni, Z.; Albrecht, J.; Alessio, F.; Alexander, M.; et al. Measurement of b -hadron branching fractions for two-body decays into charmless charged hadrons. *J. High Energy Phys.* **2012**, *10*, 037. [[CrossRef](#)]
299. Aaij, R.; Abellan Beteta, C.; Adametz, A.; Adeva, B.; Adinolfi, M.; Adrover, C.; Affolder, A.; Ajaltouni, Z.; Albrecht, J.; Alessio, F.; et al. Measurement of the ratio of branching fractions $BR(B_0 \rightarrow K^{*0}\gamma)/BR(B_{s0} \rightarrow \phi\gamma)$ and the direct CP asymmetry in $B_0 \rightarrow K^{*0}\gamma$. *Nucl. Phys. B* **2013**, *867*, 1–18. [[CrossRef](#)]
300. Aaij, R.; Abellan Beteta, C.; Adametz, A.; Adeva, B.; Adinolfi, M.; Adrover, C.; Affolder, A.; Ajaltouni, Z.; Albrecht, J.; Alessio, F.; et al. Measurement of the fragmentation fraction ratio f_s/f_d and its dependence on B meson kinematics. *J. High Energy Phys.* **2013**, *04*, 001. [[CrossRef](#)]
301. Aaij, R.; Abellán Beteta, C.; Adeva, B.; Adinolfi, M.; Aidala, C.A.; Ajaltouni, Z.; Akar, S.; Albicocco, P.; Albrecht, J.; Alessio, F.; et al. Measurement of b hadron fractions in 13 TeV pp collisions. *Phys. Rev. D* **2019**, *100*, 031102. [[CrossRef](#)]
302. Aaij, R.; Beteta, C. Abellán; Ackernley, T.; Adeva, B.; Adinolfi, M.; Afsharnia, H.; Aidala, C.A.; Aiola, S.; Ajaltouni, Z.; Akar, S.; et al. Precise measurement of the f_s/f_d ratio of fragmentation fractions and of B_s^0 decay branching fractions. *Phys. Rev. D* **2021**, *104*, 032005. [[CrossRef](#)]
303. LHCb Collaboration. Study of B_c^+ meson decays to charmonia plus multihadron final states. *arXiv* **2022**, arXiv:2208.08660.
304. LHCb Collaboration. Measurement of the ratio of branching fractions $\mathcal{B}(B_c^+ \rightarrow B_s^0\pi^+)/\mathcal{B}(B_c^+ \rightarrow J/\psi\pi^+)$. *arXiv* **2022**, arXiv:2210.12000.
305. LHCb Collaboration. Study of the $B^- \rightarrow \Lambda_c^+ \bar{\Lambda}_c^- K^-$ decay. *arXiv* **2022**, arXiv:2211.00812.
306. Aaij, R.; Abdelmotteleb, A. S.W.; Abellan Beteta, C.; Abudinén, F.; Ackernley, T.; Adeva, B.; Adinolfi, M.; Adlarson, P.; Afsharnia, H.; Agapopoulou, C.; et al. Study of charmonium decays to $K_S^0 K\pi$ in the $B \rightarrow (K_S^0 K\pi)K$ channels. *arXiv* **2023**, arXiv:2304.14891.
307. Aubert, B.; Boutigny, D.; Gaillard, J. -M.; Hicheur, A.; Karyotakis, Y.; Lees, J.P.; Robbe, P.; Tisserand, V.; Palano, A.; Chen, G.P.; et al. Observation of CP violation in the B^0 meson system. *Phys. Rev. Lett.* **2001**, *87*, 091801. [[CrossRef](#)]
308. Aubert, B.; Boutigny, D.; de Bonis, I.; Gaillard, J. -M.; Jeremie, A.; Karyotakis, Y.; Lees, J.P.; Robbe, P.; Tisserand, V.; Palano, A.; et al. Measurement of CP violating asymmetries in B^0 decays to CP eigenstates. *Phys. Rev. Lett.* **2001**, *86*, 2515–2522. [[CrossRef](#)] [[PubMed](#)]
309. Aubert, B.; Boutigny, D.; Gaillard, J.-M.; Hicheur, A.; Karyotakis, Y.; Lees, J.P.; Robbe, P.; Tisserand, V.; Zghich, A.; Palano, A.; et al. Measurement of $\sin 2\beta$ in $B^0 \rightarrow \phi K_S^0$. In Proceedings of the 31st International Conference on High Energy Physics, Amsterdam, The Netherlands, 25–31 July 2002.
310. Aubert, B.; Boutigny, D.; Gaillard, J. -M.; Hicheur, A.; Karyotakis, Y.; Lees, J.P.; Robbe, P.; Tisserand, V.; Palano, A.; Pompili, A.; et al. A study of time dependent CP-violating asymmetries and flavor oscillations in neutral B decays at the $Y(4S)$. *Phys. Rev. D* **2002**, *66*, 032003. [[CrossRef](#)]
311. Aubert, B.; Barate, R.; Boutigny, D.; Couderc, F.; Gaillard, J. -M.; Hicheur, A.; Karyotakis, Y.; Lees, J.P.; Tisserand, V.; Zghiche, A.; et al. Observation of direct CP violation in $B^0 \rightarrow K^+ \pi^-$ decays. *Phys. Rev. Lett.* **2004**, *93*, 131801. [[CrossRef](#)]
312. Aubert, B.; Barate, R.; Boutigny, D.; Couderc, F.; Gaillard, J. -M.; Hicheur, A.; Karyotakis, Y.; Lees, J.P.; Tisserand, V.; Zghiche, A.; et al. Improved measurement of CP asymmetries in $B^0 \rightarrow (c\bar{c})K^{(*)0}$ decays. *Phys. Rev. Lett.* **2005**, *94*, 161803. [[CrossRef](#)]
313. Aubert, B.; Barate, R.; Boutigny, D.; Couderc, F.; Gaillard, J. -M.; Karyotakis, Y.; Lees, J.P.; Poireau, V.; Tisserand, V.; Zghiche, A.; et al. Ambiguity-free measurement of $\cos(2\beta)$: Time-integrated and time-dependent angular analyses of $B \rightarrow J/\psi K\pi$. *Phys. Rev. D* **2005**, *71*, 032005. [[CrossRef](#)]
314. Aubert, B.; Bona, M.; Boutigny, D.; Karyotakis, Y.; Lees, J.P.; Poireau, V.; Prudent, X.; Tisserand, V.; Zghiche, A.; Garra Tico, J.; et al. Observation of CP violation in $B^0 \rightarrow K^+ \pi^-$ and $B^0 \rightarrow \pi^+ \pi^-$. *Phys. Rev. Lett.* **2007**, *99*, 021603. [[CrossRef](#)]
315. Aubert, B.; Karyotakis, Y.; Lees, J.P.; Poireau, V.; Prencipe, E.; Prudent, X.; Tisserand, V.; Tico, J. Garra; Grauges, E.; Lopez, L.; et al. Measurement of Time-Dependent CP Asymmetry in $B^0 \rightarrow c$ anti- c $K^{(*)0}$ Decays. *Phys. Rev. D* **2009**, *79*, 072009. [[CrossRef](#)]
316. Adachi, I.; Adye, T.; Ahmed, H.; Ahn, J.K.; Aihara, H.; Akar, S.; Alam, M.S.; Albert, J.; Anulli, F.; Arnaud, N.; et al. Measurement of $\cos 2\beta$ in $B^0 \rightarrow D^{(*)} h^0$ with $D \rightarrow K_S^0 \pi^+ \pi^-$ decays by a combined time-dependent Dalitz plot analysis of BaBar and Belle data. *Phys. Rev. D* **2018**, *98*, 112012. [[CrossRef](#)]
317. Aubert, B.; Bona, M.; Karyotakis, Y.; Lees, J.P.; Poireau, V.; Prencipe, E.; Prudent, X.; Tisserand, V.; Garra Tico, J.; Grauges, E.; et al. Evidence for Direct CP Violation from Dalitz-plot analysis of $B^\pm \rightarrow K^\pm \pi^\mp \pi^\pm$. *Phys. Rev. D* **2008**, *78*, 012004. [[CrossRef](#)]
318. Del Amo Sanchez, P.; Lees, J.P.; Poireau, V.; Prencipe, E.; Tisserand, V.; Garra Tico, J.; Grauges, E.; Martinelli, M.; Palano, A.; Pappagallo, M.; et al. Evidence for direct CP violation in the measurement of the Cabibbo-Kobayashi-Maskawa angle gamma with $B^+ \rightarrow D^{(*)} K^{*+}$ decays. *Phys. Rev. Lett.* **2010**, *105*, 121801. [[CrossRef](#)] [[PubMed](#)]
319. Lees, J.P.; Poireau, V.; Tisserand, V.; Garra Tico, J.; Grauges, E.; Milanese, D.A.; Palano, A.; Pappagallo, M.; Eigen, G.; Stugu, B.; et al. Study of CP violation in Dalitz-plot analyses of $B^0 \rightarrow K+K-K0(S)$, $B^+ \rightarrow K+K-K+$, and $B^+ \rightarrow K0(S)K0(S)K+$. *Phys. Rev. D* **2012**, *85*, 112010. [[CrossRef](#)]
320. Lees, J.P.; Poireau, V.; Tisserand, V.; Garra Tico, J.; Grauges, E.; Palano, A.; Eigen, G.; Stugu, B.; Brown, D.N.; Kerth, L.T.; et al. Measurement of $\mathcal{B}(B \rightarrow X_s \gamma)$, the $B \rightarrow X_s \gamma$ photon energy spectrum, and the direct CP asymmetry in $B \rightarrow X_{s+d} \gamma$ decays. *Phys. Rev. D* **2012**, *86*, 112008. [[CrossRef](#)]
321. Aubert, B.; Boutigny, D.; Gaillard, J. -M.; Hicheur, A.; Karyotakis, Y.; Lees, J.P.; Robbe, P.; Tisserand, V.; Palano, A.; Chen, G.P.; et al. Measurement of branching fractions and search for CP-violating charge asymmetries in charmless two-body B decays into pions and kaons. *Phys. Rev. Lett.* **2001**, *87*, 151802. [[CrossRef](#)] [[PubMed](#)]

322. Aubert, B.; Boutigny, D.; Gaillard, J. -M.; Hicheur, A.; Karyotakis, Y.; Lees, J.P.; Robbe, P.; Tisserand, V.; Zghiche, A.; Palano, A.; et al. Measurements of branching fractions and CP-violating asymmetries in $B^0 \rightarrow \pi^+ \pi^-, K^+ \pi^-, K^+ K^-$ decays. *Phys. Rev. Lett.* **2002**, *89*, 281802. [[CrossRef](#)]
323. Aubert, B.; Barate, R.; Boutigny, D.; Gaillard, J. -M.; Hicheur, A.; Karyotakis, Y.; Lees, J.P.; Robbe, P.; Tisserand, V.; Zghiche, A.; et al. Measurements of branching fractions and CP-violating asymmetries in $B^0 \rightarrow \rho^\pm h^\mp$ decays. *Phys. Rev. Lett.* **2003**, *91*, 201802. [[CrossRef](#)]
324. Aubert, B.; Barate, R.; Boutigny, D.; Couderc, F.; Gaillard, J. -M.; Hicheur, A.; Karyotakis, Y.; Lees, J.P.; Tisserand, V.; Zghiche, A.; et al. Measurement of branching fractions, and CP and isospin asymmetries, for $B \rightarrow K^* \gamma$. *Phys. Rev. D* **2004**, *70*, 112006. [[CrossRef](#)]
325. Aubert, B.; Barate, R.; Bona, M.; Boutigny, D.; Couderc, F.; Karyotakis, Y.; Lees, J.P.; Poireau, V.; Tisserand, V.; Zghiche, A.; et al. Measurement of the branching fraction and photon energy moments of $B \rightarrow X_s \gamma$ and $A_{CP}(B \rightarrow X_{s+d} \gamma)$. *Phys. Rev. Lett.* **2006**, *97*, 171803. [[CrossRef](#)]
326. Lees, J.P.; Poireau, V.; Tisserand, V.; Garra Tico, J.; Grauges, E.; Palano, A.; Eigen, G.; Stugu, B.; Brown, D.N.; Kerth, L.T.; et al. Precision Measurement of the $B \rightarrow X_s \gamma$ Photon Energy Spectrum, Branching Fraction, and Direct CP Asymmetry $A_{CP}(B \rightarrow X_{s+d} \gamma)$. *Phys. Rev. Lett.* **2012**, *109*, 191801. [[CrossRef](#)] [[PubMed](#)]
327. Aubert, B.; Barate, R.; Boutigny, D.; Couderc, F.; Gaillard, J. -M.; Hicheur, A.; Karyotakis, Y.; Lees, J.P.; Tisserand, V.; Zghiche, A.; et al. Study of the decay $B^0(\bar{B}^0) \rightarrow \rho^+ \rho^-$, and constraints on the CKM angle α . *Phys. Rev. Lett.* **2004**, *93*, 231801. [[CrossRef](#)] [[PubMed](#)]
328. Aubert, B.; Barate, R.; Boutigny, D.; Couderc, F.; Karyotakis, Y.; Lees, J.P.; Poireau, V.; Tisserand, V.; Zghiche, A.; Grauges, E.; et al. Measurement of γ in $B^\mp \rightarrow D^{(*)} K^\mp$ decays with a Dalitz analysis of $D \rightarrow K_S^0 \pi^- \pi^+$. *Phys. Rev. Lett.* **2005**, *95*, 121802. [[CrossRef](#)] [[PubMed](#)]
329. Aubert, B.; Bona, M.; Boutigny, D.; Karyotakis, Y.; Lees, J.P.; Poireau, V.; Prudent, X.; Tisserand, V.; Zghiche, A.; Tico, J.G.; et al. A Study of $B^0 \rightarrow \rho^+ \rho^-$ Decays and Constraints on the CKM Angle α . *Phys. Rev. D* **2007**, *76*, 052007. [[CrossRef](#)]
330. Aubert, B.; Bona, M.; Karyotakis, Y.; Lees, J.P.; Poireau, V.; Principe, E.; Prudent, X.; Tisserand, V.; Garra Tico, J.; Grauges, E.; et al. Improved measurement of the CKM angle γ in $B^\mp \rightarrow D^{(*)} K^{(*)\mp}$ decays with a Dalitz plot analysis of D decays to $K_S^0 \pi^+ \pi^-$ and $K_S^0 K^+ K^-$. *Phys. Rev. D* **2008**, *78*, 034023. [[CrossRef](#)]
331. Aubert, B.; Boutigny, D.; Gaillard, J. -M.; Hicheur, A.; Karyotakis, Y.; Lees, J.P.; Robbe, P.; Tisserand, V.; Palano, A.; Chen, G.P.; et al. Measurement of the $B \rightarrow J/\psi K^*(892)$ decay amplitudes. *Phys. Rev. Lett.* **2001**, *87*, 241801. [[CrossRef](#)]
332. Aubert, B.; Boutigny, D.; Gaillard, J. -M.; Hicheur, A.; Karyotakis, Y.; Lees, J.P.; Robbe, P.; Tisserand, V.; Palano, A.; Chen, G.P.; et al. Measurement of branching fractions for exclusive B decays to charmonium final states. *Phys. Rev. D* **2002**, *65*, 032001. [[CrossRef](#)]
333. Aubert, B.; Barate, R.; Boutigny, D.; Gaillard, J. -M.; Hicheur, A.; Karyotakis, Y.; Lees, J.P.; Robbe, P.; Tisserand, V.; Zghiche, A.; et al. Rates, polarizations, and asymmetries in charmless vector-vector B meson decays. *Phys. Rev. Lett.* **2003**, *91*, 171802. [[CrossRef](#)]
334. Aubert, B.; Barate, R.; Boutigny, D.; Couderc, F.; Gaillard, J. -M.; Hicheur, A.; Karyotakis, Y.; Lees, J.P.; Tisserand, V.; Zghiche, A.; et al. Measurement of the $B^0 \rightarrow \phi K^0$ decay amplitudes. *Phys. Rev. Lett.* **2004**, *93*, 231804. [[CrossRef](#)]
335. Aubert, B.; Barate, R.; Boutigny, D.; Couderc, F.; Karyotakis, Y.; Lees, J.P.; Poireau, V.; Tisserand, V.; Zghiche, A.; Grauges, E.; et al. Measurements of the $B \rightarrow X_s \gamma$ branching fraction and photon spectrum from a sum of exclusive final states. *Phys. Rev. D* **2005**, *72*, 052004. [[CrossRef](#)]
336. Aubert, B.; Barate, R.; Boutigny, D.; Couderc, F.; Karyotakis, Y.; Lees, J.P.; Poireau, V.; Tisserand, V.; Zghiche, A.; Grauges, E.; et al. Measurement of the $B^+ \rightarrow p \bar{p} K^+$ branching fraction and study of the decay dynamics. *Phys. Rev. D* **2005**, *72*, 051101. [[CrossRef](#)]
337. Aubert, B.; Barate, R.; Boutigny, D.; Couderc, F.; Karyotakis, Y.; Lees, J.P.; Poireau, V.; Tisserand, V.; Zghiche, A.; Grauges, E.; et al. Measurements of the absolute branching fractions of $B^\pm \rightarrow K^\pm X(c\bar{c})$. *Phys. Rev. Lett.* **2006**, *96*, 052002. [[CrossRef](#)] [[PubMed](#)]
338. Aubert, B.; Barate, R.; Bona, M.; Boutigny, D.; Couderc, F.; Karyotakis, Y.; Lees, J.P.; Poireau, V.; Tisserand, V.; Zghiche, A.; et al. Dalitz plot analysis of the decay $B^\pm \rightarrow K^\pm K^\pm K^\mp$. *Phys. Rev. D* **2006**, *74*, 032003. [[CrossRef](#)]
339. Aubert, B.; Bona, M.; Boutigny, D.; Karyotakis, Y.; Lees, J.P.; Poireau, V.; Prudent, X.; Tisserand, V.; Zghiche, A.; Tico, J.G.; et al. Study of $B^0 \rightarrow \pi^0 \pi^0$, $B^\pm \rightarrow \pi^\pm \pi^0$, and $B^\pm \rightarrow K^\pm \pi^0$ Decays, and Isospin Analysis of $B \rightarrow \pi\pi$ Decays. *Phys. Rev. D* **2007**, *76*, 091102. [[CrossRef](#)]
340. Aubert, B.; Bona, M.; Boutigny, D.; Karyotakis, Y.; Lees, J.P.; Poireau, V.; Prudent, X.; Tisserand, V.; Zghiche, A.; Tico, J.G.; et al. Measurement of decay amplitudes of $B \rightarrow J/\psi K^*, \psi(2S) K^*$, and $\chi_{c1} K^*$ with an angular analysis. *Phys. Rev. D* **2007**, *76*, 031102. [[CrossRef](#)]
341. Aubert, B.; Bona, M.; Karyotakis, Y.; Lees, J.P.; Poireau, V.; Prudent, X.; Tisserand, V.; Zghiche, A.; Tico, J. Garra ; Grauges, E.; et al. Measurement of the $B \rightarrow X_s \gamma$ branching fraction and photon energy spectrum using the recoil method. *Phys. Rev. D* **2008**, *77*, 051103. [[CrossRef](#)]
342. Lees, J.P.; Poireau, V.; Tisserand, V.; Garra Tico, J.; Grauges, E.; Palano, A.; Eigen, G.; Stugu, B.; Brown, D.N.; Kerth, L.T.; et al. Exclusive Measurements of $b \rightarrow s \gamma$ Transition Rate and Photon Energy Spectrum. *Phys. Rev. D* **2012**, *86*, 052012. [[CrossRef](#)]
343. Aubert, B.; Barate, R.; Boutigny, D.; Couderc, F.; Karyotakis, Y.; Lees, J.P.; Poireau, V.; Tisserand, V.; Zghiche, A.; Grauges, E.; et al. Dalitz-plot analysis of the decays $B^\pm \rightarrow K^\pm \pi^\mp \pi^\pm$. *Phys. Rev. D* **2005**, *72*, 072003; Erratum in *Phys. Rev. D* **2006**, *74*, 099903. [[CrossRef](#)]
344. Aubert, B.; Bona, M.; Boutigny, D.; Karyotakis, Y.; Lees, J.P.; Poireau, V.; Prudent, X.; Tisserand, V.; Zghiche, A.; Tico, J.G.; et al. Study of Resonances in Exclusive B Decays to anti- $D^{(*)} D^{(*)} K$. *Phys. Rev. D* **2008**, *77*, 011102. [[CrossRef](#)]

345. Aubert, B.; Karyotakis, Y.; Lees, J.P.; Poireau, V.; Prencipe, E.; Prudent, X.; Tisserand, V.; Tico, J. Garra ; Grauges, E.; Lopez, L.; et al. Dalitz Plot Analysis of $B^+ \rightarrow \pi^+ \pi^+ \pi^-$ Decays. *Phys. Rev. D* **2009**, *79*, 072006. [[CrossRef](#)]
346. Aubert, B.; Barate, R.; Boutigny, D.; Couderc, F.; Gaillard, J. -M.; Hicheur, A.; Karyotakis, Y.; Lees, J.P.; Tisserand, V.; Zghiche, A.; et al. Observation of the decay $B \rightarrow J/\psi \eta K$ and search for $X(3872) \rightarrow J/\psi \eta$. *Phys. Rev. Lett.* **2004**, *93*, 041801. [[CrossRef](#)]
347. Aubert, B.; Barate, R.; Boutigny, D.; Couderc, F.; Gaillard, J. -M.; Hicheur, A.; Karyotakis, Y.; Lees, J.P.; Tisserand, V.; Zghiche, A.; et al. Study of the $B \rightarrow J/\psi K^- \pi^+ \pi^-$ decay and measurement of the $B \rightarrow X(3872) K^-$ branching fraction. *Phys. Rev. D* **2005**, *71*, 071103. [[CrossRef](#)]
348. Aubert, B.; Barate, R.; Boutigny, D.; Couderc, F.; Karyotakis, Y.; Lees, J.P.; Poireau, V.; Tisserand, V.; Zghiche, A.; Grauges-Pous, E.; et al. Search for a charged partner of the $X(3872)$ in the B meson decay $B \rightarrow X^- K$, $X^- \rightarrow J/\psi \pi^- \pi^0$. *Phys. Rev. D* **2005**, *71*, 031501. [[CrossRef](#)]
349. Aubert, B.; Barate, R.; Bona, M.; Boutigny, D.; Couderc, F.; Karyotakis, Y.; Lees, J.P.; Poireau, V.; Tisserand, V.; Zghiche, A.; et al. Search for $B^+ \rightarrow X(3872) K^+$, $X_{3872} \rightarrow J/\psi \gamma$. *Phys. Rev. D* **2006**, *74*, 071101. [[CrossRef](#)]
350. Aubert, B.; Barate, R.; Boutigny, D.; Couderc, F.; Karyotakis, Y.; Lees, J.P.; Poireau, V.; Tisserand, V.; Zghiche, A.; Grauges, E.; et al. Study of the $X(3872)$ and $Y(4260)$ in $B^0 \rightarrow J/\psi \pi^+ \pi^- K^0$ and $B^- \rightarrow J/\psi \pi^+ \pi^- K^-$ decays. *Phys. Rev. D* **2006**, *73*, 011101. [[CrossRef](#)]
351. Aubert, B.; Bona, M.; Karyotakis, Y.; Lees, J.P.; Poireau, V.; Prencipe, E.; Prudent, X.; Tisserand, V.; Garra Tico, J.; Grauges, E.; et al. A Study of $B \rightarrow X(3872) K$, with $X_{3872} \rightarrow J/\psi \pi^+ \pi^-$. *Phys. Rev. D* **2008**, *77*, 111101. [[CrossRef](#)]
352. Aubert, B.; Bona, M.; Karyotakis, Y.; Lees, J.P.; Poireau, V.; Prencipe, E.; Prudent, X.; Tisserand, V.; Tico, J. Garra ; Grauges, E.; et al. Evidence for $X(3872) \rightarrow \psi_{2S} \gamma$ in $B^\pm \rightarrow X_{3872} K^\pm$ decays, and a study of $B \rightarrow c \bar{c} \gamma K$. *Phys. Rev. Lett.* **2009**, *102*, 132001. [[CrossRef](#)]
353. Del Amo Sanchez, P.; Lees, J.P.; Poireau, V.; Prencipe, E.; Tisserand, V.; Garra Tico, J.; Grauges, E.; Martinelli, M.; Palano, A.; Pappagallo, M.; et al. Evidence for the decay $X(3872) \rightarrow J/\psi \omega$. *Phys. Rev. D* **2010**, *82*, 011101. [[CrossRef](#)]
354. Lees, J.P.; Poireau, V.; Tisserand, V.; Grauges, E.; Palano, A.; Eigen, G.; Brown, D.N.; Kolomensky, Yu. G.; Fritsch, M.; Koch, H.; et al. Measurements of the Absolute Branching Fractions of $B^\pm \rightarrow K^\pm X_{c\bar{c}}$. *Phys. Rev. Lett.* **2020**, *124*, 152001. [[CrossRef](#)]
355. Choi, S. -K.; Olsen, S.L.; Abe, K.; Abe, T.; Adachi, I.; Ahn, Byoung Sup ; Aihara, H.; Akai, K.; Akatsu, M.; Akemoto, M.; et al. Observation of a narrow charmonium-like state in exclusive $B^\pm \rightarrow K^\pm \pi^+ \pi^- J/\psi$ decays. *Phys. Rev. Lett.* **2003**, *91*, 262001. [[CrossRef](#)]
356. Choi, S. -K.; Olsen, S.L.; Adachi, I.; Aihara, H.; Aulchenko, V.; Aushev, T.; Aziz, T.; Bakich, A.M.; Balagura, V.; Bedny, I.; et al. Observation of a resonance-like structure in the $\pi^\pm \psi'$ mass distribution in exclusive $B \rightarrow K \pi^\pm \psi'$ decays. *Phys. Rev. Lett.* **2008**, *100*, 142001. [[CrossRef](#)] [[PubMed](#)]
357. Choi, S. -K.; Olsen, S.L.; Abe, K.; Abe, K.; Adachi, I.; Aihara, H.; Asano, Y.; Bahinipati, S.; Bakich, A.M.; Ban, Y.; et al. Observation of a near-threshold $\omega J/\psi$ mass enhancement in exclusive $B \rightarrow K \omega J/\psi$ decays. *Phys. Rev. Lett.* **2005**, *94*, 182002. [[CrossRef](#)]
358. Abe, K.; Abe, K.; Adachi, I.; Aihara, H.; Aoki, K.; Arinstein, K.; Asano, Y.; Aso, T.; Aulchenko, V.; Aushev, T.; et al. Experimental constraints on the possible J^{PC} quantum numbers of the $X(3872)$. In Proceedings of the 22nd International Symposium on Lepton-Photon Interactions at High Energy (LP 2005), Uppsala, Sweden, 30 June–5 July 2005.
359. Gokhroo, G.; Majumder, G.; Abe, K.; Abe, K.; Adachi, I.; Aihara, H.; Anipko, D.; Aushev, T.; Aziz, T.; Bakich, A.M.; et al. Observation of a Near-threshold D^0 anti- D^0 π^0 Enhancement in $B \rightarrow D^0$ anti- D^0 π^0 K Decay. *Phys. Rev. Lett.* **2006**, *97*, 162002. [[CrossRef](#)] [[PubMed](#)]
360. Mizuk, R.; Chistov, R.; Adachi, I.; Aihara, H.; Arinstein, K.; Aulchenko, V.; Aushev, T.; Bakich, A.M.; Balagura, V.; Barberio, E.; et al. Observation of two resonance-like structures in the $\pi^+ \chi_{c1}$ mass distribution in exclusive anti- $B^0 \rightarrow K^- \pi^+ \chi_{c1}$ decays. *Phys. Rev. D* **2008**, *78*, 072004. [[CrossRef](#)]
361. Aushev, T.; Zwahlen, N.; Adachi, I.; Aihara, H.; Bakich, A.M.; Balagura, V.; Bay, A.; Belous, K.; Bhardwaj, V.; Bischofberger, M.; et al. Study of the $B \rightarrow X(3872) (D^*0 \text{ anti-} D^0) K$ decay. *Phys. Rev. D* **2010**, *81*, 031103. [[CrossRef](#)]
362. Mizuk, R.; Adachi, I.; Aihara, H.; Arinstein, K.; Aushev, T.; Bakich, A.M.; Balagura, V.; Barberio, E.; Bay, A.; Belous, K.; et al. Dalitz analysis of $B \rightarrow K \pi^+ \psi'$ decays and the $Z(4430)^+$. *Phys. Rev. D* **2009**, *80*, 031104. [[CrossRef](#)]
363. Choi, S. -K.; Olsen, S.L.; Trabelsi, K.; Adachi, I.; Aihara, H.; Arinstein, K.; Asner, D.M.; Aushev, T.; Bakich, A.M.; Barberio, E.; et al. Bounds on the width, mass difference and other properties of $X(3872) \rightarrow \pi^+ \pi^- J/\psi$ decays. *Phys. Rev. D* **2011**, *84*, 052004. [[CrossRef](#)]
364. Bhardwaj, V.; Trabelsi, K.; Singh, J.B.; Choi, S. -K.; Olsen, S.L.; Adachi, I.; Adamczyk, K.; Asner, D.M.; Aulchenko, V.; Aushev, T.; et al. Observation of $X(3872) \rightarrow J/\psi \gamma$ and search for $X(3872) \rightarrow \psi' \gamma$ in B decays. *Phys. Rev. Lett.* **2011**, *107*, 091803. [[CrossRef](#)]
365. Bhardwaj, V.; Miyabayashi, K.; Adachi, I.; Aihara, H.; Asner, D.M.; Aulchenko, V.; Aushev, T.; Aziz, T.; Bakich, A.M.; Bala, A.; et al. Evidence of a new narrow resonance decaying to $\chi_{c1} \gamma$ in $B \rightarrow \chi_{c1} \gamma K$. *Phys. Rev. Lett.* **2013**, *111*, 032001. [[CrossRef](#)]
366. Chilikin, K.; Mizuk, R.; Adachi, I.; Aihara, H.; Said, S. Al ; Arinstein, K.; Asner, D.M.; Aulchenko, V.; Aushev, T.; Ayad, R.; et al. Observation of a new charged charmoniumlike state in $\bar{B}^0 \rightarrow J/\psi K^- \pi^+$ decays. *Phys. Rev. D* **2014**, *90*, 112009. [[CrossRef](#)]
367. Hirata, H.; Iijima, T.; Kato, Y.; Tanida, K.; Adachi, I.; Ahn, J.K.; Aihara, H.; Al Said, S.; Asner, D.M.; Atmacan, H.; et al. Study of the lineshape of $X(3872)$ using B decays to $D^0 \bar{D}^{*0} K$. *arXiv* **2023**, arXiv:2302.02127.
368. Abe, K.; Abe, K.; Abe, R.; Adachi, I.; Ahn, Byoung Sup ; Aihara, H.; Akatsu, M.; Alimonti, G.; Asai, K.; Asai, M.; et al. Observation of large CP violation in the neutral B meson system. *Phys. Rev. Lett.* **2001**, *87*, 091802. [[CrossRef](#)] [[PubMed](#)]
369. Abe, K.; Abe, K.; Abe, T.; Adachi, I.; Aihara, H.; Akatsu, M.; Asano, Y.; Aso, T.; Aulchenko, V.; Aushev, T.; et al. An Improved measurement of mixing induced CP violation in the neutral B meson system. *Phys. Rev. D* **2002**, *66*, 071102. [[CrossRef](#)]

370. Abe, K.; Abe, K.; Abe, N.; Abe, T.; Adachi, I.; Aihara, H.; Akai, K.; Akatsu, M.; Akemoto, M.; Asano, Y.; et al. Observation of large CP violation and evidence for direct CP violation in $B^0 \rightarrow \pi^+ \pi^-$ decays. *Phys. Rev. Lett.* **2004**, *93*, 021601. [[CrossRef](#)]
371. Chao, Y.; Chang, P.; Abe, K.; Abe, K.; Abe, N.; Adachi, I.; Aihara, H.; Akai, K.; Akatsu, M.; Akemoto, M.; et al. Evidence for direct CP violation in $B^0 \rightarrow K^+ \pi^-$ decays. *Phys. Rev. Lett.* **2004**, *93*, 191802. [[CrossRef](#)]
372. Abashian, A.; Abe, K.; Abe, K.; Adachi, I.; Ahn, Byoung Sup; Aihara, H.; Akatsu, M.; Alimonti, G.; Aoki, K.; Asai, K.; et al. Measurement of the CP violation parameter $\sin 2\phi_1$ in B_d^0 meson decays. *Phys. Rev. Lett.* **2001**, *86*, 2509–2514. [[CrossRef](#)]
373. Abe, K.; Abe, K.; Abe, N.; Abe, T.; Adachi, I.; Aihara, H.; Akai, K.; Akatsu, M.; Akemoto, M.; Asano, Y.; et al. Evidence for CP violating asymmetries $B^0 \rightarrow \pi^+ \pi^-$ decays and constraints on the CKM angle $\phi(2)$. *Phys. Rev. D* **2003**, *68*, 012001. [[CrossRef](#)]
374. Abe, K.; Abe, K.; Abe, T.; Adachi, I.; Aihara, H.; Akai, K.; Akatsu, M.; Asano, Y.; Aso, T.; Aushev, T.; et al. Measurement of time dependent CP violating asymmetries in $B^0 \rightarrow \phi K^0(s)$, $K^+ K^- K^0(s)$, and η -prime $K^0(s)$ decays. *Phys. Rev. Lett.* **2003**, *91*, 261602. [[CrossRef](#)]
375. Poluektov, A.; Abe, K.; Abe, T.; Aihara, H.; Asano, Y.; Aushev, T.; Aziz, T.; Bahinipati, S.; Bakich, A.M.; Bedny, I.; et al. Measurement of $\phi(3)$ with Dalitz plot analysis of $B^{+-} \rightarrow D^{**(*)} K^{+-}$ decay. *Phys. Rev. D* **2004**, *70*, 072003. [[CrossRef](#)]
376. Chen, K.-F.; Fang, F.; Garmash, A.; Hara, K.; Hazumi, M.; Higuchi, T.; Kakuno, H.; Kusaka, A.; Shibata, T.; Tajima, O.; et al. Time-dependent CP-violating asymmetries in $b \rightarrow s$ anti-q q transitions. *Phys. Rev. D* **2005**, *72*, 012004. [[CrossRef](#)]
377. Itoh, R.; Onuki, Y.; Abe, K.; Abe, K.; Adachi, I.; Aihara, H.; Asano, Y.; Aushev, T.; Bakich, A.M.; Ban, Y.; et al. Studies of CP violation in $B \rightarrow J/\psi K^*$ decays. *Phys. Rev. Lett.* **2005**, *95*, 091601. [[CrossRef](#)]
378. Garmash, A.; Abe, K.; Abe, K.; Adachi, I.; Aihara, H.; Asano, Y.; Aushev, T.; Aziz, T.; Bahinipati, S.; Bakich, A.M.; et al. Evidence for large direct CP violation in $B^{+-} \rightarrow \rho(770)0 K^{+-}$ from analysis of the three-body charmless $B^{+-} \rightarrow K^{+-} \pi^+ \pi^-$ decay. *Phys. Rev. Lett.* **2006**, *96*, 251803. [[CrossRef](#)] [[PubMed](#)]
379. Poluektov, A.; Abe, K.; Abe, K.; Adachi, I.; Aihara, H.; Anipko, D.; Arinstein, K.; Aushev, T.; Bahinipati, S.; Bakich, A.M.; et al. Measurement of $\phi(3)$ with Dalitz plot analysis of $B^+ \rightarrow D^{(*)} K^{*+}$ decay. *Phys. Rev. D* **2006**, *73*, 112009. [[CrossRef](#)]
380. Mohapatra, D.; Nakao, M.; Nishida, S.; Abe, K.; Abe, K.; Adachi, I.; Aihara, H.; Anipko, D.; Arinstein, K.; Asano, Y.; et al. Observation of $b \rightarrow d$ gamma and determination of $|V(td)/V(ts)|$. *Phys. Rev. Lett.* **2006**, *96*, 221601. [[CrossRef](#)] [[PubMed](#)]
381. Ushiroda, Y.; Sumisawa, K.; Abe, K.; Abe, K.; Adachi, I.; Aihara, H.; Anipko, D.; Arinstein, K.; Bakich, A.M.; Barberio, E.; et al. Time-Dependent CP Asymmetries in $B^0 \rightarrow K_S^0 \pi^0 \gamma$ transitions. *Phys. Rev. D* **2006**, *74*, 111104. [[CrossRef](#)]
382. Somov, A.; Schwartz, A.J.; Abe, K.; Abe, K.; Adachi, I.; Aihara, H.; Anipko, D.; Arinstein, K.; Asano, Y.; Aulchenko, V.; et al. Measurement of the branching fraction, polarization, and CP asymmetry for $B^0 \rightarrow \rho^+ \rho^-$ decays, and determination of the CKM phase $\phi(2)$. *Phys. Rev. Lett.* **2006**, *96*, 171801. [[CrossRef](#)]
383. Chen, K.-F.; Hara, K.; Hazumi, M.; Higuchi, T.; Miyabayashi, K.; Nakahama, Y.; Sumisawa, K.; Tajima, O.; Ushiroda, Y.; Yusa, Y.; et al. Observation of time-dependent CP violation in $B^0 \rightarrow \eta$ -prime K^0 decays and improved measurements of CP asymmetries in $B^0 \rightarrow \phi K^0$, $K^0(s) K^0(s) K^0(s)$ and $B^0 \rightarrow J/\psi K^0$ decays. *Conf. Proc. C* **2006**, *060726*, 823–826. [[CrossRef](#)]
384. Ishino, H.; Abe, K.; Abe, K.; Adachi, I.; Aihara, H.; Anipko, D.; Arinstein, K.; Aushev, T.; Bakich, A.M.; Barberio, E.; et al. Observation of Direct CP-Violation in $B^0 \rightarrow \pi^+ \pi^-$ Decays and Model-Independent Constraints on $\phi(2)$. *Phys. Rev. Lett.* **2007**, *98*, 211801. [[CrossRef](#)]
385. Lin, S.-W.; Unno, Y.; Hou, W.-S.; Chang, P.; Adachi, I.; Aihara, H.; Akai, K.; Arinstein, K.; Aulchenko, V.; Aushev, T.; et al. Difference in direct charge-parity violation between charged and neutral B meson decays. *Nature* **2008**, *452*, 332–335. [[CrossRef](#)]
386. Poluektov, A.; Bondar, A.; Yabsley, B.D.; Adachi, I.; Aihara, H.; Arinstein, K.; Aulchenko, V.; Aushev, T.; Bakich, A.M.; Balagura, V.; et al. Evidence for direct CP violation in the decay $B \rightarrow D^{(*)} K$, $D \rightarrow K_S \pi^+ \pi^-$ and measurement of the CKM phase $\phi(3)$. *Phys. Rev. D* **2010**, *81*, 112002. [[CrossRef](#)]
387. Adachi, I.; Aihara, H.; Asner, D.M.; Aulchenko, V.; Aushev, T.; Aziz, T.; Bakich, A.M.; Bay, A.; Bhardwaj, V.; Bhuyan, B.; et al. Precise measurement of the CP violation parameter $\sin 2\phi_1$ in $B^0 \rightarrow (c\bar{c})K^0$ decays. *Phys. Rev. Lett.* **2012**, *108*, 171802. [[CrossRef](#)] [[PubMed](#)]
388. Duh, Y.-T.; Wu, T.-Y.; Chang, P.; Mohanty, G.B.; Unno, Y.; Adachi, I.; Aihara, H.; Asner, D.M.; Aulchenko, V.; Aushev, T.; et al. Measurements of branching fractions and direct CP asymmetries for $B \rightarrow K\pi$, $B \rightarrow \pi\pi$ and $B \rightarrow KK$ decays. *Phys. Rev. D* **2013**, *87*, 031103. [[CrossRef](#)]
389. Kang, K.H.; Park, H.; Higuchi, T.; Miyabayashi, K.; Sumisawa, K.; Adachi, I.; Ahn, J.K.; Aihara, H.; Al Said, S.; Asner, D.M.; et al. Measurement of time-dependent CP violation parameters in $B^0 \rightarrow K_S^0 K_S^0 K_S^0$ decays at Belle. *Phys. Rev. D* **2021**, *103*, 032003. [[CrossRef](#)]
390. Adachi, I.; Adamczyk, K.; Aggarwal, L.; Ahmed, H.; Aihara, H.; Akopov, N.; Aloisio, A.; Ky, N.A.; Asner, D.M.; Atmacan, H.; et al. Measurement of CP violation in $B^0 \rightarrow K_S^0 \pi^0$ decays at Belle II. *arXiv* **2023**, arXiv:2305.07555.
391. Abudinén, F.; Adachi, I.; Aggarwal, L.; Ahmed, H.; Aihara, H.; Akopov, N.; Aloisio, A.; Ky, N.A.; Asner, D.M.; Atmacan, H.; et al. Measurement of the B^0 lifetime and flavor-oscillation frequency using hadronic decays reconstructed in 2019–2021 Belle II data. *Phys. Rev. D* **2023**, *107*, L091102. [[CrossRef](#)]
392. Adachi, I.; Aggarwal, L.; Ahmed, H.; Aihara, H.; Akopov, N.; Aloisio, A.; Ky, N.A.; Asner, D.M.; Atmacan, H.; Aushev, T.; et al. Measurement of decay-time-dependent CP violation in $B^0 \rightarrow J/\psi K_S^0$ decays using 2019–2021 Belle II data. *arXiv* **2023**, arXiv:2302.12898.
393. Abe, K.; Abe, K.; Adachi, I.; Ahn, B.S.; Aihara, H.; Akatsu, M.; Alimonti, G.; Aoki, K.; Asai, K.; Asano, Y.; et al. A Measurement of the branching fraction for the inclusive $B \rightarrow X(s)$ gamma decays with BELLE. *Phys. Lett. B* **2001**, *511*, 151–158. [[CrossRef](#)]

394. Abe, K.; Abe, K.; Adachi, I.; Ahn, Byoung Sup ; Aihara, H.; Akatsu, M.; Alimonti, G.; Asano, Y.; Aso, T.; Aulchenko, V.; et al. Measurement of branching fractions for $B \rightarrow \pi \pi$, $K \pi$ and $K K$ decays. *Phys. Rev. Lett.* **2001**, *87*, 101801. [[CrossRef](#)]
395. Garmash, A.; Abe, K.; Abe, K.; Abe, N.; Abe, T.; Adachi, I.; Aihara, H.; Asano, Y.; Aso, T.; Aulchenko, V.; et al. Study of three-body charmless B decays. *Phys. Rev. D* **2002**, *65*, 092005. [[CrossRef](#)]
396. Garmash, A.; Abe, K.; Abe, K.; Abe, T.; Adachi, I.; Aihara, H.; Akatsu, M.; Asano, Y.; Aushev, T.; Bakich, A.M.; et al. Study of B meson decays to three body charmless hadronic final states. *Phys. Rev. D* **2004**, *69*, 012001. [[CrossRef](#)]
397. Nakao, M.; Abe, K.; Abe, K.; Abe, T.; Adachi, I.; Aihara, H.; Akatsu, M.; Asano, Y.; Aso, T.; Aulchenko, V.; et al. Measurement of the $B \rightarrow K^* \gamma$ branching fractions and asymmetries. *Phys. Rev. D* **2004**, *69*, 112001. [[CrossRef](#)]
398. Abe, K.; Abe, K.; Abe, T.; Adachi, I.; Aihara, H.; Akatsu, M.; Asano, Y.; Aso, T.; Aushev, T.; Bakich, A.M.; et al. Study of $B \rightarrow D^{*0} \pi^- (D^{*0} \rightarrow D^{*+} \pi^-)$ decays. *Phys. Rev. D* **2004**, *69*, 112002. [[CrossRef](#)]
399. Garmash, A.; Abe, K.; Abe, K.; Aihara, H.; Akatsu, M.; Asano, Y.; Aulchenko, V.; Aushev, T.; Aziz, T.; Bahinipati, S.; et al. Dalitz analysis of the three-body charmless decays $B^+ \rightarrow K^+ \pi^+ \pi^-$ and $B^+ \rightarrow K^+ K^+ K^-$. *Phys. Rev. D* **2005**, *71*, 092003. [[CrossRef](#)]
400. Limosani, A.; Aihara, H.; Arinstein, K.; Aushev, T.; Bakich, A.M.; Balagura, V.; Barberio, E.; Bay, A.; Belous, K.; Bischofberger, M.; et al. Measurement of Inclusive Radiative B-meson Decays with a Photon Energy Threshold of 1.7-GeV. *Phys. Rev. Lett.* **2009**, *103*, 241801. [[CrossRef](#)] [[PubMed](#)]
401. Chen, Y.Q.; Li, L.K.; Yan, W.B.; Adachi, I.; Aihara, H.; Al Said, S.; Asner, D.M.; Atmacan, H.; Aulchenko, V.; Aushev, T.; et al. Dalitz analysis of $D^0 \rightarrow K^- \pi^+ \eta$ decays at Belle. *Phys. Rev. D* **2020**, *102*, 012002. [[CrossRef](#)]
402. Abudinén, F.; Adachi, I.; Adamczyk, K.; Aggarwal, L.; Ahmed, H.; Aihara, H.; Akopov, N.; Aloisio, A.; Anh Ky, N.; Asner, D.M.; et al. Measurement of the branching fraction and CP asymmetry of $B^0 \rightarrow \pi^0 \pi^0$ decays using $198 \times 10^6 B \bar{B}$ pairs in Belle II data. *arXiv* **2023**, arXiv:2303.08354.
403. Abe, K.; Abe, K.; Abe, R.; Abe, T.; Adachi, I.; Ahn, Byoung Sup ; Aihara, H.; Akatsu, M.; Asano, Y.; Aso, T.; et al. Observation of $B^{*-} \rightarrow p \text{ anti-} p K^+$. *Phys. Rev. Lett.* **2002**, *88*, 181803. [[CrossRef](#)]
404. Choi, S.-K.; Olsen, S.L.; Abe, K.; Abe, K.; Abe, R.; Abe, T.; Adachi, I.; Ahn, Byoung Sup ; Aihara, H.; Akatsu, M.; et al. Observation of the eta(c)(2S) in exclusive $B \rightarrow K K(S) K^- \pi^+$ decays. *Phys. Rev. Lett.* **2002**, *89*, 102001; Erratum in *Phys. Rev. Lett.* **2002**, *89*, 129901. [[CrossRef](#)]
405. Abe, K.; Abe, K.; Abe, R.; Abe, T.; Ahn, Byoung Sup ; Aihara, H.; Akatsu, M.; Asano, Y.; Aso, T.; Aulchenko, V.; et al. Observation of anti- $B^0 \rightarrow D^0(*) p \text{ anti-} p$. *Phys. Rev. Lett.* **2002**, *89*, 151802. [[CrossRef](#)]
406. Lee, S.H.; Suzuki, K.; Abe, K.; Abe, K.; Abe, T.; Adachi, I.; Ahn, Byoung Sup ; Aihara, H.; Akai, K.; Akatsu, M.; et al. Evidence for $B^0 \rightarrow \pi^0 \pi^0$. *Phys. Rev. Lett.* **2003**, *91*, 261801. [[CrossRef](#)]
407. Krokovny, P.; Abe, K.; Abe, K.; Abe, T.; Adachi, I.; Aihara, H.; Akai, K.; Akatsu, M.; Akemoto, M.; Asano, Y.; et al. Observation of the D(sj)(2317) and D(sj)(2457) in B decays. *Phys. Rev. Lett.* **2003**, *91*, 262002. [[CrossRef](#)] [[PubMed](#)]
408. Zhang, J.; Nakao, M.; Abe, K.; Abe, K.; Abe, T.; Adachi, I.; Aihara, H.; Akatsu, M.; Asano, Y.; Aso, T.; et al. Observation of $B^+ \rightarrow \rho^+ \rho^0$. *Phys. Rev. Lett.* **2003**, *91*, 221801. [[CrossRef](#)] [[PubMed](#)]
409. Wang, M.-Z.; Abe, K.; Abe, K.; Abe, T.; Adachi, I.; Aihara, H.; Asano, Y.; Aso, T.; Aulchenko, V.; Aushev, T.; et al. Observation of $B^+ \rightarrow p \text{ anti-} p \pi^+$, $B^0 \rightarrow p \text{ anti-} p K^0$, and $B^+ \rightarrow p \text{ anti-} p K^{*+}$. *Phys. Rev. Lett.* **2004**, *92*, 131801. [[CrossRef](#)] [[PubMed](#)]
410. Brodzicka, J.; Palka, H.; Adachi, I.; Aihara, H.; Aulchenko, V.; Bakich, A.M.; Barberio, E.; Bay, A.; Bedny, I.; Bitenc, U.; et al. Observation of a new D(sj) meson in $B^+ \rightarrow \text{anti-} D^0 D^0 K^+$ decays. *Phys. Rev. Lett.* **2008**, *100*, 092001. [[CrossRef](#)] [[PubMed](#)]
411. Li, Y.B.; Shen, C.P.; Adachi, I.; Ahn, J.K.; Aihara, H.; Al Said, S.; Asner, D.M.; Aushev, T.; Ayad, R.; Babu, V.; et al. Observation of $\Xi_c(2930)^0$ and updated measurement of $B^- \rightarrow K^- \Lambda_c^+ \bar{\Lambda}_c^-$ at Belle. *Eur. Phys. J. C* **2018**, *78*, 252. [[CrossRef](#)]
412. Chen, K.-F.; Bozek, A.; Abe, K.; Abe, K.; Abe, T.; Adachi, I.; Aihara, H.; Akatsu, M.; Asano, Y.; Aso, T.; et al. Measurement of branching fractions and polarization in $B \rightarrow \phi K^*$ decays. *Phys. Rev. Lett.* **2003**, *91*, 201801. [[CrossRef](#)]
413. Chen, K.-F.; Abe, K.; Abe, K.; Aihara, H.; Asano, Y.; Aulchenko, V.; Aushev, T.; Bahinipati, S.; Bakich, A.M.; et al. Measurement of polarization and triple-product correlations in $B \rightarrow \phi K^*$ decays. *Phys. Rev. Lett.* **2005**, *94*, 221804. [[CrossRef](#)] [[PubMed](#)]
414. Koppenburg, P.; Abe, K.; Abe, K.; Abe, T.; Adachi, I.; Aihara, H.; Akatsu, M.; Asano, Y.; Aulchenko, V.; Aushev, T.; et al. An Inclusive measurement of the photon energy spectrum in $b \rightarrow s \gamma$ decays. *Phys. Rev. Lett.* **2004**, *93*, 061803. [[CrossRef](#)]
415. Abudinén, F.; Adachi, I.; Adamczyk, K.; Aggarwal, L.; Ahlburg, P.; Ahmed, H.; Ahn, J.K.; Aihara, H.; Akopov, N.; Aloisio, A.; et al. Measurement of the photon-energy spectrum in inclusive $B \rightarrow X_s \gamma$ decays identified using hadronic decays of the recoil B meson in 2019-2021 Belle II data. *arXiv* **2022**, arXiv:2210.10220.
416. Cabibbo, N. Unitary Symmetry and Leptonic Decays. *Phys. Rev. Lett.* **1963**, *10*, 531–533. [[CrossRef](#)]
417. Kobayashi, M.; Maskawa, T. CP Violation in the Renormalizable Theory of Weak Interaction. *Prog. Theor. Phys.* **1973**, *49*, 652–657. [[CrossRef](#)]
418. Bander, M.; Silverman, D.; Soni, A. CP Noninvariance in the Decays of Heavy Charged Quark Systems. *Phys. Rev. Lett.* **1979**, *43*, 242. [[CrossRef](#)]
419. Carter, A.B.; Sanda, A.I. CP Violation in B Meson Decays. *Phys. Rev. D* **1981**, *23*, 1567. [[CrossRef](#)]
420. Bigi, I.I.Y.; Sanda, A.I. Notes on the Observability of CP Violations in B Decays. *Nucl. Phys. B* **1981**, *193*, 85–108. [[CrossRef](#)]
421. Chernyak, V.L.; Zhitnitsky, A.R. Asymptotic Behavior of Exclusive Processes in QCD. *Phys. Rept.* **1984**, *112*, 173. [[CrossRef](#)]
422. Godfrey, S.; Isgur, N. Mesons in a Relativized Quark Model with Chromodynamics. *Phys. Rev. D* **1985**, *32*, 189–231. [[CrossRef](#)]
423. Bauer, M.; Stech, B.; Wirbel, M. Exclusive Nonleptonic Decays of D, D(s), and B Mesons. *Z. Phys. C* **1987**, *34*, 103. [[CrossRef](#)]

424. Buras, A.J.; Jamin, M.; Lautenbacher, M.E.; Weisz, P.H. Effective Hamiltonians for $\Delta S = 1$ and $\Delta B = 1$ nonleptonic decays beyond the leading logarithmic approximation. *Nucl. Phys. B* **1992**, *370*, 69–104; Addendum *Nucl. Phys. B* **1992**, *375*, 501. [[CrossRef](#)]
425. Isgur, N.; Wise, M.B. Spectroscopy with heavy quark symmetry. *Phys. Rev. Lett.* **1991**, *66*, 1130–1133. [[CrossRef](#)]
426. Neubert, M.; Stech, B. Nonleptonic weak decays of B mesons. *Adv. Ser. Direct. High Energy Phys.* **1998**, *15*, 294–344. [[CrossRef](#)]
427. Chetyrkin, K.G.; Misiak, M.; Munz, M. Weak radiative B meson decay beyond leading logarithms. *Phys. Lett. B* **1997**, *400*, 206–219; Erratum in *Phys. Lett. B* **1998**, *425*, 414. [[CrossRef](#)]
428. Ciuchini, M.; Franco, E.; Martinelli, G.; Silvestrini, L. Charming penguins in B decays. *Nucl. Phys. B* **1997**, *501*, 271–296. [[CrossRef](#)]
429. Kagan, A.L.; Neubert, M. QCD anatomy of $B \rightarrow X(s \gamma)$ decays. *Eur. Phys. J. C* **1999**, *7*, 5–27. [[CrossRef](#)]
430. Dunietz, I.; Rosner, J.L. Time Dependent CP Violation Effects in B_0 anti- B_0 Systems. *Phys. Rev. D* **1986**, *34*, 1404. [[CrossRef](#)]
431. Gronau, M.; London, D. Isospin analysis of CP asymmetries in B decays. *Phys. Rev. Lett.* **1990**, *65*, 3381–3384. [[CrossRef](#)]
432. Ali, A.; Kramer, G.; Lu, C.D. Experimental tests of factorization in charmless nonleptonic two-body B decays. *Phys. Rev. D* **1998**, *58*, 094009. [[CrossRef](#)]
433. Beneke, M.; Buchalla, G.; Neubert, M.; Sachrajda, C.T. QCD factorization for exclusive, nonleptonic B meson decays: General arguments and the case of heavy light final states. *Nucl. Phys. B* **2000**, *591*, 313–418. [[CrossRef](#)]
434. Beneke, M.; Buchalla, G.; Neubert, M.; Sachrajda, C.T. QCD factorization in $B \rightarrow \pi K, \pi\pi$ decays and extraction of Wolfenstein parameters. *Nucl. Phys. B* **2001**, *606*, 245–321. [[CrossRef](#)]
435. Bauer, C.W.; Pirjol, D.; Stewart, I.W. A Proof of factorization for $B \rightarrow D\pi$. *Phys. Rev. Lett.* **2001**, *87*, 201806. [[CrossRef](#)]
436. Beneke, M.; Neubert, M. QCD factorization for $B \rightarrow PP$ and $B \rightarrow PV$ decays. *Nucl. Phys. B* **2003**, *675*, 333–415. [[CrossRef](#)]
437. Bauer, C.W.; Pirjol, D.; Rothstein, I.Z.; Stewart, I.W. $B \rightarrow M(1)M(2)$: Factorization, charming penguins, strong phases, and polarization. *Phys. Rev. D* **2004**, *70*, 054015. [[CrossRef](#)]
438. Buras, A.J.; Fleischer, R.; Recksiegel, S.; Schwab, F. $B \rightarrow \pi\pi$, new physics in $B \rightarrow \pi K$ and implications for rare K and B decays. *Phys. Rev. Lett.* **2004**, *92*, 101804. [[CrossRef](#)]
439. Buras, A.J.; Fleischer, R.; Recksiegel, S.; Schwab, F. Anatomy of prominent B and K decays and signatures of CP violating new physics in the electroweak penguin sector. *Nucl. Phys. B* **2004**, *697*, 133–206. [[CrossRef](#)]
440. Cheng, H.Y.; Chua, C.K.; Soni, A. Final state interactions in hadronic B decays. *Phys. Rev. D* **2005**, *71*, 014030. [[CrossRef](#)]
441. Ball, P.; Zwicky, R. New results on $B \rightarrow \pi, K, \eta$ decay formfactors from light-cone sum rules. *Phys. Rev. D* **2005**, *71*, 014015. [[CrossRef](#)]
442. Gorbahn, M.; Haisch, U. Effective Hamiltonian for non-leptonic $|\Delta F| = 1$ decays at NNLO in QCD. *Nucl. Phys. B* **2005**, *713*, 291–332. [[CrossRef](#)]
443. Beneke, M.; Rohrer, J.; Yang, D. Branching fractions, polarisation and asymmetries of $B \rightarrow VV$ decays. *Nucl. Phys. B* **2007**, *774*, 64–101. [[CrossRef](#)]
444. Charles, J.; Deschamps, O.; Descotes-Genon, S.; Lacker, H.; Menzel, A.; Monteil, S.; Niess, V.; Ocariz, J.; Orloff, J.; Perez, A.; et al. Current status of the Standard Model CKM fit and constraints on $\Delta F = 2$ New Physics. *Phys. Rev. D* **2015**, *91*, 073007. [[CrossRef](#)]
445. Dubnicka, S.; Dubnickova, A.Z.; Ivanov, M.A.; Liptaj, A. Decays $B_s \rightarrow J/\psi + \eta$ and $B_s \rightarrow J/\psi + \eta'$ in the framework of covariant quark model. *Phys. Rev. D* **2013**, *87*, 074201. [[CrossRef](#)]
446. Ambrosino, F.; Antonelli, A.; Antonelli, M.; Bacci, C.; Beltrame, P.; Bencivenni, G.; Bertolucci, S.; Bini, C.; Bloise, C.; Bocchetta, S.; et al. Measurement of the pseudoscalar mixing angle and eta-prime gluonium content with KLOE detector. *Phys. Lett. B* **2007**, *648*, 267–273. [[CrossRef](#)]
447. Li, J.; et al. First observation of $B_s^0 \rightarrow J/\psi\eta$ and $B_s^0 \rightarrow J/\psi\eta'$. *Phys. Rev. Lett.* **2012**, *108*, 181808. [[CrossRef](#)]
448. Aaij, R.; Abellan Beteta, C.; Adametz, A.; Adeva, B.; Adinolfi, M.; Adrover, C.; Affolder, A.; Ajaltouni, Z.; Albrecht, J.; Alessio, F.; et al. Evidence for the decay $B^0 \rightarrow J/\psi\omega$ and measurement of the relative branching fractions of B_s^0 meson decays to $J/\psi\eta$ and $J/\psi\eta'$. *Nucl. Phys. B* **2013**, *867*, 547–566. [[CrossRef](#)]
449. Dubnička, S.; Dubničková, A.Z.; Ivanov, M.A.; Liptaj, A. Decays $B \rightarrow D(s)(*)h$ ($h = \pi, \rho$) in a confined covariant quark model. *Phys. Rev. D* **2022**, *106*, 033006. [[CrossRef](#)]
450. Huber, T.; Kränkl, S.; Li, X.Q. Two-body non-leptonic heavy-to-heavy decays at NNLO in QCD factorization. *J. High Energy Phys.* **2016**, *09*, 112. [[CrossRef](#)]
451. Bordone, M.; Gubernari, N.; Huber, T.; Jung, M.; van Dyk, D. A puzzle in $\bar{B}_{(s)}^0 \rightarrow D_{(s)}^{(*)+} \{\pi^-, K^-\}$ decays and extraction of the f_s/f_d fragmentation fraction. *Eur. Phys. J. C* **2020**, *80*, 951. [[CrossRef](#)]
452. Iguro, S.; Kitahara, T. Implications for new physics from a novel puzzle in $\bar{B}_{(s)}^0 \rightarrow D_{(s)}^{(*)+} \{\pi^-, K^-\}$ decays. *Phys. Rev. D* **2020**, *102*, 071701. [[CrossRef](#)]
453. Ivanov, M.A.; Korner, J.G.; Pakhomova, O.N. The Nonleptonic decays $B_c^+ \rightarrow D_s^+ \bar{D}^0$ and $B_c^+ \rightarrow D_s^+ D^0$ in a relativistic quark model. *Phys. Lett. B* **2003**, *555*, 189–196. [[CrossRef](#)]
454. Dubnicka, S.; Dubnickova, A.Z.; Issadykov, A.; Ivanov, M.A.; Liptaj, A. Study of B_c decays into charmonia and D mesons. *Phys. Rev. D* **2017**, *96*, 076017. [[CrossRef](#)]
455. Aad, G.; Abbott, B.; Abdallah, J.; Abidinov, O.; Aben, R.; Abolins, M.; AbouZeid, O.S.; Abramowicz, H.; Abreu, H.; Abreu, R.; et al. Study of the $B_c^+ \rightarrow J/\psi D_s^+$ and $B_c^+ \rightarrow J/\psi D_s^{*+}$ decays with the ATLAS detector. *Eur. Phys. J. C* **2016**, *76*, 4. [[CrossRef](#)]
456. Ivanov, M.A.; Tyulemissov, Z.; Tyulemissova, A. Weak nonleptonic decays of vector B-mesons. *Phys. Rev. D* **2023**, *107*, 013009. [[CrossRef](#)]

457. Aaij, R.; Abellán Beteta, C.; Ackernley, T.; Adeva, B.; Adinolfi, M.; Afsharnia, H.; Aidala, C.A.; Aiola, S.; Ajaltouni, Z.; Akar, S.; et al. Measurement of the $B_s^0 \rightarrow \mu^+ \mu^-$ decay properties and search for the $B^0 \rightarrow \mu^+ \mu^-$ and $B_s^0 \rightarrow \mu^+ \mu^- \gamma$ decays. *Phys. Rev. D* **2022**, *105*, 012010. [[CrossRef](#)]
458. Aad, G.; Abbott, B.; Abbott, D.C.; Abed Abud, A.; Abeling, K.; Abhayasinghe, D.K.; Abidi, S.H.; Aboulhorma, A.; Abramowicz, H.; Abreu, H.; et al. Study of $B_c^+ \rightarrow J/\psi D_s^+$ and $B_c^+ \rightarrow J/\psi D_s^{*+}$ decays in pp collisions at $\sqrt{s} = 13$ TeV with the ATLAS detector. *J. High Energy Phys.* **2022**, *8*, 87. [[CrossRef](#)]

Disclaimer/Publisher's Note: The statements, opinions and data contained in all publications are solely those of the individual author(s) and contributor(s) and not of MDPI and/or the editor(s). MDPI and/or the editor(s) disclaim responsibility for any injury to people or property resulting from any ideas, methods, instructions or products referred to in the content.